

Regulation of Vascular Smooth Muscle Cell Function by Mechanical Strain

by

George Chen-hsi Cheng

S.M., Massachusetts Institute of Technology, 1993
A.B., Harvard College, 1988

Submitted to the Harvard-MIT
Division of Health Sciences and Technology
in Partial Fulfillment of the Requirements
for the Degree of

Doctor of Philosophy
in Medical Engineering

at the

Massachusetts Institute of Technology
June 1996

© Massachusetts Institute of Technology, 1996

MIT LIBRARIES

JUL 2 1996

SCHERING

Signature of Author _____

Harvard-MIT Division of Health Sciences and Technology
May 1996

Certified by _____

Richard T. Lee, Thesis Supervisor
Assistant Professor of Medicine, Harvard Medical School
Lecturer, Department of Mechanical Engineering, MIT

Accepted by _____

Martha L. Gray, Co-Director
Harvard-MIT Division of Health Sciences and Technology

MASSACHUSETTS INSTITUTE
OF TECHNOLOGY

JUN 03 1996

SCHERING-PLOUGH

LIBRARIES

Regulation of Vascular Smooth Muscle Cell Function by Mechanical Strain

by

George Cheng

Submitted to the Harvard-MIT Division of Health Sciences and Technology
on May 24, 1996 in Partial Fulfillment of the Requirements for the Degree of
Doctor of Philosophy in Medical Engineering

Abstract

Although smooth muscle cells participate in the remodeling associated with atherosclerosis and other vascular diseases, the mechanisms by which these cells interact with their mechanical environment are incompletely characterized. This thesis serves to elucidate the capacity of smooth muscle cells to modulate their matrix and respond to mechanical loading.

Because integrins mediate many cell-matrix interactions, the role of integrins in reorganization and mechanical contraction of collagen by smooth muscle cells was assessed in blocking antibody studies. Of the collagen-specific integrins ($\alpha^1\beta_1$, $\alpha^2\beta_1$, and $\alpha^3\beta_1$) found to be expressed by these cells, only the α^1 and α^2 integrins mediated smooth muscle cell adhesion to collagen. In addition collagen gel contraction was mediated by α^2 , but not by α^1 or α^3 integrins. Interestingly, gel contraction was inhibited by an anti- β_1 antibody known for its stimulatory effect on cell adhesion.

To evaluate the mechanical regulation of smooth muscle cell function in a three-dimensional matrix, collagen gel cultures were subjected to uniaxial, unconfined compression. Sustained static compression led to a decrease in DNA and glycosaminoglycan synthesis, respectively, as measured by ^3H -thymidine and ^{35}S -sulfate incorporation. Decreased incorporation was not due to diffusive limitation of the radiolabel into the gel. A brief transient compression led to a delayed induction of DNA synthesis but a decrease in glycosaminoglycan synthesis. The induction of DNA synthesis increased with the compressive gel strain, and was mediated by autocrine release of FGF-2 as demonstrated by antibody-blocking studies and ELISA. Thus mechanical loading differentially regulates metabolic functions of smooth muscle cells in a three-dimensional culture.

Cellular strain was hypothesized to control the release of FGF-2 from smooth muscle cells; however, these strains cannot be readily assessed theoretically or experimentally from the bulk gel strain. Thus, a second method which imposes homogeneous and biaxially uniform strains to monolayer cells was developed. Oscillatory

strain induced FGF-2 release dependent on the amplitude (0-30%), frequency (0 - 1 Hz), and number of cycles of strain (0 - 10^5). There was a strain amplitude-threshold (10%) below which FGF-2 was not released. Above this threshold, FGF-2 release increased with the frequency, amplitude, and cycle number, but was maximally released by only $\sim 10^2$ cycles of strain. Thus cellular strain amplitude and/or strain rate tightly regulate the release of FGF-2 from vascular smooth muscle cells. In addition, heparin studies demonstrated that cellular strain causes a transfer of intracellular FGF-2 to the extracellular low-affinity receptors.

Thesis Supervisor: Richard T. Lee, M.D.
Assistant Professor of Medicine, Harvard Medical School
Lecturer, Department of Mechanical Engineering, MIT

Thesis Committee Chair: Alan J. Grodzinsky, Sc.D.
Professor of Electrical, Mechanical, and Bioengineering
MIT

Thesis Reader: Peter Libby, M.D.
Director of Vascular Medicine
Brigham and Women's Hospital

Thesis Reader: Roger D. Kamm, Ph.D.
Professor of Mechanical Engineering
MIT

Acknowledgments

I would first like to thank my thesis supervisor, Dr. Rich Lee. I first met Rich about five years ago while finishing the second year of med school and searching for a decent research project with which to kill the subsequent n years of my (then) young life. Although I must have met with at least a dozen investigators, it was through Rich's persistence that I joined his group and am here today writing about vascular smooth muscle cells. I am grateful for that persistence, because as it turns out all the other cardiologists with whom I met have since left Boston, and were it not for my decision I would probably be writing in Cleveland or not yet writing at all. Through the years I have learned a great deal and have received invaluable support from him in many capacities. His ability to exert a sublethal stress and respond appropriately to my oscillatory strain has played an essential role in the completion of this work. The lab meetings/free meals have also been critical.

I thank the HST-MEMP program for financial support, Dr. Roger Mark for academic advice, and Keiko Oh for administering all the checks and for answering all my last minute questions. This work was also supported, in part, by the NIH MSTP program.

My gratitude also goes to Dr. Elaine Lee, fellow grad student who tolerated my mess for three years before she (understandably) decided to graduate and leave. During the past year, I have missed the luxury of, without warning, turning my head to the left and griping to a receptive ear. Elaine was a constant source of personal and technical support, and her finishing the program with flying colors has been inspirational.

In retrospect, Prof. Alan Grodzinsky must also be sorry that Elaine left, because the clutter on my desk has been mounting at an alarming rate ever since. I am fortunate to have worked in Al's lab. How I managed to get through without ever cutting a joint, I will never know. His expertise, guidance, and humor have contributed greatly to my work. I am especially thankful for his helping me get past "that same sentence" during the writing of this document.

Dr. Peter Libby and members of his lab, including Marysia and Elyssa, have helped us on many aspects of the project. Without their assistance, we would still be growing our first batch of smooth muscle cells, not knowing, of course, that they are actually fibroblasts. Many of the turns taken in the research have been steered by Peter's helpful feedback.

Prof. Roger Kamm has continued to support me through the years, as teacher, collaborator, and more recently thesis committee member.

Prof. Martin Hemler and Dr. Feodor Berdichevski at the Dana-Farber Cancer Institute collaborated with us on the integrin study and have helped us with other technical issues along the way.

I thank Prof. Martha Gray for introducing us to the biaxial strain device and for allowing us to collaborate on its further development. Matt Mikulics helped with many of the design modifications, and Dave Gerson was instrumental in producing multiple devices and performing the necessary strain validations.

Special thanks go to Smruti Parikh and Bill Briggs for their technical assistance, maintenance of the lab, and ability to be in two places at the same time. Not only were they responsive to my occasional inordinate demands (i.e. I need a dozen flasks of cells tomorrow), but they assisted me in many experiments. This work would not have been possible without them. I also thank Grace Timlin and Lisa Cook for making my life easier.

A number of people in the lab have made for an entertaining environment and/or have saved me from stumbling over the years -- Tom, Larry, Greg, Marc, Steve, Soph, Ann, Jen, Paula, Scott, Eliot, and many more. I have especially appreciated commiserating/strategizing with Minerva this past year. I also thank Linda for disrupting the daily humdrum and for basically running the entire show.

I thank my parents for their endless love, support, and inspiration, and am grateful to my sister Deborah for sharing her infinite wisdom. Finally, much of this work is dedicated to Annie who probably knows it better than I do and has been by my side throughout. I assure her that I will not be reporting another experiment in excruciating detail any time soon.

George C. Cheng
May 1996

Table of Contents

Abstract	3
Acknowledgments	5
List of Figures	10
List of Tables	18
Chapter 1. Introduction	19
1.1 Atherosclerosis	19
1.2 The Vascular Smooth Muscle Cell	20
1.3 Mechanical Forces in Blood Vessels	22
1.4 Evidence for Vascular Responses to Mechanical Loading	25
1.4.1 In Vivo Studies	26
1.4.2 In Vitro Studies	26
1.5 Limitations of Previous Studies	28
1.5.1 Response in a Three-dimensional Matrix	28
1.5.2 Relationship between Cellular Strain and Function	29
1.6 Objectives	30
1.7 Primary Hypotheses	30
Chapter 2. Collagen Matrix Contraction and Reorganization by Human Vascular Smooth Muscle Cells: Role of Integrins	32
2.1 Abstract	32
2.2 Introduction	33
2.3 Materials and Methods	35
2.3.1 Monoclonal Antibodies	35
2.3.2 Cell Preparation and Culture	36
2.3.3 Immunoprecipitation	37
2.3.4 Cell Adhesion Assays	37
2.3.5 Collagen Gel Contraction	38
2.4 Results	38
2.4.1 Immunoprecipitation and Adhesion to Collagen	38
2.4.2 Collagen Gel Contraction	43
2.5 Discussion	48
Chapter 3. Biosynthetic Response to Compression of the Three- Dimensional Matrix Culture	52
3.1 Abstract	52
3.2 Introduction	53
3.3 Materials and Methods	55

3.3.1 Cell Culture.....	55
3.3.2 Mechanical Compression.....	56
3.3.3 Equilibrium Stress-Strain Relation of Gel Culture.....	58
3.3.4 ³ H-Thymidine Incorporation.....	60
3.3.5 ³⁵ S-Sulfate Incorporation.....	60
3.3.6 Total Radiolabel in Gel.....	61
3.3.7 Measurement of Total DNA Content.....	61
3.3.8 Measurement of Glycosaminoglycans.....	61
3.3.9 Statistics.....	61
3.4 Results.....	62
3.4.1 Effect of Static Compression on Biosynthesis.....	62
3.4.2 Diffusion of Thymidine.....	64
3.4.3 Dependence of DNA Synthesis on Static Compressive Strain.....	68
3.4.4 Effect of Release of Compression.....	70
3.4.5 Effect of Transient Compression on DNA and Glycosaminoglycan Synthesis.....	70
3.5 Discussion.....	72
Chapter 4. Characterization of DNA Synthetic Induction by Transient Compression	75
4.1 Abstract.....	75
4.2 Introduction.....	76
4.3 Materials and Methods.....	78
4.3.1 Cell Culture.....	78
4.3.2 Mechanical Compression.....	79
4.3.3 ³ H-Thymidine Incorporation.....	81
4.3.4 Conditioned-Media Experiments.....	82
4.3.5 Antibody Neutralization Experiments.....	82
4.3.6 Measurement of FGF-2 and Lactate Dehydrogenase Activity.....	83
4.3.7 Measurement of Total DNA Content.....	84
4.3.8 Measurement of FGF-2 mRNA.....	84
4.3.9 Statistics.....	85
4.4 Results.....	85
4.4.1 DNA Synthesis Following Transient Strain.....	85
4.4.2 Autocrine Growth Factor Studies.....	89
4.5 Discussion.....	93
Chapter 5. Development of Membrane Strain Device: Preliminary Assessment of FGF-2 and IL-1α Release by Cellular Strain	98
5.1 Abstract.....	98
5.2 Introduction.....	99
5.3 Materials and Methods.....	106
5.3.1 Prototype Device Modifications.....	106
5.3.2 Cell Culture on Matrix-Coated Membranes.....	110
5.3.3 Compatibility of Lubricant.....	110
5.3.4 Displacement of Platen (oscillatory, impulse, or step).....	111
5.3.5 Estimation of Strain Distribution.....	112
5.3.6 Dependence of Strain Magnitude on Oscillatory Platen Displacement.....	114

5.3.7 Measurement of Strain Distribution.....	115
5.3.8 Measurement of FGF-2 and IL-1 α	118
5.4 Results.....	118
5.4.1 Cellular Growth on Matrix-Coated Membrane.....	118
5.4.2 Sterilization of Membrane Dishes.....	120
5.4.3 Effect of Lubricant on Cell Morphology and FGF-2 Release.....	121
5.4.4 Strain Distribution.....	122
5.4.5 Clearance Between Dish Lid and Dish.....	126
5.4.6 Release of FGF-2 From Human Vascular Smooth Muscle Cells.....	129
5.4.7 Release of IL-1a from Human Keratinocytes.....	133
5.5 Discussion.....	134
Chapter 6. Characterization of FGF-2 Release in Response to Oscillatory Cellular Strain	136
6.1 Abstract.....	136
6.2 Introduction.....	137
6.3 Materials and Methods.....	140
6.3.1 Cell Culture.....	140
6.3.2 Application of Mechanical Strain.....	141
6.3.3 Measurement of FGF-2.....	141
6.3.4 Measurement of Cellular Injury.....	141
6.3.5 Immunofluorescence.....	142
6.3.6 Statistics.....	143
6.4 Results.....	143
6.4.1 Release of FGF-2 During Dynamic Strain.....	143
6.4.2 Dependence of FGF-2 Release on Characteristics of Strain.....	144
6.4.3 Cellular Injury.....	151
6.4.4 Role of Matrix Reservoir in FGF-2 Release.....	154
6.4.5 Localization of Release.....	158
6.5 Discussion.....	159
Chapter 7. Conclusions	166
7.1 Summary of Experiments: Relevance to Disease.....	166
7.1.1 Reorganization of Matrix.....	166
7.1.2 Mechanical Response in Three-dimensional Matrix.....	166
7.1.3 Role of Cellular Strain.....	168
7.2 Limitations and Future Work.....	169
7.2.1 Integrins in Cellular Responses.....	169
7.2.2 Growth Factor Responsiveness.....	170
7.2.3 Tissue Stress and Cellular Strain.....	170
7.2.4 Substrate Deformation and Cellular Strain.....	171
7.2.5 Improving the Three-Dimensional Configuration.....	171
7.2.6 Injury and IL-1 Release.....	172
7.2.7 Other Responses.....	172
References	173

List of Figures

- Figure 1.1 The role of smooth muscle cells in vascular remodeling. Smooth muscle cells synthesize extracellular matrix and degradative enzymes, and also secrete growth factors and other cytokines which can act in autocrine or paracrine fashions. Certain growth factors can bind to extracellular matrix and are subsequently released by matrix degradative enzymes. 21
- Figure 1.2 Mechanical loads associated with a segment of blood vessel. Applied forces (normal (A) and shear (B) forces intraluminally and (C) normal forces externally) give rise to reaction forces (normal (D) and shear (E) forces internally). 24
- Figure 2.1. Integrin expression in cultured human vascular smooth muscle cells. Cells were surface-labelled with Na¹²⁵I, lysed in 1% Brij 96 extraction buffer and immunoprecipitated with specific monoclonal antibodies against different integrin subunits. Immunoprecipitates were resolved by SDS-PAGE and autoradiography. The anti-integrin antibodies were: lane 1, TS2/7 (anti- α^1); lane 2, IIE10 (anti- α^2); lane 3, IA3 (anti- α^3); lane 4, B5G (anti- α^4); lane 5, mAB16 (anti- α^5); lane 6, A6-ELE (anti- α^6); lane 7, mAB13 (anti- β_1); lane 8, P3-nonspecific control. 40
- Figure 2.2. Effect of specific anti-integrin monoclonal antibodies on the adhesion of the human smooth muscle cells to collagen type 1. The plastic surface was coated with collagen type I (5 μ g/ml) and blocked with heat-denaturated bovine serum albumin. Cells labeled with fluorescent dye were pre-incubated with antibodies for 30 min at 4°C and allowed to attach to the adhesion surface for 30 min at 37°C. Non-adherent cells were removed in three consecutive washes and the attachment was analyzed using CytoFluor 2300. P3 is a control non-integrin antibody. 1B3.1 is an inhibitory anti- $\alpha^1\beta_1$ antibody, P1H5 and IIE10 are inhibitory anti- $\alpha^2\beta_1$ antibodies, Mab13 is an inhibitory anti- β_1 antibody, and TS2/16 is an anti- β_1 antibody known to stimulate adhesion. Error bars denote one standard deviation. 42
- Figure 2.3. Effect of inhibition of $\alpha^2\beta_1$ function on contraction of collagen matrices by vascular smooth muscle cells. ○ are Mab13, 1 ug/ml, and ▲ are without antibody. A. Effect of antibody IIE10. B. Effect of antibody 3E9. In both panels A and B, ● represent antibody diluted 1:500, ◆ are 1:100, ▼ are 1:20, and □ are 1:10 dilutions of monoclonal antibody culture supernatants. Points are average of duplicate matrices. 44

Figure 2.4.	Effect of inhibition of $\alpha^1\beta_1$ or $\alpha^3\beta_1$ function on contraction of collagen matrices by vascular smooth muscle cells. \circ are Mab13, 1 $\mu\text{g/ml}$, and \blacktriangle are without antibody. A. Effect of antibody 1B3.1 in concentrations of 1:2500, 1:500, and 1:250 as dilutions of ascites fluid. B. Effect of antibody IA3 in concentrations of 0.2, 2.0, and 20 $\mu\text{g/ml}$. Points are average of duplicate matrices.	45
Figure 2.5.	Effect of inhibition of $\alpha^1\beta_1$ and $\alpha^2\beta_1$ function on contraction of collagen matrices by vascular smooth muscle cells. Open \blacktriangle are without antibody. \blacksquare are with 1:100 dilution of antibody 1B3.1 ascites fluid. \bullet are with 1:20 dilution of antibody IIE10 culture supernatant. Open \blacktriangledown are with both 1B3.1 and IIE10. Means and standard deviations of triplicates are shown.	46
Figure 2.6.	Effect of stimulating anti- β_1 antibody TS2/16 on contraction of collagen matrices by vascular smooth muscle cells. \blacktriangledown are Mab13, 1 $\mu\text{g/ml}$, and \blacktriangle are in the absence of antibody. \blacklozenge are 1:5000, \square are 1:2000, and \circ are 1:500 dilutions of ascites fluid. Points are average of triplicate matrices.	47
Figure 3.1.	Static compression of vascular smooth muscle cell-collagen gel in a well of a standard 24-well culture plate. Gel is mounted between two porous polyethylene platens and compressed by a cylindrical weight. Alternatively, teflon spacers are inserted between platens to control gel compressive displacement.	
Figure 3.2.	Vessel wall under internal pressure, P. Unconfined gel compression in this study simulates radial compressive and circumferential tensile deformations indicated on element.	57
Figure 3.2.	Vessel wall under intraluminal pressure, P. Unconfined gel compression in this study simulates radial (r) compressive and circumferential (θ) tensile deformations indicated on element.	58
Figure 3.3.	Equilibrium stress-strain relationship for smooth muscle cell-collagen gel under unconfined compression (displacement control). Stress represents the compressive load normalized to the initial gel-platen contact area. Strain represents the decrease in gel thickness normalized to the initial gel thickness.	59
Figure 3.4.	^3H -thymidine incorporation by human vascular smooth muscle cells in collagen gel culture during 24 hr static compression (load control). Stress represents the compressive load normalized to the initial gel-platen contact area. Data represent mean \pm sem for n=3 or 4.	63
Figure 3.5.	^{35}S -sulfate incorporation by human vascular smooth muscle cells in collagen gel culture during 24 hr static compression. Stress represents the compressive load normalized to the initial gel-platen contact area. Data represent mean \pm sem for n=3 or 4.	64

Figure 3.6.	Time course of total (incorporated + unincorporated) ³ H-thymidine in smooth muscle cell-collagen gel cultures during sustained static compression of 10 (○), 50 (■), 250 (□), and 1000 Pa (▼) stress applied at time 0, relative to control (●). Data represent mean ± sd for n=3.	66
Figure 3.7.	(A) Total (incorporated + unincorporated) ³ H-thymidine in smooth muscle cell-collagen gel cultures after 24 hr compression and radiolabeling. (B) Wet weight of the gels after 24 hr compression. Data represent mean ± sd for n=1 to 3.	67
Figure 3.8.	Total ³ H-thymidine in gel normalized to gel wet weight after 24 hr static compression and radiolabeling. Data represent mean ± sd for n=1 to 3.	68
Figure 3.9.	³ H-thymidine incorporation by vascular smooth muscle cell in collagen gel culture during 24 hr static compression (displacement control). Gel strain represents the decrease in gel thickness normalized to the initial thickness. Data represent mean + sd for n = 3.	69
Figure 3.10.	Time course of ³ H-thymidine incorporation by vascular smooth muscle cells in collagen gel culture after a transient (5 min, 0.50 strain) compression and release of compression at time 0 (■), relative to unloaded control (●). Data represent mean ± sd for n=3.	71
Figure 3.11.	Time course of ³⁵ S-sulfate incorporation by vascular smooth muscle cells in collagen gel culture after a transient (5 min, 0.50 strain). compression at time 0 (■), relative to unloaded control (●). Data represent mean ± sd for n = 4.	72
Figure 4.1	Diagram of apparatus used to apply transient mechanical compression to three dimensional vascular smooth muscle cell cultures (SMC-Gel). A Compression Plate was lowered on to the gel cultures, and strain was limited by Teflon disks. After a brief period (usually 5 min), the Compression Plate was removed.	81
Figure 4.2.	Increase in ³ H-thymidine incorporation by human vascular smooth muscle cells following a 5 min compression at time 0 in the presence of 10% fetal calf serum at strains of 60% (●) or 80% (■). Control 12-hour incorporated counts were 710 ± 220, 560 ± 210, 1290 ± 207, and 930 ± 140 cpm, at 0, 12, 24, and 36 hours following compression. n = 3 or 4 for each measurement, error bars denote one standard deviation.	86
Figure 4.3.	Increase in ³ H-thymidine incorporation by human vascular smooth muscle cells following a 5 min compression at time 0 in defined serum-free conditions at strains of 60% (●) or 80% (■). Control 12-hour incorporated counts were 730 ± 200, 350 ± 70, and 590 ± 120 cpm, at 12, 24, and 36 hours following compression. n = 4 for each measurement, error bars denote one standard deviation.	88

Figure 4.4.	³ H-thymidine incorporation by human vascular smooth muscle cells 12-24 hr following a 5 min, 60% compression (Comp) in serum-free conditions. Control cell-gels received no stimulation. (A) Addition of a neutralizing polyclonal antibody to PDGF-A immediately following compression (Comp+anti-AA) did not inhibit the effect of transient compression (Comp) (p = ns). Addition of PDGF-AA in the absence of compression led to an increase in ³ H-thymidine incorporation (PDGF-AA) that was inhibited by the polyclonal antibody (AA+anti-AA). (B) Addition of a neutralizing polyclonal antibody to PDGF-B immediately following compression (Comp+anti-BB) did not inhibit the effect of transient compression (Comp) (p = ns). Addition of PDGF-BB in the absence of compression led to an increase in ³ H-thymidine incorporation (PDGF-BB) that was inhibited by the polyclonal antibody (BB+anti-BB). n = 3 or 4 for each measurement, error bars denote one standard deviation.	90
Figure 4.5.	³ H-thymidine incorporation by human vascular smooth muscle cells 12-24 hr following a 5 min, 65% compression (Comp) in serum-free conditions. Control cell-gels received no stimulation. The effect of transient compression was inhibited by a neutralizing monoclonal antibody to FGF-2 (10 mg/ml, p < 0.005) added immediately following compression (Comp+antiF10), but was unaffected by a mouse non-immune IgG (10 µg/ml) (Comp+IgG10). Nonsignificant inhibitory effects of lower concentrations of antibody to FGF-2 are shown (comp+antiF1, 1 µg/ml; comp+antiF.1, 0.1 µg/ml). Addition of FGF-2 in the absence of compression led to an increase in ³ H-thymidine incorporation (FGF-2) that was inhibited by the monoclonal antibody (FGF-2+anti-F10). n = 3 or 4 for each measurement, error bars denote one standard deviation.	91
Figure 4.6.	Ability of conditioned media from transiently compressed vascular smooth muscle cell-gel cultures to increase ³ H-thymidine incorporation by unstimulated gel cultures. Media harvested 12 hr following a 5 min, 60% compression (Comp) or no compression (Control) were transferred to unstimulated gel cultures, and ³ H-thymidine incorporation was measured from 12-36 hr later. The stimulatory effect of the compression-conditioned media was reversed by a neutralizing monoclonal antibody to FGF-2 (Comp+anti-FGF-2) (p < 0.001 vs. Comp). n = 4 for each measurement, error bars denote one standard deviation.	92
Figure 5.1	Uniaxial unconfined compression of cylindrical gel. Macroscopic strain profile is complicated by friction at the top and bottom surfaces of the gel, but these edge effects could be minimized by confined compression.	100

Figure 5.2	One-dimensional lumped-parameter mechanical model of cells (thin springs, k) and matrix elements (thick springs, K) bearing compressive force embedded in series and parallel orientations. Although overall gel strain is constrained by the platen displacement, the strains of the individual internal components may be spatially variable due to random density and orientation of these elements. In reality, both tension and compression-bearing elements resist the compression of the gel.	101
Figure 5.3	Viscoelastic response of gel culture after brief transient compression and release. Thickness (T) returns to 90 % of its initial value after $t \sim 1$ hr.	102
Figure 5.4	One-dimensional lumped-parameter mechanical model of cells (thin springs, k) and membrane (thick springs, K) under tensile force T . Assuming cells are rigidly constrained to the membrane through a thin matrix coating, the deformation of the ensemble is dominated by the membrane because it is much stiffer than the cell layer.	104
Figure 5.5	Schematic diagram of cellular deformation under tensile deformation of membrane (dotted boundary). Focal adhesions (x) move with membrane displacement, so that average cell strain is determined by membrane strain.	105
Figure 5.6	Side view of the prototype device to impose homogeneous and equi-biaxial strain to cells growth on a circular membrane.	107
Figure 5.7	Side view of current device illustrating modifications made to simplify operation and improve performance.	108
Figure 5.8	Side view of deformation of circular membrane by circular platen displacement, x .	113
Figure 5.9	Predicted membrane strain amplitudes for various cam displacement amplitudes.	114
Figure 5.10	Time course of membrane strain for cam displacement amplitudes of 3.1 mm (■), 5.4 mm (▲), 7.3 mm (×), 19.3 mm (*). For each cam, data are normalized to the maximum strain yielded for the hypothetical condition $R = r$ (◆).	115
Figure 5.11	Side view of platen for viewing cells microscopically under static strain. Membrane is deformed as dish is lowered manually into well and secured with locking collar.	116
Figure 5.12	Method used to compute strain components from the relative planar displacements of a triad of points.	118
Figure 5.13	Growth of human vascular smooth muscle cells on plastic (●), Silastic (■), Vitrogen-coated Silastic (▲), fibronectin-coated Silastic (▼), and silicone membrane pre-coated with collagen (◆). Cells were plated on day 0 and media were changed on days 1, 2, and 3.	120
Figure 5.14	Effect of lubricants on the release of FGF-2 by human vascular smooth muscle cells. Cells growing on membrane with an undercoating of Crisco (▲) released FGF-2 during the first	

	day, while cells growing on membrane with Braycote 804 (■) or without lubricant (●) released no growth factor during the four days. Error bars denote one standard deviation; n = 3 for each measurement.	122
Figure 5.15	The dependence of strain components e_{11} (●), e_{12} (■), and e_{22} (▲) on radial (A) and angular (B) location on membrane during static deformation (5.4 mm platen displacement). Data represent mean \pm sd for n = 4 to 6.	123
Figure 5.16	The dependence of strain components e_{11} (●), e_{12} (■), and e_{22} (▲) on radial location, computed from the displacements of microspheres adhered to the collagen coating (A), the fibronectin coating (B), and to cells on collagen-coated membrane (C) under static deformation (5.4 mm platen displacement). Data represent mean \pm sd for n = 4 to 6.	125
Figure 5.17	The dependence of strain components e_{11} (●) and e_{22} (■) on radial (A) and angular (B) membrane location computed from the displacements of ink markings on membrane under dynamic deformation (9.7 mm platen displacement amplitude). Data represent mean \pm sd for n = 4 to 6.	126
Figure 5.18	Evaporation of culture media from dishes with different lid configurations with or without membrane strain (1 Hz, 15%) as follows: uncovered + strain (●), uncovered - strain (■), propped lid + strain (▲), 0.1" lid clearance + strain (▼), 0.1" lid clearance - strain (○), covered + strain (□), and covered - strain (open ▲). Data represent mean for n = 2.	128
Figure 5.19	Maintenance of media volume under dynamic membrane strain (15%, 0.5Hz, ■) relative to control (●) when incubator humidity is maintained > 85%. Data represent mean for n = 2.	129
Figure 5.20	A) Time course of FGF-2 in media. FGF-2 is released by human vascular smooth muscle cells in response to a sustained step (●) and to 10 impulses (■) of strain at 55% magnitude relative to control (▲). B) FGF-2 remaining in the cell layers at 24 hours. Data represent mean + sd for n = 3 per measurement.	130
Figure 5.21	Time course of FGF-2 in media. FGF-2 is released by human vascular smooth muscle cells in response to a single strain impulse of 15% (■), 25% (▲), 40% (▼), and 55% (◆) magnitude relative to control (●). Data represent measurement of n = 2 pooled samples.	132
Figure 5.22	Time course of FGF-2 in media. FGF-2 is released by human vascular smooth muscle cells in response to single strain impulses of 5% (■) and 15% (▲), and to continuous cyclic strain of 15% (▼), relative to control (●). Data represent mean \pm sd for n = 4.	132

Figure 5.23	A) Time course of IL-1 α in media. IL-1 α is released from human keratinocytes in response to a single impulse of 40% strain (\blacktriangle) and to continuous cyclic strain of 15% magnitude (\blacksquare), relative to control (\bullet). B) IL-1 α remaining in cell layer after 150 min. Data represent measurement of n = 3 pooled samples.	134
Figure 6.1.	Cumulative FGF-2 in culture media during continuous oscillatory strain (1 Hz, 15% amplitude, \blacksquare) of human vascular smooth muscle cells, relative to control (\bullet). Data represent mean \pm sd for n=3 to 7.	144
Figure 6.2.	Dependence of FGF-2 release from human vascular smooth muscle cells on the number of cycles of mechanical strain (1 Hz, 15% amplitude). Relative to control (\bullet), cumulative FGF-2 in the media increased with cycle number for 1 cycle (\blacksquare), 9 cycles (\blacktriangle), and 90 cycles (\blacktriangledown) of strain (1 Hz, 15% amplitude); however, FGF-2 was not further increased for 900 cycles (\blacklozenge). Data represent mean \pm sd for n=3.	146
Figure 6.3.	Acute FGF-2 release from human vascular smooth muscle cells in response to both brief and prolonged dynamic strain. Relative to control (\bullet), strain (1 Hz, 15%) of 90 cycles (\blacksquare) and 90,000 cycles (\blacktriangle) initiated at t=0 min. were associated with rapid increases in FGF-2 in the media; however, FGF-2 was not further released after change to fresh media at t=150 min. Data represents measurement of n = 3 pooled samples.	147
Figure 6.4.	The dependence of release of FGF-2 from human vascular smooth muscle cells on the frequency of mechanical strain (90 cycles, 15% amplitude). Relative to control (\bullet), cumulative FGF-2 in media increased with frequency for 0.25 Hz (\blacksquare), 0.5 Hz (\blacktriangle), and 1 Hz (\blacktriangledown). Data represent mean \pm sd for n=3.	149
Figure 6.5.	The dependence of FGF-2 release from human vascular smooth muscle cells on the amplitude of mechanical strain (90 cycles, 1 Hz). Relative to control (\bullet), cumulative FGF-2 in media did not increase for 5% amplitude strain (\blacksquare) but increased with amplitude for 15% (\blacktriangle) and 30% (\blacktriangledown) strain. Data represent mean \pm sd for n = 3.	150
Figure 6.6.	The release of FGF-2 from human vascular smooth muscle cells by mechanical strain above and below 10% amplitude. Relative to control (\bullet), 90 cycles of 15% strain (\blacksquare) induced rapid release of FGF-2, but 90,000 cycles of 5% strain (\blacktriangle) caused no release. Data represents measurement of n = 3 pooled samples.	151
Figure 6.7.	Dependence of cellular injury on mechanical strain. Fluoresceinated dextran uptake by cells for control and after 15%, and 30% amplitude strain (90 cycles, 1 Hz).	153

Figure 6.8.	Effect of pre-treatment with heparin on FGF-2 release from human vascular smooth muscle cells in response to mechanical strain. FGF-2 in the media is increased in media by heparin treatment (second column). Strain (90 cycles, 1 Hz, 30%) after heparin pre-treatment caused release of FGF-2 (third column) that was less than that caused by strain alone (fourth column).	155
Figure 6.9.	Ability of heparin to increase FGF-2 in the culture media after mechanical strain. Human vascular smooth muscle cells were subjected to strain (90 cycles, 1 Hz, 30%) or received no mechanical strain and further incubated in the presence or absence of heparin (5 μ g/mL). After 60 min. FGF-2 in the media was increased by heparin treatment (column 2). Strain in the presence of heparin (column 4) released a greater amount of FGF-2 than strain alone (column 3). Data represent mean + sd for n = 3.	157
Figure 6.10.	Transfer of FGF-2 to media and low-affinity receptors by mechanical strain of 5%, 15%, and 30% amplitude. FGF-2 in the media 60 min. after mechanical strain (90 cycles, 1 Hz) in the presence (black column) or absence (gray) of heparin (5 μ g/ml). After 5% strain (second pair of columns), FGF-2 was not increased in the media (gray column) or low-affinity receptor pool (difference between gray and black columns). Strain of 15% amplitude (third pair of columns) increased FGF-2 in both the media and receptor pool; however strain of 30% amplitude (fourth pair of columns) caused further increase of FGF-2 in the media only. Data represent mean + sd for n = 3.	158

List of Tables

Table 2.1. Monoclonal antibodies against integrins. *Ability to block cell adhesion to integrin ligand. **TS2/16 is stimulatory.	36
Table 4.1 FGF-2 and LDH in culture media 12 hr following 5 min, 60% compression of the three-dimensional smooth muscle cell gel cultures in serum-free condition. Parallel gel cultures were subjected to three cycles of freezing and thawing without compression. The lower limit sensitivity of the LDH assay was 40 units/ml. * $p < 0.005$ vs. control, $n = 4$	93
Table 5.1 Duration of three impulse stages for various platen displacements performed manually. Data represent mean \pm sd for $n = 10$ measurements.	112

Chapter
I

Introduction

Mechanical forces regulate the functions of various cells including osteocytes,¹⁻⁴ chondrocytes,^{5,6} fibroblasts,⁷⁻⁹ cardiac¹⁰⁻¹⁴ and skeletal^{15,16} myocytes, and endothelial cells.¹⁷⁻¹⁹ This thesis serves to assess relationships between vascular smooth muscle cells and their mechanical environment. The experimental results may lend insight to general mechanisms of cellular responses to mechanical stimuli but may be particularly relevant to vascular physiology and disease.

1.1 Atherosclerosis

Atherosclerosis, a chronic disease affecting the intimal layer of medium- and large-sized arteries, is the principal etiology of myocardial and cerebral infarction and the leading cause of mortality in the U.S., and other developed countries.²⁰ The atherosclerotic lesion may begin early in life as an intimal aggregation of lipid-rich macrophages and T-lymphocytes, the "fatty streak", and may evolve over many years to a more advanced lesion or plaque.²¹ Although several classifications have been defined, plaques are typically characterized by hyperplastic smooth muscle cells and foam cells, abundant dense extracellular matrix, and deposits of lipid and cholesterol.²⁰ In an atherosclerotic coronary artery, a raised plaque may stenose the lumen and chronically obstruct the supply of blood to the myocardium, resulting in stable angina. Acutely, the surface of the plaque may rupture, potentially leading to thrombosis.²² Although plaque rupture may occur frequently during the evolution of

coronary lesions and without clinical symptoms, plaque rupture occasionally leads to occlusive thrombi and is probably the primary mechanism underlying acute coronary syndromes.^{21,23-25}

Experiments with hypercholesterolemic animals demonstrate a sequence of vascular changes consistent with human postmortem pathology and provide the basis for the “response-to-injury” model of atherogenesis, first proposed by Glomset and Ross in 1976. In this model, injury to the endothelium leads to an excessive fibro-proliferative inflammatory response beginning with 1) adhesion of inflammatory cells, including monocytes and T lymphocytes, to the endothelium, and followed by 2) migration of these cells into the vessel wall, 3) migration of vascular smooth muscle cells from the media into the intima, 4) proliferation of vascular smooth muscle cells and macrophages, 5) sequestration of lipid by macrophages and subsequent foam cell formation 6) excessive accumulation of extracellular matrix and 7) deposition of lipid and cholesterol in the matrix.²⁰ These activities are coordinated by biochemical, and perhaps mechanical, interactions among smooth muscle cells, endothelial cells, monocytes and macrophages, T-lymphocytes, platelets, and the extracellular matrix.^{20,26}

1.2 The Vascular Smooth Muscle Cell

Besides regulating short-term vascular tone myogenically, smooth muscle cells participate in vascular remodeling by synthesizing and secreting extracellular matrix, matrix-degradative enzymes, and also growth factors and other cytokines (Figure 1.1). Vascular smooth muscle cells produce much of the extracellular matrix in the vessel wall. Serving both structural and biological functions, these matrix components include collagens which provide tensile stiffness, elastin which confers properties of elastic recoil,

and proteoglycans which help regulate permeability and visco-elasticity, cell adhesion and migration,²⁷ and also low-density lipoprotein accumulation and foam cell formation.²⁸⁻³⁰

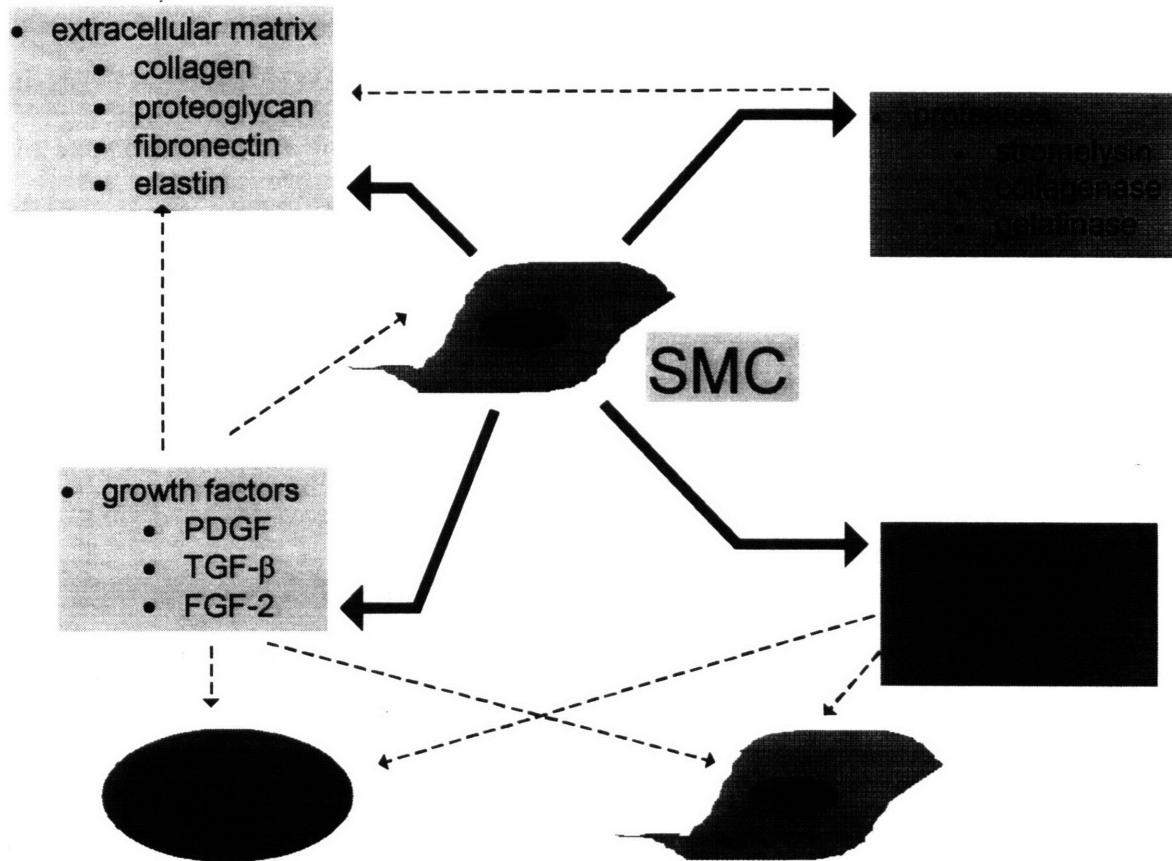


Figure 1.1 The role of smooth muscle cells in vascular remodeling. Smooth muscle cells synthesize extracellular matrix and degradative enzymes, and also secrete growth factors and other cytokines which can act in autocrine or paracrine fashions. Certain growth factors can bind to extracellular matrix and are subsequently released by matrix degradative enzymes.

Vascular smooth muscle cells also synthesize and secrete matrix degradative enzymes. Smooth muscle cells can digest extracellular matrix using both plasminogen-dependent and plasminogen-independent proteinases.³¹ Stromelysin mRNA has been detected in human atherosclerotic lesions,³² and expression of activated members of all three matrix metalloproteinase classes is increased in vulnerable regions of atherosclerotic tissue.³³ Vascular remodeling mediated by the synthesis and degradation of matrix components may be important for migration of smooth muscle cells³⁴ and other cells, lesion progression and regression,³⁵ and plaque structural properties such as failure strength.^{36,37}

In addition, smooth muscle cells coordinate cellular functions by synthesizing and secreting growth factors and other cytokines, which act in autocrine or paracrine fashion.²⁶ Matrix metabolism can be regulated by smooth muscle cell-derived cytokines. Collagen synthesis may be modulated by transforming growth factor- β (TGF- β)³⁸ and interleukin-1 (IL-1),³⁹ in turn, the synthesis of interstitial collagenase⁴⁰ and stromelysin,⁴¹ respectively, may be induced by platelet-derived growth factor (PDGF) and IL-1. Smooth muscle cell proliferation may also be regulated by TGF- β , PDGF, and fibroblast growth factor-2 (FGF-2).^{42,43} Macrophage recruitment may be mediated by chemotactic factors such as monocyte chemoattractant protein-1 (MCP-1).⁴⁴

1.3 Mechanical Forces in Blood Vessels

Blood vessels are continuously exposed to various mechanical loads (Figure 1.2), including pressure and shear forces exerted on the lumen, and resultant tensile,

compressive, and torsional forces borne within the wall. A primary hypothesis of this thesis is that cellular deformation, or strain, as a result of these loads, regulates cellular function. The distribution of mechanical stress in the vessel, as in any structure, is dependent on both the loads and certain structural parameters, such as geometry and constitutive material properties. These physical parameters may vary widely between and within vessels, depending on the structural organization of cells, extracellular matrix, and any lipid or calcified regions. To understand the potential effect of externally applied loads on the internal structure, it is useful to consider a simple general case. Under quasistatic mechanical loading, the resulting deformations within a heterogeneous structure composed of linear elastic materials may be discretely modeled. The deformations, $[U]$, are related to the loads, $[R]$ (applied, as well as reactions due to boundary conditions) by the equilibrium equation

$$[K][U] = [R] \quad (1.1)$$

where $[K]$ is the global stiffness matrix formulated from the stiffnesses of the individual structural elements. The internal strains $[e]$ may be derived from the displacements $[U]$ through an appropriate strain-displacement interpolation transformation. The internal stresses, $[\tau]$, are then obtained from the strains $[e]$ by

$$[\tau] = [C][e] \quad (1.2)$$

where $[C]$ is the matrix of elasticity also derived from the stiffness matrix and the strain-displacement transformation. The addition of dynamic loading, in general, would

introduce additional inertial and damping terms; however, these equations reveal that for a given loading condition, local strains may vary widely within a heterogeneous structure.

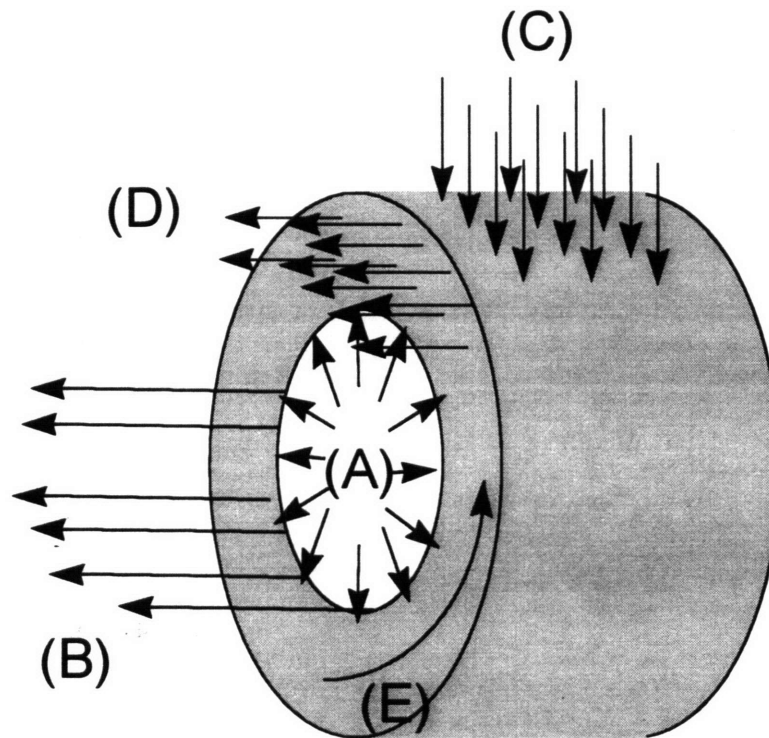


Figure 1.2 Mechanical loads associated with a segment of blood vessel. Applied forces (normal (A) and shear (B) forces intraluminally and (C) normal forces externally) give rise to reaction forces (normal (D) and shear (E) forces internally).

For example, under physiological conditions, the externally applied fluid shear stress and pressure, respectively, range from 0 to 10^2 Pa⁴⁵ and from 10^3 to 10^4 Pa. The resultant internal stresses may range from 0 to 10^5 Pa. From the above equations, strains may vary widely and within a small region because they are related to the loads through a matrix of elemental compliances. In the vascular wall, material compliance can vary by two or three orders of magnitude depending on the density and organization of collagen

and proteoglycan fibrils. Furthermore, still greater heterogeneity exists in the local vicinity of a single cell; at that level, cells and matrix fibrils are discrete elements which form a structure similar to an engineering truss; as is the case for truss elements under a given loading condition, individual cells may experience dramatically different strains depending on their location and orientation within the mechanically loaded tissue. Thus, the deformation of an individual cell cannot be generally determined from the loading condition, the general shape of the tissue, and the overall global stiffness. In the biological literature, the terms “stress” and “strain” are sometimes used interchangeably to refer to many different types of mechanical stimuli. However, in this thesis, different terms are used to describe, with varying degrees of specificity, a mechanical stimulus. Mechanical “loading” or “deformation” are used to refer to a general mechanical stimulus. The terms “stress” or “strain”, respectively, are used to refer to a mechanical load in which the average bulk stress (force/area) or strain (change in length/initial length) is controlled. Finally, the term “cellular strain” is reserved to refer to a mechanical load in which strain at the cellular level is regulated.

1.4 Evidence for Vascular Responses to Mechanical Loading

The modulation of vascular biology by mechanical loading has been observed at several levels. Clinically, the medial hypertrophy of hypertension^{46,47} and restenosis associated with percutaneous transluminal coronary angioplasty^{48,49} suggest adaptive vascular remodeling in response to mechanical forces and/or cell injury. Finite element analytical studies on actual human atherosclerotic lesions demonstrate a correlation

between mechanical stress concentrations and locations of plaque rupture.³⁷ Specific cellular responses are revealed by *in vivo* and *in vitro* studies.

1.4.1 In Vivo Studies

The anatomical sites of initiation and progression of atherosclerosis have been shown to correlate with locations of low-magnitude oscillatory fluid shear stress.⁵⁰ In addition, an endothelial-dependent negative-feedback process appears to control long-term vessel wall structure to maintain shear stress magnitude at 15 dyne/cm².⁵¹ Coarctation and congenital models of hypertension reveal increased proteoglycan synthesis by arterial smooth muscle cells.^{52,53}

1.4.2 In Vitro Studies

Previous *in vitro* studies have demonstrated responses to mechanical loading both in endothelial and smooth muscle cells. The endothelium, by virtue of its location at the interface between vessel wall and blood flow, is subjected to fluid shear stress as well as internal wall stresses and appears to act as a mediator in regulating arterial diameter both acutely and chronically.⁵⁴ Fluid shear stress applied to cultured endothelial cells leads to changes in cell topography,⁵⁵ cell shape,⁵⁶ pinocytosis,⁵⁷ alignment,^{58,59} cytoskeletal architecture, and in the expression of genes. These changes include a down-regulation of endothelin-1⁶⁰ (ET-1) and thrombomodulin,⁶¹ as well as an induction of FGF-2,⁶² tissue plasminogen activator,⁶³ TGF β -1, and PDGF A and B. Furthermore, the PDGF B gene has been shown to be regulated by a cis-acting shear-stress-responsive element in its promoter⁶⁴ and shear stress has been shown to stimulate DNA binding activities of nuclear factor kappa B and nuclear factor activator protein-1 (AP-1).⁶⁵

Endothelial cell responses may be tightly controlled by specific components of the stress. In endothelial cells, pinocytotic rates are dependent on the frequency of shear stress imposed.⁵⁷ Shear stress regulation of PDGF-B, FGF-2, and endothelin-1 in endothelial cells is magnitude- and frequency-dependent.^{62,66} In addition, the regulation of proliferation by fluid shear stress is observed with turbulent⁶⁷ but not with laminar shear stress⁶¹ of comparable magnitude.

In contrast to what is known about the endothelial cell, regulation of vascular smooth muscle cell function by mechanical loading is less well understood. Previous experiments have been performed primarily in monolayer culture.⁶⁸ Rat,⁶⁹ bovine,⁵⁹ and porcine⁷⁰ aortic vascular smooth muscle cells cultured on elastic substrates and subjected to cyclic deformation tend to align perpendicularly to the direction of membrane strain. In similar experiments, changes in cellular proliferation and DNA synthesis have been demonstrated. Although DNA synthesis is decreased in porcine aortic vascular smooth muscle cells subjected to oscillatory loading of 0.05 Hz, synthesis is increased in neonatal rat⁷¹ and in human saphenous vein vascular smooth muscle cells⁷² deformed at a frequency of 1 Hz. On the other hand, deformation applied at 1 Hz did not alter growth of rabbit aortic,⁶⁸ human internal mammary artery,⁷² and rat and lamb pulmonary arterial smooth muscle cells.⁷³ Mechanical deformation of smooth muscle cells has also been shown to increase^{68,74} or decrease⁷³ collagen synthesis, increase proteoglycan synthesis,⁶⁸ and increase⁶⁸ or decrease⁷³ general protein synthesis. In addition, static deformation of porcine aortic smooth muscle cells increases elastin synthesis.⁷⁵ The diversity of responses in these studies suggests that cellular responses may depend not only on the

type, species, and anatomical origin of the cell, but also on the characteristics of the mechanical loading.

1.5 Limitations of Previous Studies

1.5.1 Response in a Three-dimensional Matrix.

Although the ability of mechanical loading to alter smooth muscle function in a monolayer configuration has been demonstrated, the effect of mechanical deformation on cells in a three-dimensional matrix culture has not been completely characterized. Cells adhere to their surrounding matrix through integrins, heterodimeric transmembrane receptors. Integrins bind to specific amino acid sequences of extracellular matrix constituents.⁷⁶ Integrin cytoplasmic domains are physically associated with cytoskeletal components which interlink with microfilaments⁷⁶ and participate in bi-directional communication between the cell and matrix.

Integrins can transmit various forces exerted by cells upon their extracellular matrix. Cell migration is mediated by force generation via distinct α subunit cytoplasmic domains.⁷⁷ Dermal fibroblasts exert measurable forces⁷⁸ which mediate collagen gel contraction and reorganization. Although human vascular smooth muscle cells have also been shown to contract collagen matrices,⁷⁹ the role of specific integrins in gel contraction has not been characterized. Several α subunits associate with β_1 subunits to mediate adhesion of rat vascular smooth muscle cells to fibronectin, laminin, and collagen.⁸⁰ Adhesion of lamb ductus arteriosus vascular smooth muscle cells to fibronectin, laminin,

and collagens type I and IV is dependent on β_1 integrins, while migration over these substrates is heavily dependent on the $\alpha^v\beta_3$ integrin.⁸¹

Integrins can also transmit external forces to the cell cytoskeleton,⁸² inducing changes in cell shape which may regulate growth and differentiation.⁸³ However, the ability of mechanical loading to regulate cellular function in a three-dimensional matrix is incompletely understood. Cells in a three-dimensional matrix behave differently from those in monolayer configuration.^{84,85} Collagen matrix can regulate cell phenotype and morphology,^{86,87} collagen^{38,88} and proteoglycan synthesis, and also collagenase gene expression.^{89,90} In addition, proliferation of cells⁹¹⁻⁹³ and responsiveness to soluble growth factors may be decreased by contact with a three-dimensional matrix.⁹⁴

1.5.2 Relationship between Cellular Strain and Function.

In most previous studies, cells adhered to an elastic membrane substrate have been deformed at a controlled frequency of oscillation but with an uncontrolled, spatially nonuniform strain profile. Under these conditions, both strain amplitude and strain rate depend on the cell's location on the membrane (see Chapter 6 Discussion); thus, the frequency of mechanical loading in these experiments specifies only a general stimulus intensity. Given the close regulation of endothelial function by fluid shear stress, smooth muscle cell function may also depend on specific mechanical features such as cellular stress (or strain) amplitude or rate. The ability to control these features might be critical for interpreting certain cellular responses to mechanical loading.

1.6 Objectives

The objective of this thesis was to further characterize some of the functional relationships between vascular smooth muscle cells and their mechanical environment. The thesis is divided into two general parts, each addressing one limitation discussed in Section 1.5. The first part addresses mechanical relationships between the smooth muscle cell and its three-dimensional matrix; global stress or strain is applied in a controlled fashion to the three-dimensional matrix, but no attempt is made to control these parameters at the cellular level. The second part (Chapters 5 and 6) of the thesis focuses on the role of cellular strain in responses to mechanical loading; here methods to control cellular strain are used, but the potential role of the three-dimensional matrix is de-emphasized.

1.7 Primary Hypotheses

- **Specific integrins participate in vascular smooth muscle cell contraction and reorganization of their matrix.** In Chapter 2, a subset of integrins mediating smooth muscle cell adhesion to collagen is found to participate in collagen gel contraction; however, increased adhesion through one integrin adversely affects collagen contraction.
- **Static mechanical compression regulates DNA and matrix synthesis by vascular smooth muscle cells.** In Chapter 3, the smooth muscle cell-collagen gel is used to evaluate the regulation of DNA and glycosaminoglycan synthesis by mechanical compression. Static, unconfined compression is found to decrease biosynthesis, but transient compression leads to a differential response -- increased

DNA synthesis and decreased glycosaminoglycan synthesis. In Chapter 4, the DNA synthetic induction by a single transient matrix compression is found to be mediated by autocrine FGF-2.

- **Cellular strain tightly controls cellular function.** In Chapter 5, the rationale for controlling cellular strain rather than a bulk tissue stress is discussed in further detail. A previously used prototype cell strain device is modified, built, and experimentally verified to impose homogeneous and equi-biaxial strain to cells on an elastic membrane. Preliminary experiments demonstrate cellular strain-controlled release of FGF-2 and IL-1 α , respectively, from smooth muscle cells and keratinocytes. In Chapter 6, the control of FGF-2 release by cellular strain is further assessed. Strain amplitude and/or strain rate appear to regulate both cell injury and FGF-2 release.

Collagen Matrix Contraction and Reorganization by Human Vascular Smooth Muscle Cells: Role of Integrins

2.1 Abstract

Vascular smooth muscle cells perform the important function of modulation of vascular extracellular matrix. Because integrins mediate many cell-matrix interactions, the role of integrins in reorganization of collagen by cultured human vascular smooth muscle cells was studied. Immunoprecipitation demonstrated that human vascular smooth muscle cells express multiple β_1 integrins. Monoclonal antibody IIE10 (a blocking anti- α^2 antibody) inhibited adhesion of smooth muscle cells to collagen by 31%. The blocking anti- α^1 antibody 1B3.1 inhibited adhesion by 40%, while a blocking anti- α^3 antibody had no effect on adhesion. When 1B3.1 and IIE10 were both used, a 79% reduction in adhesion was observed, indicating that active α^1 and α^2 integrins cooperatively mediate adhesion. The blocking anti- β_1 antibody Mab13 abolished smooth muscle cell-mediated gel contraction, and the α^2 blocking antibody IIE10 had a dose-dependent partial inhibitory effect (37%). In contrast, blocking antibodies to α^1 and α^3 had no effect. When anti- α^1 (1B3.1) and anti- α^2 (IIE10) monoclonal antibodies were combined, no synergistic effect on inhibition of gel contraction was observed. Surprisingly, collagen gel contraction was inhibited by 46% by an anti- β_1 antibody (TS2/16) known for its stimulatory effect on cell adhesion. Thus, while $\alpha^1\beta_1$ and $\alpha^2\beta_1$ integrins both participate in adhesion of vascular

smooth muscle cells to collagen, only $\alpha^2\beta_1$ integrins mediate collagen reorganization. In addition, collagen reorganization appears to be a dynamic process, adversely affected by excessive adhesion strengthening.

2.2 Introduction

Vascular smooth muscle cells perform many functions that are critical for determining vascular structure during development, normal homeostasis, and disease states. In response to mechanical stimuli, smooth muscle cells change orientation, growth state, and extracellular matrix synthesis, permitting homeostatic adaptations to the pulsatile stresses of blood pressure.^{71,95} In addition, vascular smooth muscle cells migrate into the intima, proliferate, and secrete the extracellular matrix of atherosclerotic lesions.^{96,97} These lesions typically contain a collagen matrix that is relatively dense compared with the normal vessel. This collagenous matrix is, in part, responsible for changes in the biomechanical behavior of the vessel that can lead to instability and, ultimately, fracture of the lesion with thrombosis and occlusion.^{21,98}

Studies of fibroblasts, melanocytes, and other cells cultured in hydrated collagen lattices have demonstrated that mammalian cells will contract and reorganize collagen fibrils.⁹⁹⁻¹⁰¹ This process of physically contracting collagen is analogous to the organization of collagen matrix that occurs in dermal wound healing and development of normal connective tissues and is mediated by integrins.^{99,101} Integrins are heterodimeric cell surface receptors for extracellular matrix molecules that can transduce mechanical signals from the extracellular environment into the cell.^{76,102,103} The integrin family includes at least 15 α subunits and 8 β subunits that can form 21 different heterodimers,

and three different α subunits (α^1 , α^2 , and α^3) can form complexes with the β_1 subunit and function as collagen receptors. In addition to ligand specificity, integrins may have cell-type specific differences in function. For example, the $\alpha^2\beta_1$ integrin may function as a collagen receptor on fibroblasts or a collagen and laminin receptor on other cells.^{104,105} The $\alpha^2\beta_1$ integrin appears to mediate collagen gel contraction, and this process has been implicated in the pathophysiology of vitreoretinal contraction and retinal detachment.^{106,107} Collagen gel contraction by $\alpha^2\beta_1$ integrins can be abolished by exchange of the cytoplasmic domain of the α^2 subunit with that of the α^4 subunit with no effect on adhesion to collagen.⁷⁷ Thus, integrins function as more than adhesion receptors for extracellular matrix.

A variety of integrins on cultured vascular smooth muscle cells have been described. Clyman et al described several α subunits associated with β_1 subunits that mediated adhesion of rat vascular smooth muscle cells to fibronectin, laminin, and collagen.^{80,108} Lamb ductus arteriosus smooth muscle cells have β_1 integrins that appear to mediate adhesion to fibronectin, laminin, and collagens type I and IV, while migration of these cells on these substrates is heavily dependent on $\alpha^v\beta_3$ integrins.⁸¹ Because integrins may play an important role in smooth muscle cell regulation of vascular structure, we studied integrin-mediated extracellular matrix reorganization by cultured human vascular smooth muscle cells. We found that $\alpha^1\beta_1$ and $\alpha^2\beta_1$ integrins both participated in mediating adhesion to collagen, while $\alpha^2\beta_1$ integrins mediated collagen gel contraction, demonstrating specificity of α subunit functions in human vascular smooth muscle cells. In addition, we report that collagen gel contraction can be inhibited by an anti- β_1 integrin

antibody that usually stimulates adhesion, suggesting that dynamic conformational changes in β_1 integrins are necessary for collagen reorganization.

2.3 Materials and Methods

2.3.1 Monoclonal Antibodies.

Monoclonal antibodies used (Table 2.1) included Mab13 (anti- β_1) and Mab16 (anti- α^5),¹⁰⁹ 1B3.1 (anti- α^1),¹¹⁰ 12F1 (anti- α^2),¹¹¹ P3 (nonspecific control),¹¹² TS2/7 (anti- α^1),¹¹³ B5G10 (anti- α^4),¹¹⁴ TS2/16 (anti- β_1)¹¹⁵⁻¹¹⁷ and P1H5 (anti- α^2).¹⁰¹ Additional monoclonal antibodies used that were developed and characterized in the laboratory of M. Hemler include IIE10 and 3E9 (both anti- α^2), 6.7 (anti- α^5), and A6-ELE (anti- α^6). Monoclonal antibody IA3 (anti- α^3) was developed and characterized by F. Berdichevsky and J. Taylor-Papadimitriou.

ANTIGENS	ANTIBODY	BLOCKING?*
α^1	TS2/7	No
	1B3.1	Yes
α^2	3E9	No
	IIE10	Yes
	P1H5	Yes
α^3	IA3	Yes
α^4	B5G10	No
α^5	6.7	?
	Mab16	Yes
α^6	A6-ELE	No
β_1	Mab13	Yes
	TS2/16	**No

Table 2.1. Monoclonal antibodies against integrins. *Ability to block cell adhesion to integrin ligand. **TS2/16 is stimulatory.

2.3.2 Cell Preparation and Culture.

Smooth muscle cells were cultured by explant out-growth from unused portions of human saphenous veins from coronary bypass surgery by a protocol approved by the Brigham and Women's Hospital Human Research Committee. The cell cultures were grown in Dulbecco's modified Eagle's medium (DMEM) (M.A. Bioproducts, Walkersville, MD) with 10% fetal calf serum (FCS). All tissue culture constituents were selected for low endotoxin levels (<40 pg/ml) by Limulus amoebocyte lysate assay (QCL 1000, M.A. Bioproducts). Experiments were performed at passage 4 or 5 following harvesting.

2.3.3 Immunoprecipitation.

Cultured human smooth muscle cells were detached from tissue culture plastic with 2mM EDTA and surface labelled with Na¹²⁵I using lactoperoxidase and glucose oxidase as previously described.¹¹⁸ Cellular proteins were solubilized in the immunoprecipitation buffer (1% of NP-40, 50mM Tris HCl, pH 7.5, 150 mM NaCl, 5mM MgCl₂, 2mM PMSF, 20µg/ml aprotinin, 20µg/ml leupeptin) for 1 hour at 4°C and the protein extract was incubated with appropriate monoclonal antibodies for 1 hour at 4°C. Immune complexes were recovered on Protein A-Sepharose beads preabsorbed with rabbit anti-mouse polyclonal antisera and washed five times with immunoprecipitation buffer. Immunoprecipitated proteins were eluted from the Protein A-Sepharose beads in Laemmli loading buffer and resolved in 8.5% SDS/polyacrylamide gels. The dried gels were exposed for 24 hours at -70°C with X-OMAT film (Kodak, Rochester, NY).

2.3.4 Cell Adhesion Assays.

96-well plates were coated overnight with a solution of collagen type I (5µg/ml), blocked with 0.1% heat-denatured bovine serum albumin (hdBSA) for 45 min at 37°C, and washed twice with phosphate-buffered saline. Cells were detached from the tissue culture plastic with 2mM EDTA, washed with phosphate-buffered saline, and labelled with the fluorescent dye BCECF-AM (2',7'-bis(2-carboxyethyl)-5(6)-carboxyfluorescein) (Molecular Probes, Inc., Eugene, OR) for 30 min at 37°C. After labelling, the cells were washed twice with phosphate-buffered saline, resuspended in 0.1% hdBSA/RPMI and preincubated with appropriate antibodies for 30 min at 4°C before addition to the matrix coated plate (50,000 cells per well). After incubation for 25-30 min at 37°C, the plates were washed three times with RPMI to remove nonadherent cells. The fluorescence

before and after washes was evaluated with a CytoFluor 2300 fluorescent analyzer machine (Millipore Co., Bedford, MA). Every measurement point was performed in triplicate, and adhesion was estimated as a number of attached cells per mm².

2.3.5 Collagen Gel Contraction.

Cell culture in hydrated collagen gels was performed with Vitrogen 100 collagen (Collagen Corp, Palo Alto, CA) as previously described.⁹⁹ Vascular smooth muscle cells were preincubated with monoclonal antibodies at various concentrations for 30 min and then diluted 10 fold to yield final gel concentrations. The preincubated cells were then added to neutralized collagen (2.5 mg/ml) at a concentration of 2×10^5 cells/ml. The collagen-cell suspensions (1.5 ml each) were then incubated in 24 well plates (Costar, Cambridge, MA) at 37°C for one hour to polymerize the collagen, and the gel was then gently cut away from the sides of the well and lifted off the bottom. At selected time points, the diameter of the hydrated gels was measured using an inverted microscope.

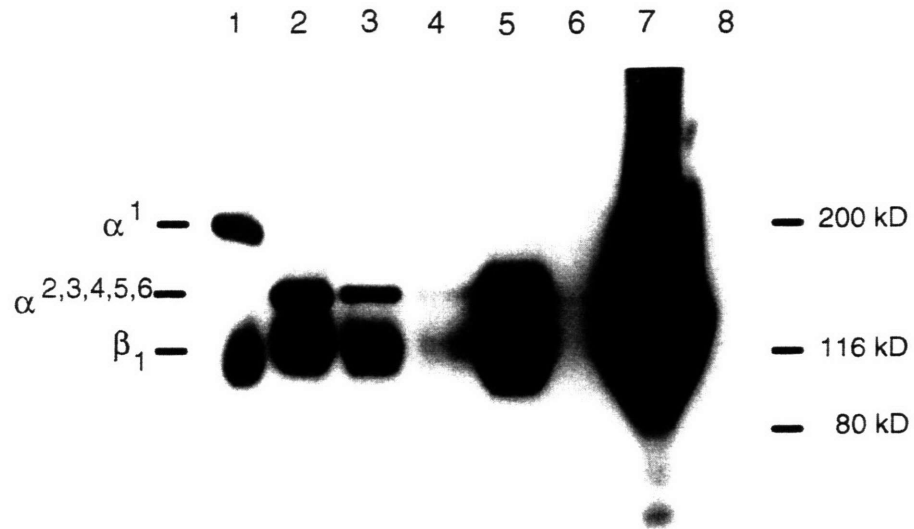
2.4 Results

2.4.1 Immunoprecipitation and Adhesion to Collagen.

To study the role of integrins in reorganization of collagenous matrix by human vascular smooth muscle cells, we first analyzed their integrin profile by immunoprecipitation using specific monoclonal antibodies (Figure 2.1). Vascular smooth muscle cells express abundant levels of several integrins of the β_1 family (lanes 1-6), including $\alpha^1\beta_1$, $\alpha^2\beta_1$, $\alpha^3\beta_1$, and $\alpha^5\beta_1$, whereas the cell surface expression of $\alpha^4\beta_1$ was low

and $\alpha^6\beta_1$ was almost undetectable. An anti- β_1 antibody precipitated all of the β_1 -containing integrins at once (lane 7).

Figure 2.1. Integrin expression in cultured human vascular smooth muscle cells. Cells were surface-labelled with Na^{125}I , lysed in 1% Brij 96 extraction buffer and immunoprecipitated with specific monoclonal antibodies against different integrin subunits. Immunoprecipitates were resolved by SDS-PAGE and autoradiography. The anti-integrin antibodies were: lane 1, TS2/7 (anti- α^1); lane 2, IIE10 (anti- α^2); lane 3, IA3 (anti- α^3); lane 4, B5G (anti- α^4); lane 5, mAB16 (anti- α^5); lane 6, A6-ELE (anti- α^6); lane 7, mAB13 (anti- β_1); lane 8, P3-nonspecific control.



To explore the role of these integrins in adhesion of vascular smooth muscle cells to collagen type I, adhesion experiments were performed in the presence of specific blocking monoclonal antibodies (Figure 2.2). Monoclonal antibodies P1H5 and IIE10 (which block α^2 -mediated adhesion) reduced adhesion by 34% and 31%, respectively, and the anti- α^1 blocking antibody 1B3.1 reduced adhesion by 40%. However, when 1B3.1 and IIE10 were both used, adhesion was reduced by 79%, indicating that these cells use both $\alpha^1\beta_1$ and $\alpha^2\beta_1$ integrins to interact with collagen. Accordingly, monoclonal antibody Mab13 (which blocks the function of all β_1 integrins) reduced adhesion to collagen by 95%. In parallel experiments, blocking anti- $\alpha^3\beta_1$ or non-blocking anti- $\alpha^1\beta_1$ and anti- $\alpha^2\beta_1$ monoclonal antibodies did not block adhesion (data not shown). Notably, adhesion to collagen was not increased by TS2/16, presumably because adhesion is already at a near maximal level.

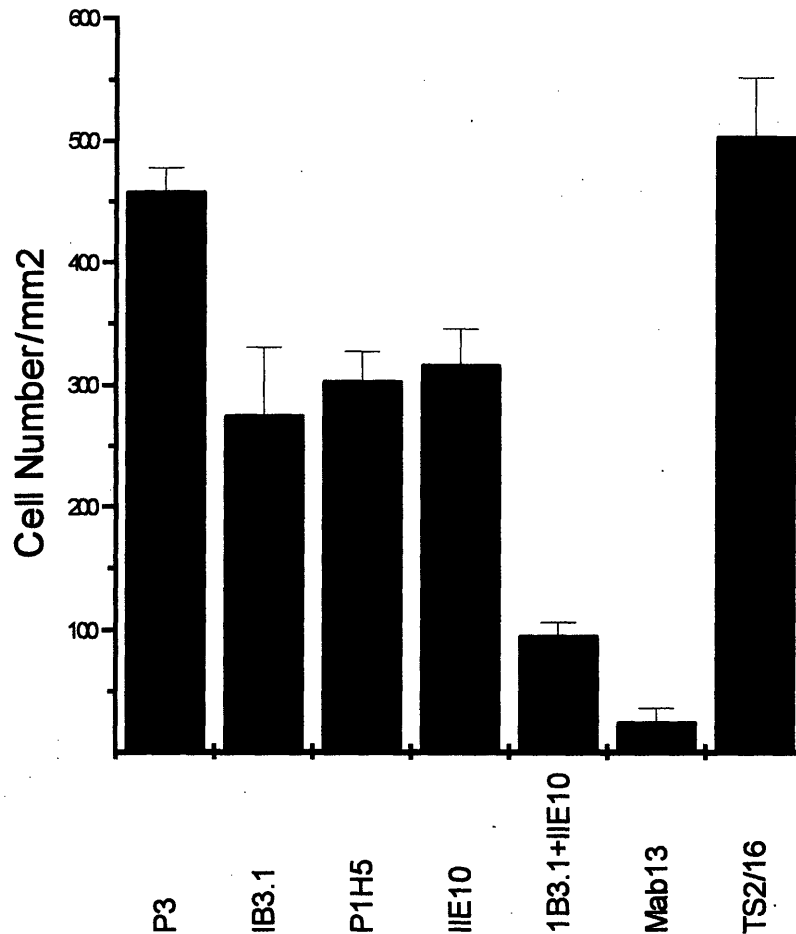


Figure 2.2. Effect of specific anti-integrin monoclonal antibodies on the adhesion of the human smooth muscle cells to collagen type I. The plastic surface was coated with collagen type I (5 μ g/ml) and blocked with heat-denaturated bovine serum albumin. Cells labeled with fluorescent dye were pre-incubated with antibodies for 30 min at 4 $^{\circ}$ C and allowed to attach to the adhesion surface for 30 min at 37 $^{\circ}$ C. Non-adherent cells were removed in three consecutive washes and the attachment was analyzed using CytoFluor 2300. P3 is a control non-integrin antibody. IB3.1 is an inhibitory anti- $\alpha^1\beta_1$ antibody, P1H5 and IIE10 are inhibitory anti- $\alpha^2\beta_1$ antibodies, Mab13 is an inhibitory anti- β_1 antibody, and TS2/16 is an anti- β_1 antibody known to stimulate adhesion. Error bars denote one standard deviation.

2.4.2 Collagen Gel Contraction.

When human vascular smooth muscle cells were cultured in floating hydrated collagen gels, the gels contracted in a highly reproducible and symmetric manner. Significant reduction in gel diameter occurred within the first 24 hr, and contraction was essentially complete after 72 hours. To evaluate the role of collagen-binding integrins in this process, collagen gel contraction experiments were performed in the presence of blocking anti-integrin monoclonal antibodies. The anti- α^2 blocking antibody IIE10 had a dose-dependent partial inhibitory effect on gel contraction (37% at 72 hr, Figure 2.3A), while the non-blocking anti- α^2 3E9 antibody had no inhibitory effect (Figure 2.3B). The anti- α^2 blocking antibody P1H5 also inhibited gel contraction by 40% at 72 hr (data not shown). In contrast, the presence of blocking antibodies to α^1 (Figure 2.4A) and α^3 (Figure 2.4B) had no effect on collagen gel contraction. Moreover, in contrast with the results of the adhesion experiments, when anti- α^1 (1B3.1) and anti- α^2 (IIE10) antibodies were combined, no synergistic effect on inhibition of gel contraction was observed (Figure 2.5). The β_1 -blocking antibody Mab13 abolished smooth muscle cell-mediated gel contraction (Figure 2.3A, 3B), but in all experiments, IIE10 and P1H5 failed to inhibit gel contraction as effectively as Mab13. Although the anti- β_1 antibody TS2/16 had no inhibitory effect on cell adhesion, it strongly inhibited collagen gel contraction in a dose-dependent manner, with 46% inhibition (at 72 hr) for the highest dose (Figure 2.6). The maximal inhibitory effect of TS2/16 was less than that observed with Mab13 (86%), but similar to the inhibitory effects of blocking anti- α^2 antibodies (37-40%).

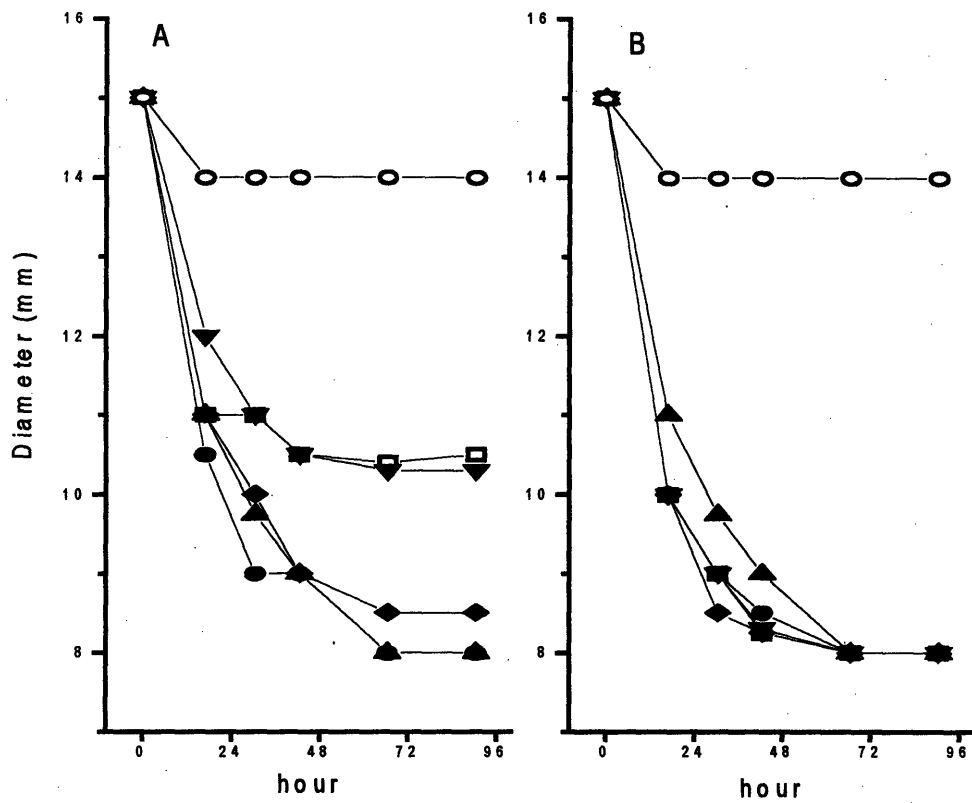


Figure 2.3. Effect of inhibition of $\alpha^2\beta_1$ function on contraction of collagen matrices by vascular smooth muscle cells. \circ are Mab13, 1 $\mu\text{g}/\text{ml}$, and \blacktriangle are without antibody. A. Effect of antibody IIE10. B. Effect of antibody 3E9. In both panels A and B, \bullet represent antibody diluted 1:500, \blacklozenge are 1:100, \blacktriangledown are 1:20, and \square are 1:10 dilutions of monoclonal antibody culture supernatants. Points are average of duplicate matrices.

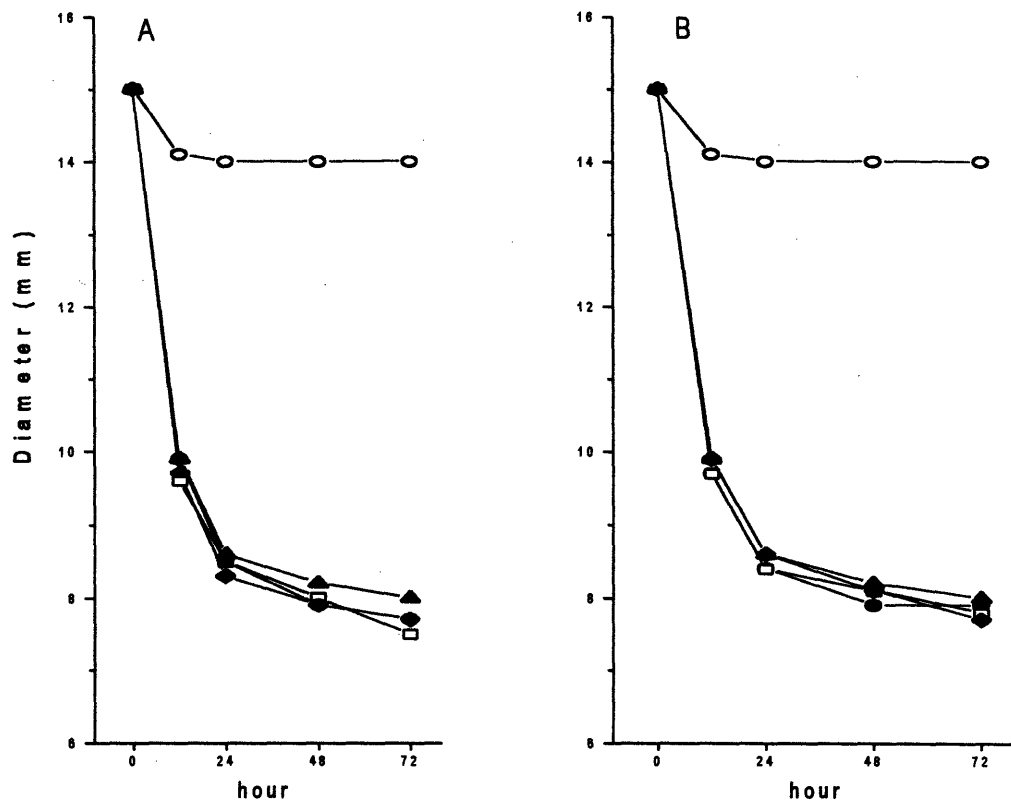


Figure 2.4. Effect of inhibition of $\alpha^1\beta_1$ or $\alpha^3\beta_1$ function on contraction of collagen matrices by vascular smooth muscle cells. ○ are Mab13, 1 $\mu\text{g/ml}$, and ▲ are without antibody. A. Effect of antibody 1B3.1 in concentrations of 1:2500, 1:500, and 1:250 as dilutions of ascites fluid. B. Effect of antibody IA3 in concentrations of 0.2, 2.0, and 20 $\mu\text{g/ml}$. Points are average of duplicate matrices.

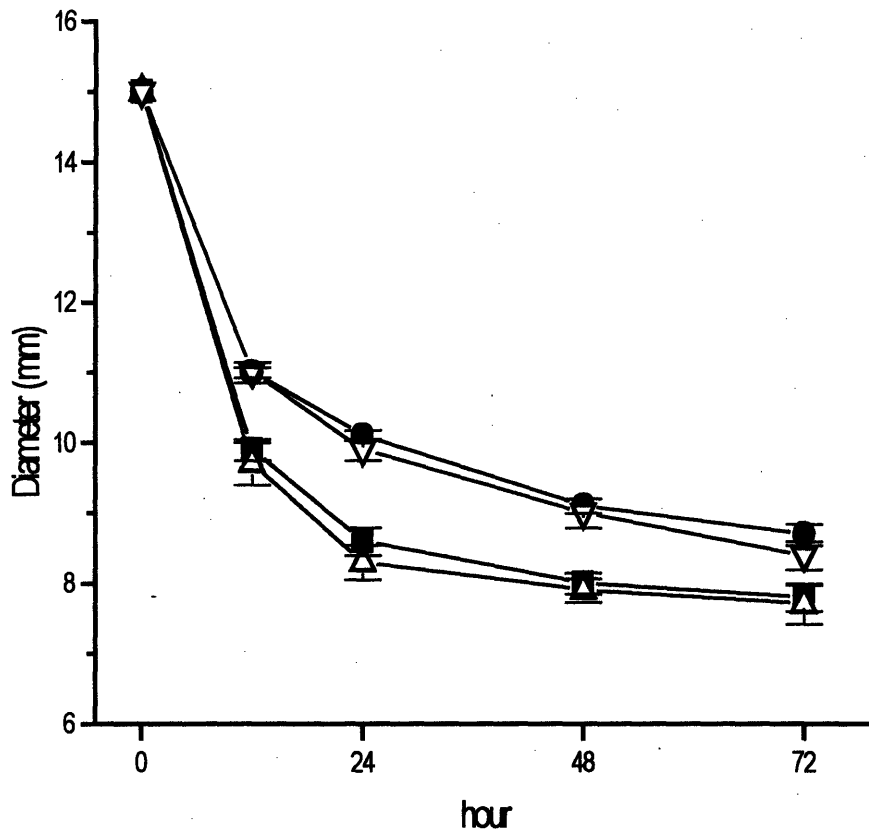


Figure 2.5. Effect of inhibition of $\alpha^1\beta_1$ and $\alpha^2\beta_1$ function on contraction of collagen matrices by vascular smooth muscle cells. Open \triangle are without antibody. \blacksquare are with 1:100 dilution of antibody 1B3.1 ascites fluid. \bullet are with 1:20 dilution of antibody IIE10 culture supernatant. Open ∇ are with both 1B3.1 and IIE10. Means and standard deviations of triplicates are shown.

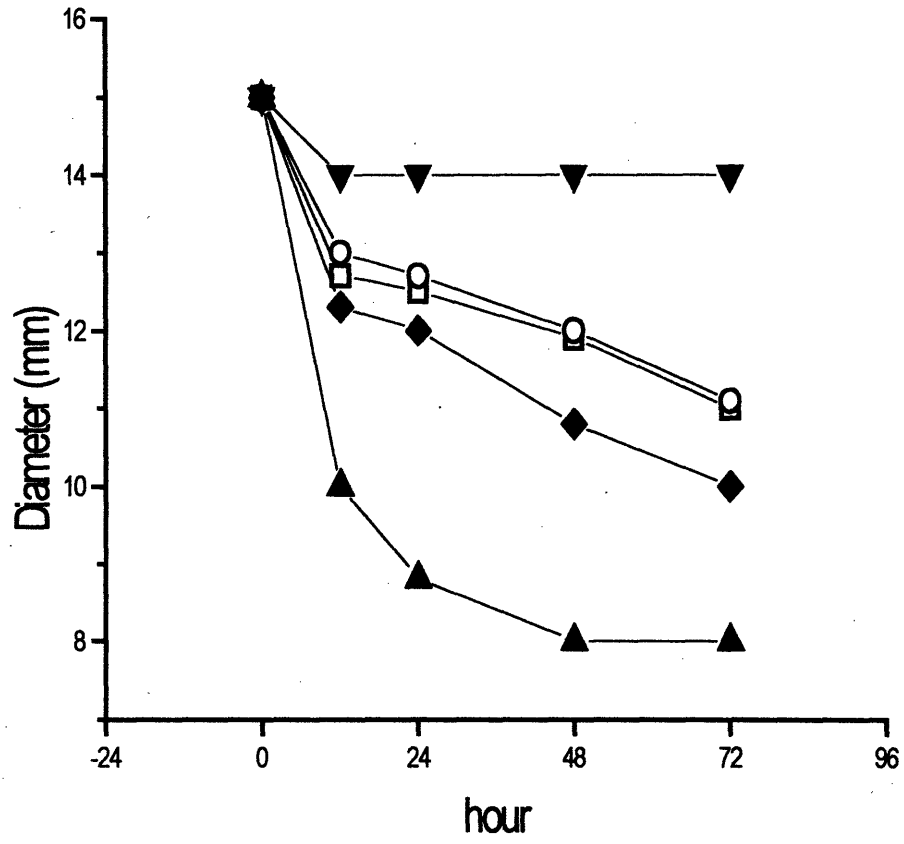


Figure 2.6. Effect of stimulating anti- β_1 antibody TS2/16 on contraction of collagen matrices by vascular smooth muscle cells. ▼ are Mab13, 1 $\mu\text{g/ml}$, and ▲ are in the absence of antibody. ◆ are 1:5000, ◻ are 1:2000, and ○ are 1:500 dilutions of ascites fluid. Points are average of triplicate matrices.

2.5 Discussion

In this study, we found that function-blocking antibodies to individual α subunits of collagen-binding integrins partially blocked vascular smooth muscle cell adhesion, while the combination of antibodies to both α^1 and α^2 subunits markedly inhibited adhesion. It is not surprising that a cell responsible for regulating structure in a collagenous matrix both acutely through active contraction and chronically through organization of matrix should have a redundant system for adhering to collagen. On the other hand, the addition of antibodies blocking α^1 function did not lead to additional inhibition of collagen gel contraction over the α^2 blocking antibody, indicating that in the collagen reorganization process, integrins function as more than simply collagen adhesion receptors. In this regard, it was previously shown that replacement of the α^2 cytoplasmic domain with that of α^4 did not alter adhesion to collagen, but did abolish gel contraction.⁷⁷

The complexity of the collagen reorganization process was further demonstrated by the effects of the stimulatory monoclonal antibody TS2/16. The TS2/16 antibody can increase adhesion in cells with β_1 integrins that are not fully active, presumably by inducing a conformational change that causes increased ligand binding. The results of this study indicate that β_1 integrins of cultured vascular smooth muscle are already in a highly active state, since adhesion was not increased by TS2/16. Although the stimulatory antibody had minimal effect on adhesion, collagen gel contraction was markedly inhibited. One potential explanation for this finding is a dynamic mechanism of collagen

reorganization that requires: 1) integrin-mediated adhesion to collagen, 2) contraction through cytoskeletal force generation, and 3) subsequent release of collagen from the integrin. The integrin could then bind to new collagen ligands, and the contraction process would begin again. This dynamic adhesion and release mechanism may be similar to proposed mechanisms of integrin-mediated cell migration.¹¹⁹ Indeed, it was recently demonstrated that the stimulatory antibody 8A2 inhibited migration, presumably by freezing eosinophil β_1 integrins in the high-avidity adhesion state.¹²⁰

Previous studies have identified $\alpha^2\beta_1$ integrins as the primary mediators of the gel contraction phenomenon.^{99,101} However, as seen in previous studies,¹⁰¹ antibodies blocking α^2 function failed to achieve the magnitude of inhibition of collagen gel contraction of Mab13 in this study. Although we observed this incomplete inhibition with two different α^2 function-blocking antibodies (IIE10 and P1H5), it is possible that Mab13 has a much higher potency for blocking integrin function than the other antibodies.

The ability of cells to contract and organize collagen is fundamental in the wound healing process. Dermal fibroblasts have been shown to generate measurable traction forces during collagen gel contraction⁷⁸ which in vivo may serve to close a skin wound and increase the strength of the loose granulation tissue, ultimately forming a strong scar. Atherosclerosis resembles the wound healing process in many ways.²⁰ In response to a variety of stimuli, smooth muscle cells migrate into the intima and secrete extracellular matrix rich in collagen and proteoglycans.²¹ It is likely that smooth muscle cells participate in organizing the collagen in this newly-synthesized matrix to form the dense network of collagen that is often seen in the advanced atheroma. The organized collagen

network is one reason that atherosclerotic tissue is several times stiffer than the normal vessel wall.¹²¹ Studies of vascular mechanics suggest that this difference in stiffness may predispose the vessel to plaque rupture and thrombosis by establishing regions of high stress near the junction of the stiffer plaque with the more normal vessel.³⁷

It is important to recognize that cultured human vascular smooth muscle cells are phenotypically different from smooth muscle cells *in vivo*.^{122,123} Previous reports have suggested that the profile of integrins on vascular smooth muscle cells changes in cell culture. Koteliansky et al found that expression of α^1 integrins by human aortic smooth muscle cells decreased during subculturing;¹²⁴ in addition, smooth muscle cells from thickened intima of human adult aorta express five times less α^1 than cells from adult aortic media.¹²⁵ Vascular smooth muscle cells cultured in collagen gels have some differences compared to cells grown on plastic; for example, smooth muscle cells reduce collagen synthesis and are less responsive to growth factors.^{94,126} Although we have not observed changes in integrin profile between smooth muscle cells grown on plastic or grown in collagen gels (preliminary studies not shown), Klein et al have found that $\alpha^2\beta_1$ integrins in some cells are upregulated by growth in collagen gels.⁹⁹ It is also possible that integrin activation state could be changed by culture in the collagen lattice.

In conclusion, this chapter serves to identify a potential mechanism used by vascular smooth muscle cells *in vivo* to mechanically contract and organize extracellular matrix, and opens the way for further studies to determine how modulating $\alpha^2\beta_1$ function might change vessel wall structure. In addition, these experiments indicate that the process of collagen reorganization by cells has stringent biological and mechanical

requirements; it does not occur if adhesion to collagen is mediated by the wrong integrin (i.e. $\alpha^1\beta_1$) or if adhesion is excessively strong (i.e. in the presence of TS2/16). In the remaining chapters, the capacity of the mechanical environment to control cellular function is discussed.

Biosynthetic Response to Compression of the Three-Dimensional Matrix Culture

3.1 Abstract

The appropriate control of smooth muscle cell proliferation and extracellular matrix metabolism may be essential for maintaining the normal vascular state. Mechanical stimuli have been shown previously to regulate these functions in vascular smooth muscle cells grown in monolayer configuration. However, the effects of mechanical loading on smooth muscle cells in a three-dimensional matrix have been incompletely characterized. The purpose of this study was to evaluate the potential regulation of DNA and glycosaminoglycan synthesis by compression of a smooth muscle cell-collagen gel culture. Static, unconfined compression inhibited ^3H -thymidine incorporation; compression for 24 hrs at 0.25, 1.0 and 2.5 kPa stress, respectively, led to incorporations of 475 ± 200 , 86 ± 7 , and 64 ± 17 cpm/gel (vs. 1000 ± 220 cpm/gel for control, $p < 0.05$ by ANOVA). Compression also decreased ^{35}S -sulfate incorporation; 24 hr of compression at 0.25, 1.0 and 2.5 kPa, respectively, led to incorporations of 230 ± 30 , 200 ± 8 and 211 ± 33 cpm/gel (vs. 460 ± 40 cpm/gel for control, $p < 0.05$). Decreased incorporation of radiolabel was not due to diffusional limitation by compression; there was no difference in total gel ^3H -thymidine concentration after 24 hr of compression at 10, 50, 250, or 1000 kPa. In addition, ^3H -thymidine incorporation decreased linearly with the magnitude of compressive gel strain, suggesting that biosynthesis was controlled by the matrix

deformation rather than the applied force. Decreased DNA synthesis was reversible after release of compression. In addition, transient compression led to a delayed induction of ³H-thymidine incorporation; at 24-48 hr after compression (5 min., 50% strain) and release, incorporation was 3000 ± 620 cpm/gel (vs. 990 ± 100 cpm/gel for control, $p < 0.005$). Thus, mechanical loading of smooth muscle cells in a three-dimensional matrix regulates DNA and glycosaminoglycan synthesis.

3.2 Introduction

The dysregulation of cellular proliferation, migration, and extracellular matrix metabolism may contribute to vascular disease states.¹²⁷⁻¹²⁹ Interactions among smooth muscle cells, macrophages, endothelial cells, platelets, and other cells as well as the extracellular matrix are coordinated by growth factors and other cytokines.^{20,130,131} In addition to biochemical signals, mechanical forces may participate in proliferative and remodeling responses. *In vivo* studies suggest that elevated intravascular pressures may accelerate the medial hypertrophy and decreased vascular compliance often associated with hypertension.^{46,132} The mechanical stress imposed during balloon angioplasty may trigger some of the early cellular responses of restenosis.^{133,134}

Vascular smooth muscle cells synthesize many of the extracellular matrix components in the vessel wall.¹³⁵ Besides synthesizing five of the six types of collagen found in blood vessels¹³⁶, smooth muscle cells also make the large proteoglycan versican as well as the small proteoglycans, decorin and biglycan. Both chondroitin sulfate and dermatan sulfate proteoglycans accumulate in atherosclerotic tissues, and may promote low-density lipoprotein accumulation and oxidation, and also foam cell formation.²⁸⁻³⁰

Proteoglycan synthesis by smooth muscle cells may be regulated by PDGF and TGF- β ¹³⁷ as well as the extracellular matrix.¹³⁸

Mechanical loading has been shown to regulate vascular smooth muscle cell proliferation and matrix synthesis, primarily in monolayer culture. Oscillatory forces induce the proliferation of neonatal rat⁷¹ and human saphenous vein⁷² smooth muscle cells, but decrease the proliferation of porcine aortic smooth muscle cells.⁷⁰ Other studies with human mammary artery,⁷² and also rat and lamb pulmonary arterial smooth muscle cells,⁷³ reveal no growth effect by mechanical stimuli. Mechanical loading may also increase^{68,74} or decrease⁷³ collagen production, and increase proteoglycan synthesis.⁶⁸ The apparent diversity of responses in these studies may reflect differences both in the species and anatomical origin of the cells as well as in the specific loading protocols used.

Although these studies demonstrate sensitivity of smooth muscle cells to the mechanical environment,¹³⁹ the regulation of vascular smooth muscle cells in a three-dimensional matrix has not been characterized. Cells grown in a three-dimensional lattice behave differently from those in monolayer. Collagen matrix affects vascular smooth muscle cell ultrastructure, proliferation, and synthesis of collagen and proteoglycans.^{38,140} In lattice culture, the vascular smooth muscle cell assumes a spindle shape similar to that observed *in vivo* and proliferates more slowly than in monolayer.¹⁴¹ The cellular response to mechanical forces may be mediated by certain cytoskeletal compression- and tension-bearing elements oriented in a three-dimensional configuration.¹⁴² Thus, in this chapter, smooth muscle cell-collagen matrix culture were subjected to compression, and DNA and glycosaminoglycan synthesis was measured.

3.3 Materials and Methods

3.3.1 Cell Culture.

Human vascular smooth muscle cells were derived from explants of discarded portions of saphenous veins obtained during coronary bypass surgery performed at Brigham and Women's Hospital. Monolayer smooth muscle cells were cultured in Dulbecco's Modified Eagle Medium (DMEM) (Whittaker Bioproducts, Inc.) with 10% fetal calf serum (FCS), at 37° C and 5% CO₂. These conditions are selective for growth of smooth muscle cells over endothelial cells.¹⁴³ The explant and culture techniques were identical to protocols used in previous studies of cultured vascular smooth muscle cells.^{39,144,145} Cells were cultured through passages 3 - 5 prior to transfer to a three-dimensional collagen gel culture system for use in compression experiments.

Cell culture in hydrated collagen gels was performed with Vitrogen 100 collagen (Celtrix Pharmaceutical) as previously described.¹⁴⁶ Cells ($2.5 - 3.0 \times 10^5$) were suspended in 1.25 ml collagen (2.8 mg/ml) and cultured in standard 24-well (16 mm diam.) culture plates (Costar Corporation). Gel cultures were maintained in DMEM supplemented with 10% FCS and 0.07 mM ascorbate-2-phosphate (Wako Pure Chemical Industries) and received a change of culture medium every two days. The contraction of collagen gel matrices by these cells may be resisted by local adhesions to the culture plate wells; thus, to facilitate uniform, axisymmetric gel contraction, on day 5 the gel cultures were gently detached from the sides of the wells. Over the course of 10 days in culture, smooth muscle cell-gels contracted uniformly to disks with nearly identical dimensions in a given experiment; the standard deviation of gel thicknesses, measured by micrometer prior

to compression, was less than 5% of the mean. Final contracted gel diameter ranged from 4.5 - 7.0 mm, and thickness ranged from 1.0 - 2.5 mm in different experiments.

3.3.2 Mechanical Compression.

In 24-well plates (Costar), smooth muscle cell-collagen gel cultures were mounted between porous (nominal pore size 40-60 μm , Porex), polyethylene platens to permit diffusion into the gel during compression (Figure 3.1). Static uniaxial, unconfined compression was applied with load-control by manually lowering a cylindrical weight onto the top platen. This configuration of loading was used to qualitatively simulate radial compressive and circumferential tensile deformations in the pressurized blood vessel (Figure 3.2). In some experiments, a Teflon spacer was inserted between the platens to control the displacement of compression.

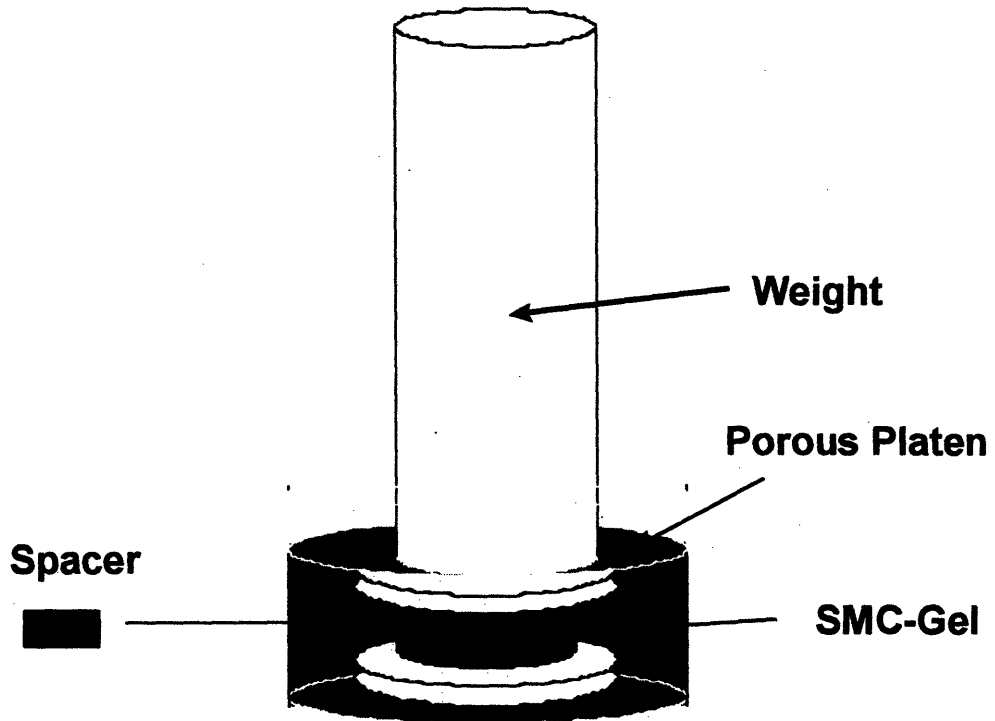


Figure 3.1. Static compression of vascular smooth muscle cell-collagen gel in a well of a standard 24-well culture plate. Gel is mounted between two porous polyethylene platens and compressed by a cylindrical weight. Alternatively, teflon spacers are inserted between platens to control gel compressive displacement. Figure 3.2. Vessel wall under internal pressure, P . Unconfined gel compression in this study simulates radial compressive and circumferential tensile deformations indicated on element.

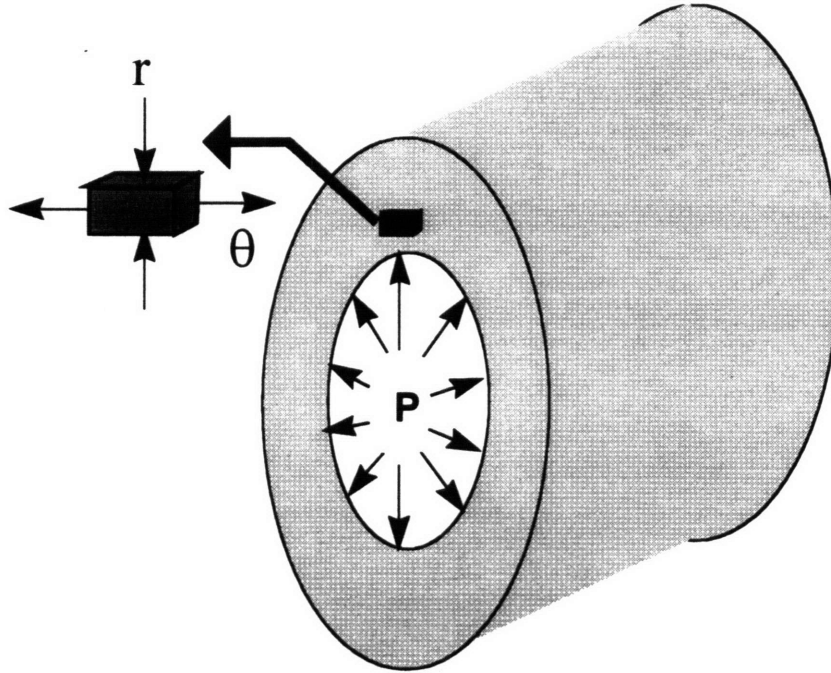


Figure 3.2. Vessel wall under intraluminal pressure, P. Unconfined gel compression in this study simulates radial (r) compressive and circumferential (θ) tensile deformations indicated on element.

3.3.3 Equilibrium Stress-Strain Relation of Gel Culture.

Smooth muscle cell-collagen gel cultures were loaded in a polysulfone, cylindrically unconfining chamber which was mounted in a servo-controlled Dynastat mechanical spectrometer (IMASS, Hingham, MA). The gel cultures were compressed in displacement control between the porous polyethylene platens in DMEM supplemented with 10% FCS; the initial gel thickness was determined by micrometer before the gel was loaded. Gel cultures were compressed by sequential increments of 10% strain, estimated as the vertical displacement divided by the initial thickness, up to a maximum of ~90%

strain. At each displacement, the load was recorded after a stress relaxation period. The stress was estimated as the load normalized to the initial area of the gel face (Figure 3.3)

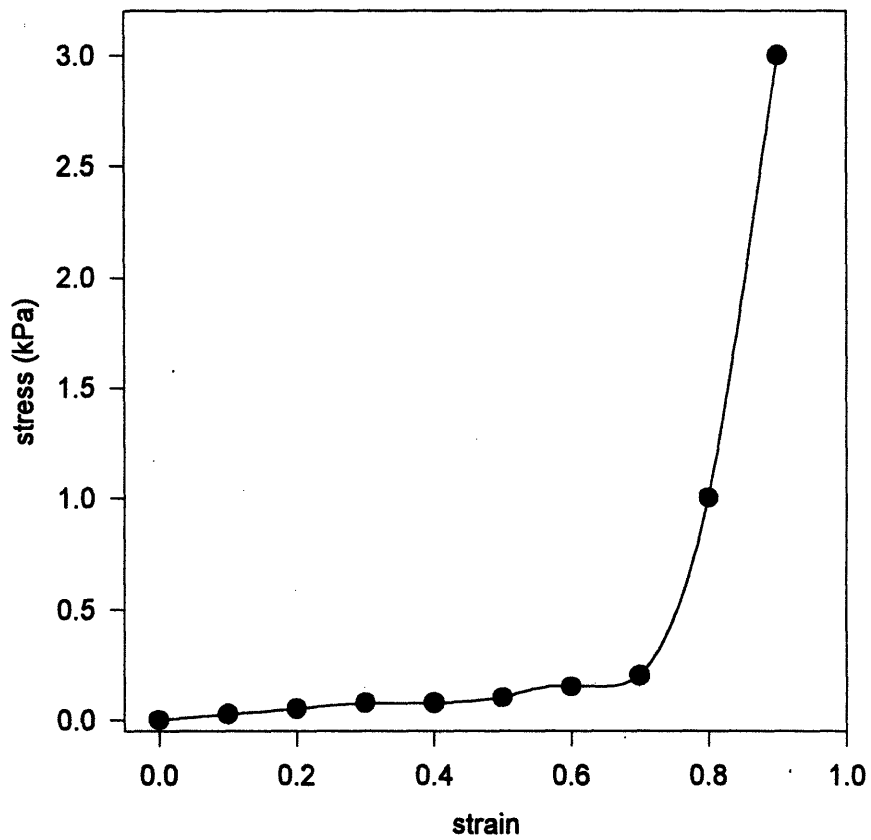


Figure 3.3. Equilibrium stress-strain relationship for smooth muscle cell-collagen gel under unconfined compression (displacement control). Stress represents the compressive load normalized to the initial gel-platen contact area. Strain represents the decrease in gel thickness normalized to the initial gel thickness.

3.3.4 ³H-Thymidine Incorporation.

Smooth muscle cell-collagen gel cultures were pulse-labeled with methyl-[³H]-thymidine, 6.7 mCi/mmol, (Dupont-NEN) to measure DNA synthesis. Following radiolabeling, smooth muscle cell-collagen gel matrices were solubilized overnight in 4 mol/L urea, 0.5% sodium dodecyl sulfate (SDS), and precipitated with 10% trichloroacetic acid at 4° C. Precipitates were vacuum-collected on 0.45 µm filters (Millipore Corp.) and washed with 10% trichloroacetic acid at 4° C. Filters were air-dried, mixed with Ecolume (ICN Biomedicals) scintillation cocktail, and counted with a scintillation counter (Pharmacia LKB Nuclear). To assess nonspecific radiolabeling of the gel matrices, parallel smooth muscle cell-gel cultures in some experiments were subjected to three cycles of freezing at -80° C and thawing at 37° C prior to radiolabeling. The nonspecific counts were generally less than 5% of those in the live smooth muscle cell-gel cultures.

3.3.5 ³⁵S-Sulfate Incorporation.

Smooth muscle cell-collagen gel cultures were pulse-labeled with ³⁵S-sulfate (25 µCi/ml) to measure glycosaminoglycan synthesis. After radiolabeling, culture media were collected, and gels were washed six times in PBS at 4° C; wash fractions were pooled with the media. Following lyophilization, gels were digested in papain (0.25 mg/ml) at 60° C. Sephadex G-25 M (Pharmacia PD-10) gel-filtration chromatography was performed on gel digests and media/washes to assess the incorporation of ³⁵S-sulfate into macromolecules greater than 1-5 kDa. Samples were dissolved and eluted with 4 mol / L

Guanidine-HCl running buffer. Total ^{35}S -sulfate incorporation (combined gel, media, and wash) was determined for each gel sample by scintillation counting of the macromolecular fractions and adjusting for background cpm.

3.3.6 Total Radiolabel in Gel.

Following pulse-labeling, gels were solubilized in 4 mol / L urea, 0.5 % SDS, and total ^3H -thymidine or ^{35}S -sulfate in aliquots were determined by scintillation counting.

3.3.7 Measurement of Total DNA Content.

Smooth muscle cell-gel cultures were frozen, lyophilized, and digested in 1 ml/gel papain (Sigma, 125 mg/ml) for 24 hours at 60° C. Hoechst 33258 dye solution was added to digest aliquots in an acrylic cuvet, and DNA content was measured fluorometrically, using calf thymus DNA as a standard.¹⁴⁷

3.3.8 Measurement of Glycosaminoglycans.

Smooth muscle cell-gel cultures were frozen, lyophilized, and digested in 1 ml/gel papain (Sigma, 125 mg/ml) for 24 hours at 60° C. Aliquots of gel digests were mixed with dimethylmethylene blue dye in flat-bottom 96-well plates (Nunc), and glycosaminoglycan content was measured spectrophotometrically, using chondroitin-6-sulfate (Sigma) in Vitrogen as a standard.

3.3.9 Statistics.

Data are presented as mean \pm one standard deviation (or \pm one standard error of mean) for n = 3 or 4 measurements. For comparison among several groups of continuous variables, analysis of variance was used. For comparison between specific groups of

continuous variables, the two-sample Student's t test was used. A p value < 0.05 was considered statistically significant.

3.4 Results

3.4.1 Effect of Static Compression on Biosynthesis.

Static compression of vascular smooth muscle cell-collagen gel cultures decreased ³H-thymidine incorporation in a stress-dependent fashion (Figure 3.4). Compression for 24 hr of 0, 0.25, 1.0 and 2.5 kPa stress, respectively, led to incorporations of 1000 ± 220 , 480 ± 200 , 90 ± 10 , and 60 ± 20 cpm/gel (p < 0.05 by ANOVA). Static compression also decreased ³⁵S-sulfate incorporation (Figure 3.5); compression of 0, 0.25, 1.0, and 2.5 kPa stress, respectively, led to incorporations of 460 ± 40 , 230 ± 30 , 200 ± 10 , and 210 ± 30 cpm / gel. Total DNA and glycosaminoglycan in the gel cultures did not change during the 24 hr compressions (data not shown).

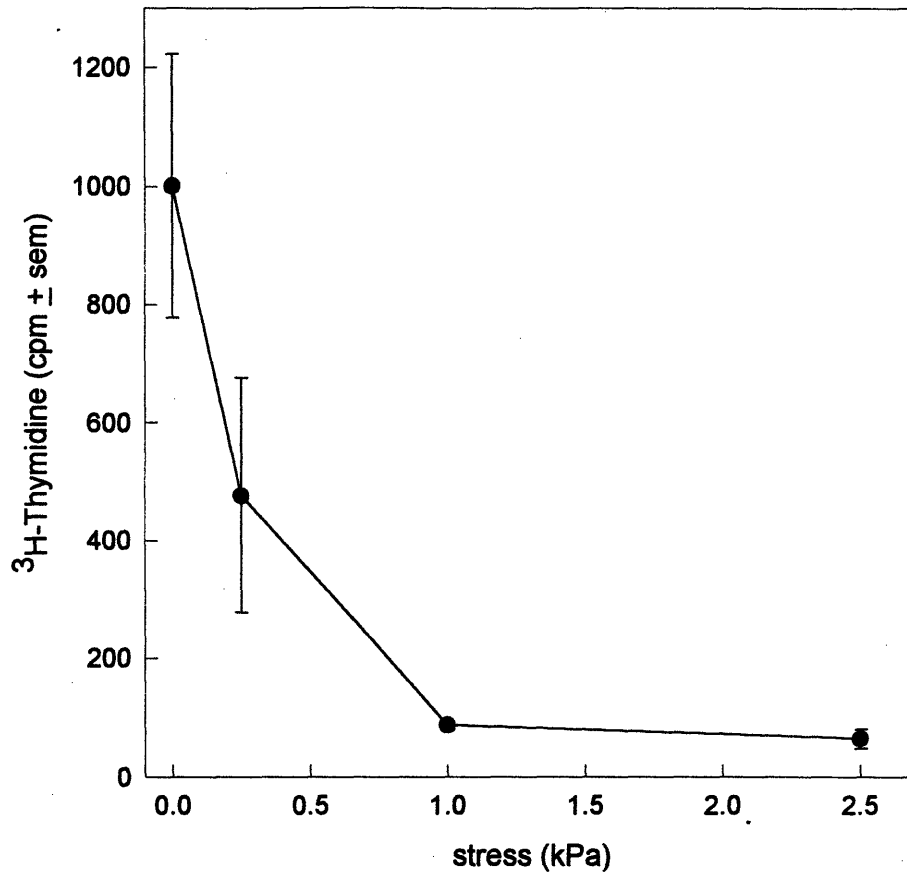


Figure 3.4. ³H-thymidine incorporation by human vascular smooth muscle cells in collagen gel culture during 24 hr static compression (load control). Stress represents the compressive load normalized to the initial gel-platen contact area. Data represent mean ± sem for n=3 or 4.

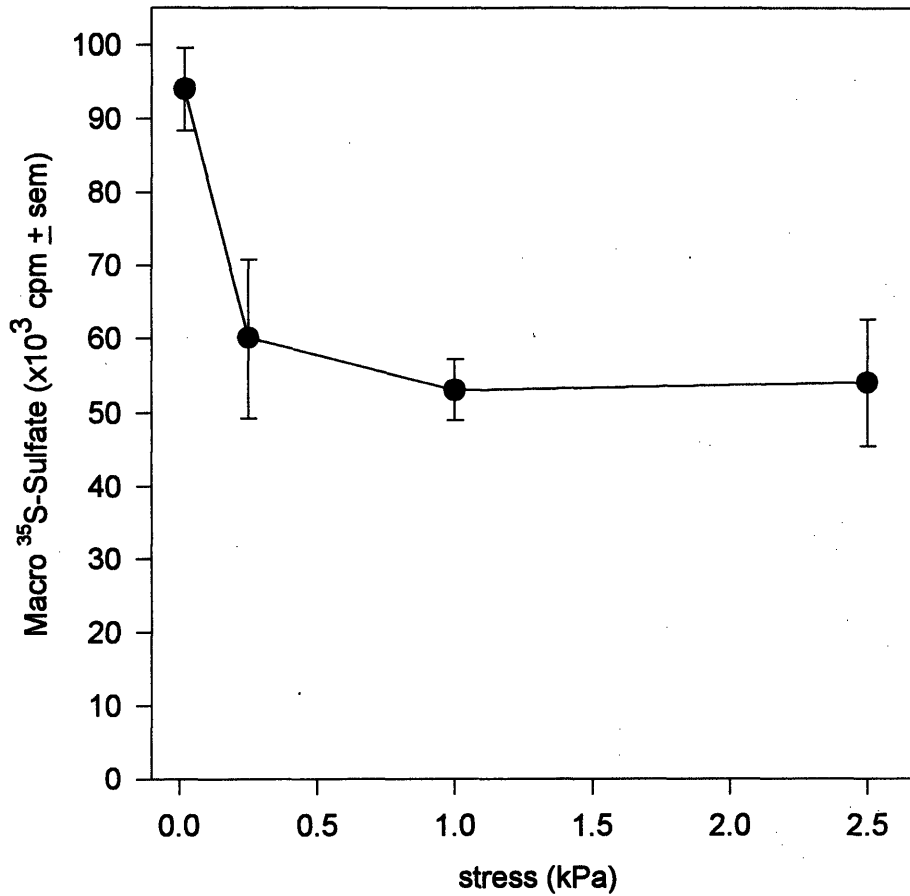


Figure 3.5. ³⁵S-sulfate incorporation by human vascular smooth muscle cells in collagen gel culture during 24 hr static compression. Stress represents the compressive load normalized to the initial gel-platen contact area. Data represent mean ± sem for n=3 or 4.

3.4.2 Diffusion of Thymidine.

To assess whether decreased radiolabel incorporation was caused simply by limited radiolabel diffusion into the compressed gel, total ³H-thymidine in the gel was measured during compression. Although ³H-thymidine equilibrated in the gel within ~ 60 min. after

pulse-labeling, the absolute amount of radiolabel in the gel decreased with the compressive stress (Figure 3.6); after 24 hr of compression at 0, 10, 50, 250, and 1000 Pa, respectively, gels contained 1150 ± 30 , 760 ± 34 , 550 ± 45 , 260 ± 7 , and 250 ± 3 cpm total ^3H -thymidine. A similar experiment was performed to evaluate whether the reduction in total radiolabel in the gel was associated with decreased gel volume; after 24 hr compression, ^3H -thymidine (Figure 3.7A) and gel wet weight (Figure 3.7B) decreased similarly with the applied stress. The effective concentration of radiolabel, estimated as the total gel ^3H -thymidine normalized to the gel wet weight, did not decrease with the compressive stress (Figure 3.8); after 24 hr of compression at 0, 10, 50, 250, and 1000 kPa, respectively, the average total ^3H -thymidine concentration in the gel was 7890, 7880 ± 1350 , 7570 ± 340 , 7090 ± 1980 , and 5780 ± 1200 ($p = \text{NS}$). Thus, gel compression was not associated with decreased radiolabel concentration.

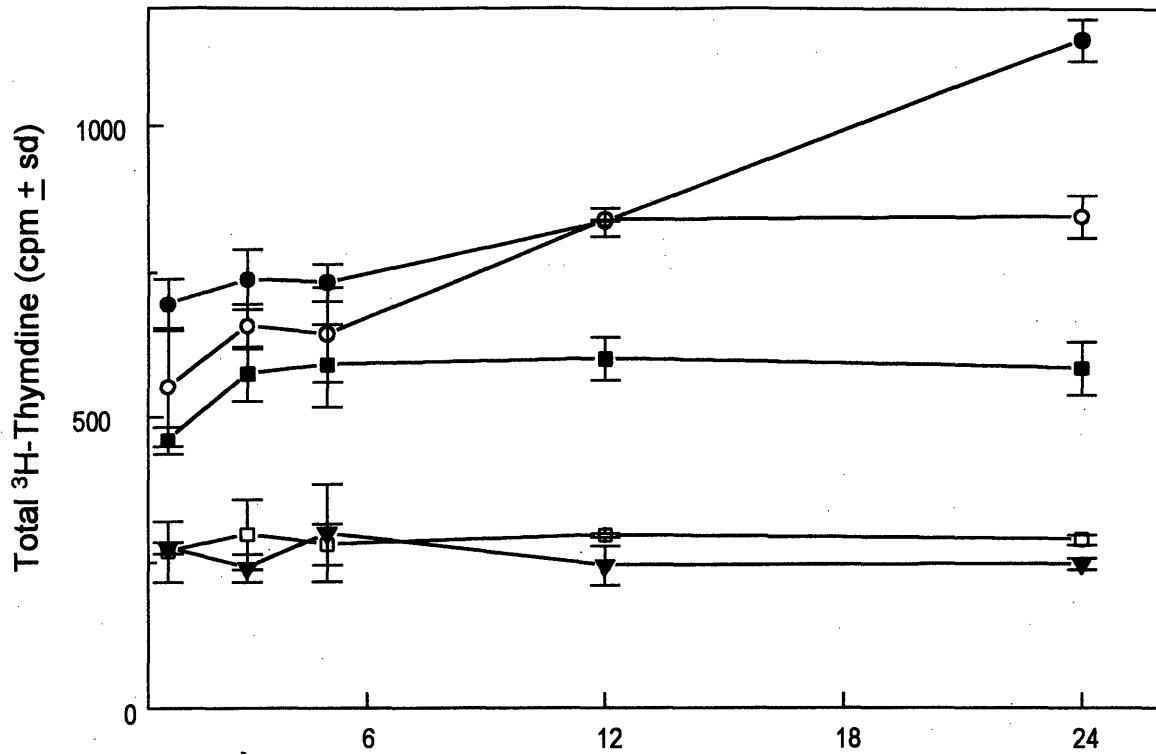


Figure 3.6. Time course of total (incorporated + unincorporated) ³H-thymidine in smooth muscle cell-collagen gel cultures during sustained static compression of 10 (○), 50 (■), 250 (□), and 1000 Pa (▼) stress applied at time 0, relative to control (●). Data represent mean ± sd for n=3.

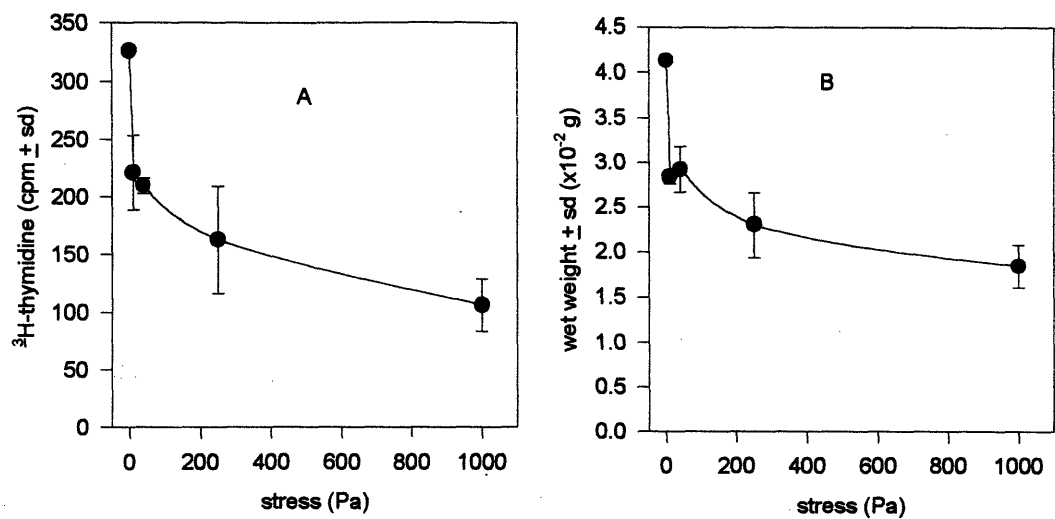


Figure 3.7. (A) Total (incorporated + unincorporated) ^3H -thymidine in smooth muscle cell-collagen gel cultures after 24 hr compression and radiolabeling. (B) Wet weight of the gels after 24 hr compression. Data represent mean \pm sd for n=1 to 3.

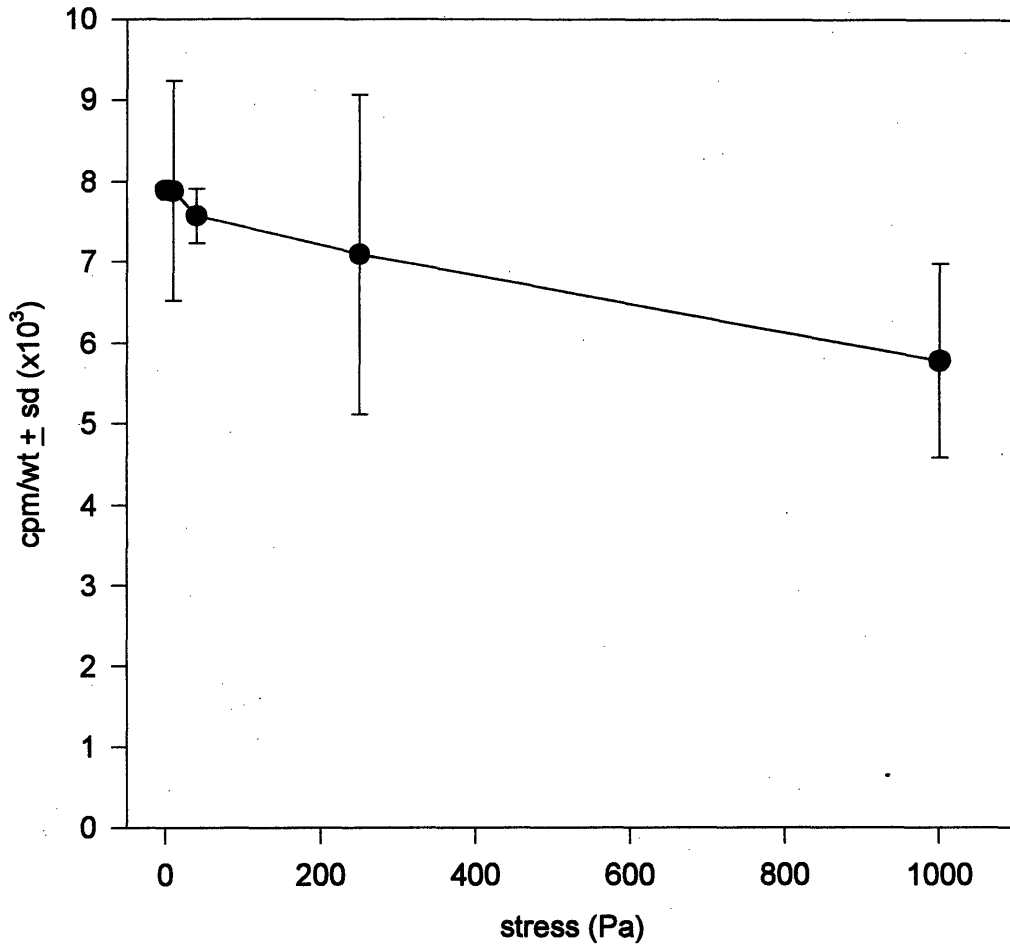


Figure 3.8. Total ^3H -thymidine in gel normalized to gel wet weight after 24 hr static compression and radiolabeling. Data represent mean \pm sd for n=1 to 3.

3.4.3 Dependence of DNA Synthesis on Static Compressive Strain.

The stress (1 kPa) required to completely inhibit DNA synthesis was much lower than normal mean intravascular pressures, but was sufficient to impose large (> 50%) gel

strains. Thus, we assessed the change in DNA synthesis with compression in displacement-control. Compressive strain of 0%, 20%, 27%, 40%, 47%, 60%, and 80%, respectively, led to incorporations of 880 ± 58 , 690 ± 39 , 680 ± 300 , 417 ± 130 , 403 ± 340 , 140 ± 154 , and 130 ± 113 cpm/gel ($p < 0.05$ by ANOVA, Figure 3.8).

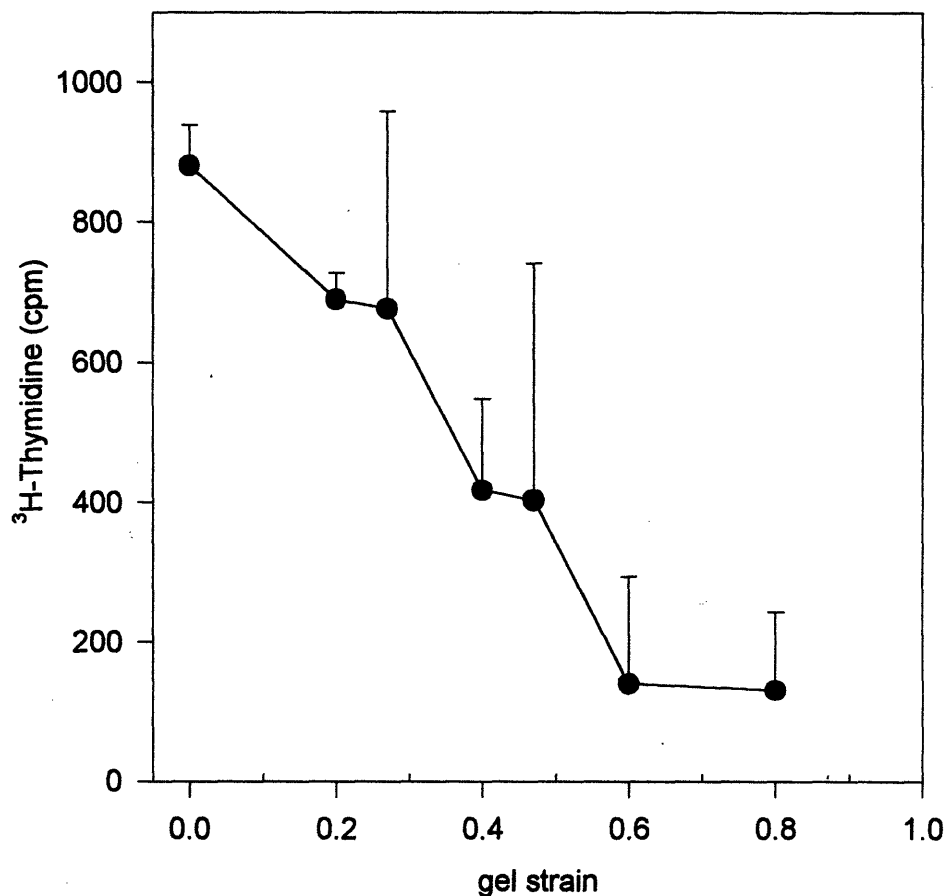


Figure 3.9. ^3H -thymidine incorporation by vascular smooth muscle cell in collagen gel culture during 24 hr static compression (displacement control). Gel strain represents the decrease in gel thickness normalized to the initial thickness. Data represent mean + sd for $n = 3$.

3.4.4 Effect of Release of Compression.

To evaluate whether the compression-induced decrease in biosynthesis was reversible, gel cultures were either compressed and pulse-labeled for 24 hours, or compressed for 24 hours, released from compression, and pulse-labeled for the subsequent 24 hours. Compression decreased ^3H -thymidine incorporation in a strain-dependent manner, and subsequent release of compression caused a delayed increase in thymidine incorporation (data not shown). Additional experiments demonstrated that this delayed DNA synthetic induction could occur in response to a brief compression followed by release of compression.

3.4.5 Effect of Transient Compression on DNA and Glycosaminoglycan Synthesis.

Smooth muscle cell-collagen gel cultures were exposed to a brief compression (5 min, 50% strain) followed by release and then were pulse-labeled with ^3H -thymidine for 24 hours at 0, 24, 48, or 72 hours after compression. Transient compression led to a delayed increase in ^3H -thymidine incorporation (Figure 3.10); at 24 hr after compression, incorporated counts were 800 ± 290 cpm/gel (vs. 750 ± 20 cpm/gel for control, $p = \text{NS}$); at 48 hr, there were 3000 ± 620 cpm/gel (vs. 990 ± 100 cpm/gel for control, $p < 0.005$); at 72 hr, there were 340 ± 90 cpm/gel (vs. 340 ± 10 cpm/gel for control, $p = \text{NS}$); and at 96 hr, there were 310 ± 140 cpm/gel (vs. 240 ± 20 cpm/gel for control, $p = \text{NS}$). However, transient compression led to a parallel decrease in ^{35}S -sulfate incorporation (Figure 3.11); at 24 hr after compression, incorporated counts were 520 ± 40 cpm/gel (vs. 500 ± 90 cpm/gel for control, $p = \text{NS}$); at 48 hr, counts were 400 ± 50 cpm/gel (vs. 450 ± 30 cpm/gel for control, $p = \text{NS}$); at 72 hr, counts were 350 ± 30 cpm/gel (vs. 430 ± 20 for

control, $p < 0.005$); at 96 hr, counts were 230 ± 20 cpm/gel (vs. 350 ± 20 for control, $p < 0.001$).

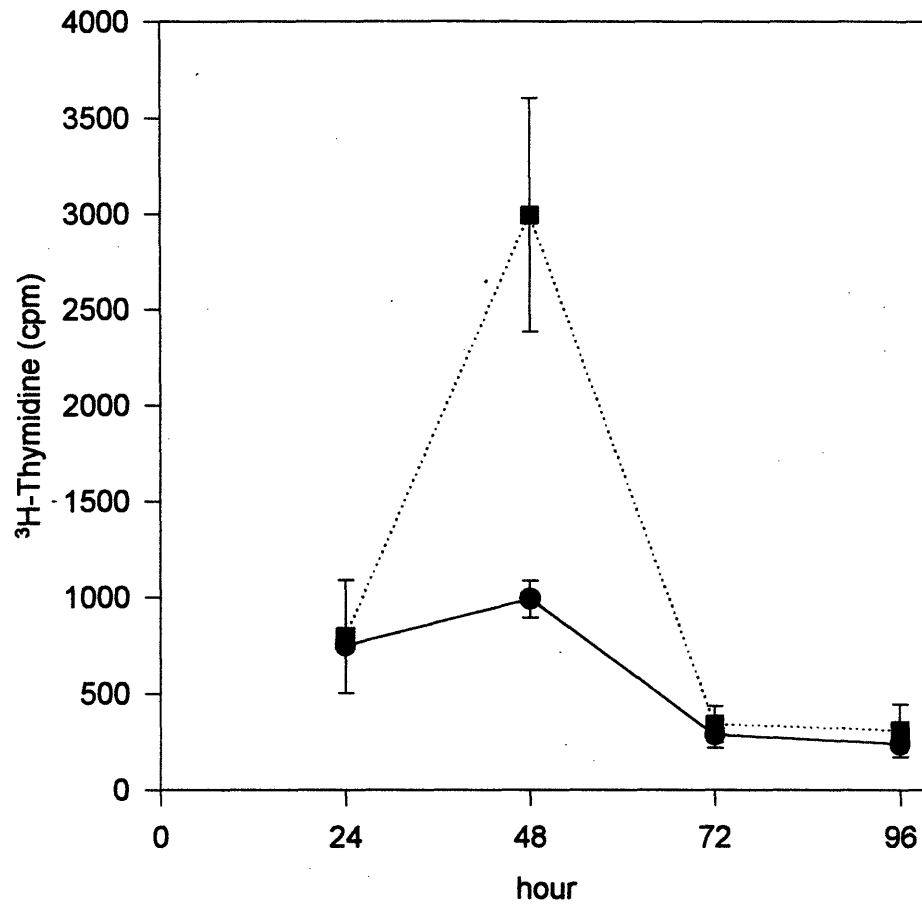


Figure 3.10. Time course of ³H-thymidine incorporation by vascular smooth muscle cells in collagen gel culture after a transient (5 min, 0.50 strain) compression and release of compression at time 0 (■), relative to unloaded control (●). Data represent mean \pm sd for $n=3$.

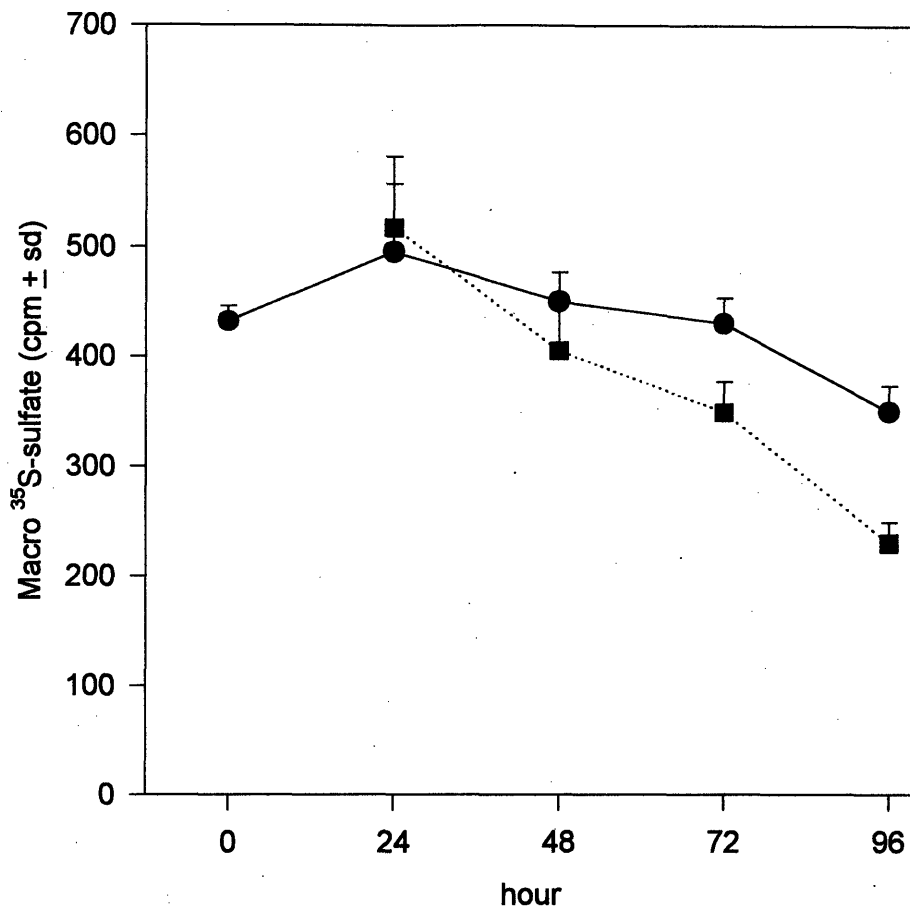


Figure 3.11. Time course of ³⁵S-sulfate incorporation by vascular smooth muscle cells in collagen gel culture after a transient (5 min, 0.50 strain) compression at time 0 (■), relative to unloaded control (●). Data represent mean ± sd for n = 4.

3.5 Discussion

Mechanical loading of vascular smooth muscle cells in a two-dimensional monolayer configuration has been shown previously to control proliferation and matrix synthesis. In this chapter, the effect of mechanical compression on smooth muscle cell DNA and glycosaminoglycan synthesis was evaluated in a three-dimensional collagen

lattice. Sustained, static uniaxial and unconfined compression decreased both DNA and glycosaminoglycan synthesis in a stress-dependent manner. Total radiolabel in the gel decreased with the compressive stress, but the equilibrium intra-gel radiolabel concentration did not decrease with stress, suggesting that incorporation was not limited by radiolabel access. Decreased ^3H -thymidine incorporation was reversed after release of 24 hr compression, and a brief transient compression caused a delayed increase in ^3H -thymidine incorporation but decreased ^{35}S -sulfate incorporation.

Because biosynthesis was maximally inhibited by a low magnitude of stress (~ 1 kPa) relative to typical mean intravascular pressure, it was hypothesized that decreased DNA synthesis was coupled to the gel deformation rather than to the absolute applied force. When the displacement rather than load was controlled, DNA synthesis decreased relatively linearly with the imposed compressive gel strain. These observations suggest that cells respond to their own deformation rather than to the absolute stress applied to the bulk tissue. As discussed in Chapter 1, cellular deformation is a function not only of the applied load, but also of the ensemble material compliances. Thus, vascular smooth muscle cells in the very compliant gel matrix may be more responsive to a given applied stress than the same cells would be in a stiffer matrix, such as in the blood vessel. This model may also suggest that decreased vascular compliance associated with hypertension is a compensatory mechanism to maintain smooth muscle cell strain.

Whether cells respond to their own deformation or to an applied bulk stress might be directly tested experimentally by constituting gel cultures of varying mechanical compliance (by altering the concentration of Vitrogen 100, for example), and comparing their biological responses to both controlled-load and -displacement compression;

however, such an experiment might be difficult to interpret given that the matrix composition itself can regulate cellular function. Indeed, given the reduction in gel volume under static compression, one mechanism for decreased biosynthesis may be increased matrix concentration. For several additional reasons, the three-dimensional gel culture is not ideal for performing experiments to dissect the specific role of cellular strain in mechanical responses. These issues and related experiments are presented in Chapters 5 and 6.

For now, additional questions remain concerning the biological mechanisms underlying the responses presented in this chapter. For example, the extent to which cells were injured by compression is unknown. Although total DNA content remained constant, decreased biosynthesis during static compression might be consistent with sublethal cell injury. In addition, the mechanism for increased DNA synthesis during release of compression was not characterized, but could involve intracrine pathways, autocrine/paracrine pathways, or a combination of both. The induction of DNA synthesis was accompanied by a decrease in glycosaminoglycan synthesis, suggesting a specific response rather than a generalized change in metabolic activity. In the next chapter, the mechanism for DNA synthetic induction by transient compression is further characterized.

Characterization of DNA Synthetic Induction by Transient Compression

4.1 Abstract

Although mechanical vascular injury leads to smooth muscle cell proliferation that contributes to restenosis following balloon angioplasty, the role of the single transient mechanical stimulation of smooth muscle cells in this process is unknown. In this chapter, the DNA synthetic response to transient compression, described in Chapter 3, was further characterized. Transient compression (5 min duration) of smooth muscle cell-collagen gel cultures in defined serum-free conditions led to delayed increases in ^3H -thymidine incorporation. At 12-24 hours after compression, there was a 3.3 ± 0.5 ($p < 0.001$ vs. control) and 3.0 ± 0.6 ($p < 0.002$ vs. control) fold increase for 60% and 80% strain, respectively; at 24-36 hours after compression there was a 1.8 ± 0.5 ($p < 0.05$ vs. control) and 4.3 ± 0.8 ($p < 0.001$ vs. control) fold increase. Additionally, serum-free media conditioned by transiently compressed gel cultures induced DNA synthesis in control, unstimulated smooth muscle cell cultures, suggesting the release of growth factors by transient compression. Although neutralizing antibodies against platelet-derived growth factor (PDGF) did not affect the mechanical induction of DNA synthesis, a neutralizing monoclonal antibody against fibroblast growth factor-2 (FGF-2) decreased this induction by 89% and completely blocked the increase in DNA synthesis caused by media conditioned by transiently compressed gels. Media conditioned by transient compression

contained elevated levels of FGF-2 (17 ± 5 pg/ml vs. 2 ± 2 pg/ml for control, $p < 0.005$) with no increase in lactate dehydrogenase activity, suggesting release of FGF-2 with sublethal cellular injury. Thus, a single transient mechanical stimulus increases DNA synthesis in human vascular smooth muscle cells, in part by autocrine or paracrine FGF-2 release.

4.2 Introduction

Although percutaneous transluminal coronary angioplasty is widely used in the treatment of coronary atheroma, the success of this procedure is often limited by late restenosis. Within months following angioplasty, 20% - 40% of patients develop recurrent neointimal lesions consisting of abundant extracellular matrix and hyperplastic vascular smooth muscle cells.¹⁴⁸ A cascade of pathways involving vascular smooth muscle cells, endothelial cells, platelets, and macrophages may mediate neointimal growth through cytokines and growth factors.¹⁴⁸ The vascular responses to the direct mechanical strain of balloon angioplasty, as well as to acute local thrombosis, may be important early events in this cascade.

Mechanical forces may influence biological responses through various signal transduction mechanisms to alter structure and function at the cellular and molecular level.^{54,82,149} Vascular smooth muscle cells *in vivo* undergo dynamic and static mechanical strains from superimposed pulsatile and mean pressure loads of the cardiac cycle, and these strains may be altered in pathological conditions such as hypertension.^{71,74,132,150} Several *in vitro* studies have assessed potential biologic responses of vascular smooth muscle cells to physiologically relevant mechanical conditions. For example, dynamic

mechanical strain can modulate cellular orientation,^{69,70} matrix synthesis,^{68,73} and proliferation^{70-72,151} of cultured vascular smooth muscle cells, and continuous static strain increases proto-oncogene expression and phosphoinositide turnover.¹⁵¹

During balloon angioplasty, smooth muscle cells and other vascular cells are exposed to a transient mechanical strain of relatively large magnitude, as the vessel is dilated briefly and then allowed to relax. *In vivo* studies of balloon injury demonstrate intimal smooth muscle cell hyperplasia caused both by migration from the media and increased proliferation,^{43,152} and these processes may be mediated by platelet-derived growth factor (PDGF) and fibroblast growth factor-2 (FGF-2). PDGF is both a mitogen and a chemoattractant for vascular smooth muscle cells,⁴² which may be synthesized and released by platelets, smooth muscle cells, and endothelial cells.¹⁵³ In animal models, vascular injury induces expression of mRNA for the PDGF-A chain and also the PDGF receptor- α and - β subunits in the neointima.^{154,155} Additionally, intimal thickening induced by injury can be inhibited by a polyclonal antibody against PDGF.¹⁵⁶ Under some conditions, PDGF can be mechanically induced in cultured vascular smooth muscle cells.⁷¹

FGF-2, also known as basic fibroblast growth factor, may be essential for the early smooth muscle cell proliferative response in injured rat arteries. Like PDGF, FGF-2 is mitogenic and chemotactic for vascular smooth muscle cells *in vitro* and can be synthesized by both vascular smooth muscle cells and endothelial cells.^{157,158} This growth factor lacks a signal sequence for classical secretion,¹⁵⁹ and may be released upon cell injury.¹⁶⁰⁻¹⁶² In rat arteries, injury-induced smooth muscle cell proliferation is significantly greater with combined injury to endothelial and smooth muscle cells than with endothelial

denudation alone,¹⁶³ can be inhibited by a neutralizing antibody against FGF-2,¹⁶⁴ and does not require circulating platelets.¹⁶⁵ In addition, balloon injury leads to increased expression of mRNA for both FGF-2 and its receptor by smooth muscle cells and endothelial cells.¹⁶⁶

Although animal models of restenosis have revealed potential mechanisms of smooth muscle cell proliferation, they have not readily dissected the specific role of the transient mechanical strain on smooth muscle cell responses. This study was designed to test the hypothesis that a single transient mechanical strain can induce DNA synthesis in human vascular smooth muscle cells, potentially mediated by autocrine growth factors.

4.3 Materials and Methods

4.3.1 Cell Culture.

Human vascular smooth muscle cells were derived from explants of discarded portions of saphenous veins obtained during coronary bypass surgery performed at Brigham and Women's Hospital. Monolayer smooth muscle cells were cultured in Dulbecco's Modified Eagle Medium (DMEM) (Whittaker Bioproducts, Inc.) with 10% fetal calf serum (FCS), at 37° C and 5% CO₂. These conditions are selective for growth of smooth muscle cells over endothelial cells.¹⁴³ The explant and culture technique was identical to the protocol used in previous studies of cultured vascular smooth muscle cells.^{39,144,145} Cells were cultured through passages 3 - 5 prior to transfer to a three-dimensional collagen gel culture system for use in transient compression experiments.

Cell culture in hydrated collagen gels was performed with Vitrogen 100 collagen (Celtrix Pharmaceutical) as previously described.¹⁴⁶ Cells ($2.5 - 3.0 \times 10^5$) were

suspended in 1.25 ml collagen (2.8 mg/ml) and cultured in standard 24-well (16 mm diameter) culture plates (Costar Corporation). Gel cultures were maintained in DMEM supplemented with 10% FCS and 0.07 mmol / L ascorbate-2-phosphate (Wako Pure Chemical Industries) and received a change of culture medium every two days. The contraction of collagen gel matrices by these cells may be resisted by local adhesions to the culture plate wells; thus, to facilitate uniform, axisymmetric gel contraction, on day 5 the gel cultures were gently detached from the sides of the wells. Over the course of 10 days in culture, smooth muscle cell-gels contracted uniformly to disks with nearly identical dimensions in a given experiment; the standard deviation of gel thickness, measured by micrometer prior to compression, was less than 5% of the mean. Final contracted gel diameter ranged from 4.5 - 7.0 mm, and thickness ranged from 1.0 - 2.5 mm in different experiments.

4.3.2 Mechanical Compression.

Smooth muscle cell-gel cultures received a final media change on day 10 and were subjected to a uniaxial, unconfined, transient compression consisting of a brief fixed-displacement static compression, followed by release of compression. For serum-free conditions, smooth muscle cell-gels were washed six times on day 9 with defined, serum-free IT medium (equal volumes of DMEM and Ham's F-12 supplemented with 1 μ M insulin and 5 μ g/ml transferrin) at 37° C and further incubated for 24 hours in this medium prior to the transient compression. The compression apparatus consisted of a base to hold the culture plate and a rigid top compression plate (Figure 4.1). Compression platens and spacer posts, machined from autoclavable polysulfone rod stock (Patriot Plastics & Supply, Inc.) to a uniform length (19.05 mm), were affixed to this top plate and

concentrically aligned with culture plate wells. By lowering the top plate assembly, static compression was applied to the gels by the compression platens at a desired strain determined by the thickness of Teflon disks positioned beneath the spacer posts within vacant adjacent wells; this imposed strain ranged from 50 - 80% of the initial gel thickness in all experiments. For most experiments, a moderate strain of 50-65% was used; the 80% strain was used for evaluating the effect of higher amplitudes of initial strain. The duration of transient compression ranged from 0.2 - 5.0 minutes; by 2 hours after removal of compression, the gels were observed to reswell to a state of <10% strain. Parallel control smooth muscle cell-gels were not compressed but were otherwise handled in identical fashions.

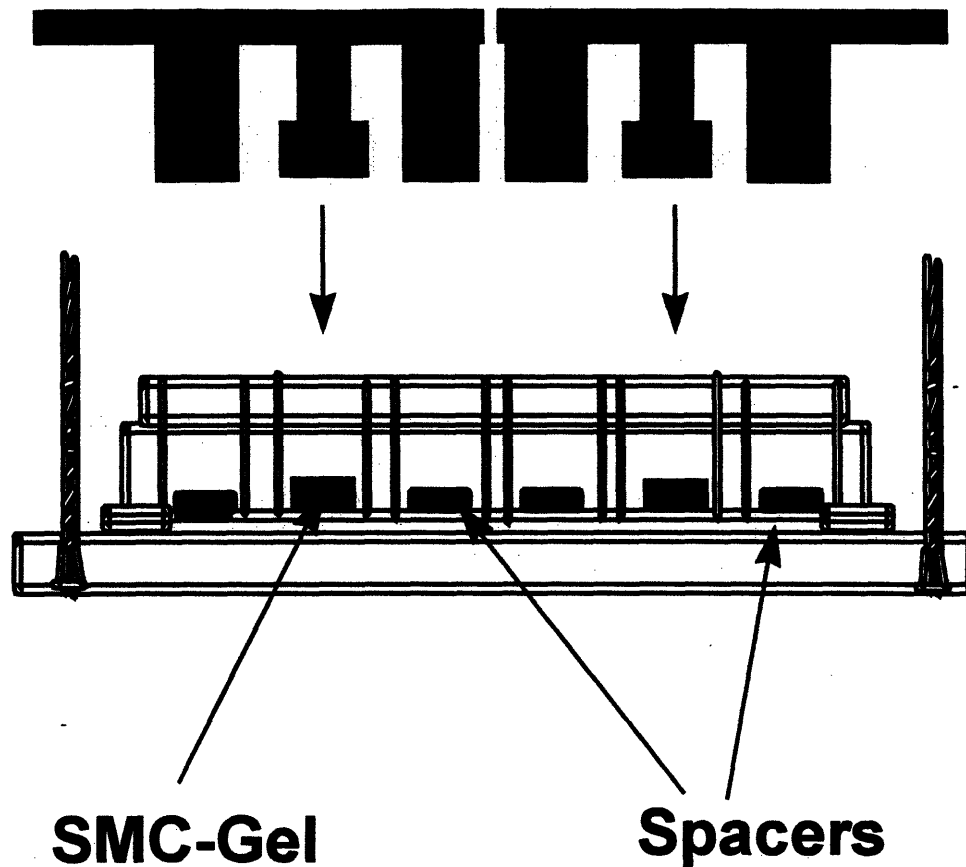


Figure 4.1 Diagram of apparatus used to apply transient mechanical compression to three dimensional vascular smooth muscle cell cultures (SMC-Gel). A Compression Plate was lowered on to the gel cultures, and strain was limited by Teflon disks. After a brief period (usually 5 min), the Compression Plate was removed.

4.3.3 ³H-Thymidine Incorporation.

Following compression, culture media were supplemented with methyl-[³H]-thymidine, 6.7 mCi / mmol, (Dupont-NEN) to measure DNA synthesis. To assess time course, designated smooth muscle cell-gels were radiolabeled during consecutive 12-hour periods; additional control gels were radiolabeled during the 12 hours preceding the transient compression and served as an initial baseline. Following radiolabeling, smooth

muscle cell-gel matrices were solubilized overnight in 4 M urea, 0.5% sodium dodecyl sulfate, and precipitated with 10% trichloroacetic acid at 4° C. Precipitates were vacuum-collected on 0.45 µm filters (Millipore Corp.) and washed with 10% trichloroacetic acid at 4° C. Filters were air-dried, mixed with Ecolume (ICN Biomedicals) scintillation cocktail, and counted with a scintillation counter (Pharmacia LKB Nuclear). To assess nonspecific radiolabeling of the gel matrices, parallel smooth muscle cell-gel cultures in some experiments were subjected to three cycles of freezing at -80° C and thawing at 37° C prior to radiolabeling. The nonspecific counts were generally less than 5% of those in the live smooth muscle cell-gel cultures.

4.3.4 Conditioned-Media Experiments.

To test the hypothesis that transient compression of the smooth muscle cell-gel cultures triggers release of mitogens from the cells, conditioned-media experiments were performed. Smooth muscle cell-gel cultures were either compressed for 5 minutes (60% strain) or were not compressed, and then further incubated for 24 hours. Culture media were then exchanged between the two groups and supplemented with 4 µCi/ml methyl-³H]-thymidine for 24 hours of radiolabeling. Uncompressed control gels were incubated for 24 hours, and the media were removed and immediately returned to the identical wells prior to radiolabeling.

4.3.5 Antibody Neutralization Experiments.

Smooth muscle cell-gel cultures, made quiescent under defined serum-free conditions as described above, were subjected to transient compression (60% strain, 5 min). In separate experiments, neutralizing polyclonal rabbit antibodies against either

human PDGF-A (10 µg/ml) or PDGF-B (5 µg/ml) (Genzyme Corporation) chain were added to designated culture media immediately following release of compression, and the gel cultures were further incubated for either 12 or 24 hours. Media were then supplemented with 4 µCi methyl-[³H]-thymidine for 12 hours of radiolabeling. For positive controls, exogenous recombinant human PDGF-AA (2 ng/ml) or PDGF-BB (4 ng/ml) (Genzyme Corporation) was added to the culture media of control (unstimulated) smooth muscle cell-gels either in the presence or absence of the appropriate neutralizing anti-PDGF antibody.

In similar experiments, we assessed the ability of a neutralizing monoclonal antibody against human FGF-2 (0.1, 1.0, or 10 µg/ml, Upstate Biotechnology Inc.) to inhibit the induction of ³H-thymidine incorporation by transient compression (65% strain, 5 minutes). A non-immune mouse IgG antibody (10 µg/ml, Sigma) was added to parallel cultures to assess the specificity of the anti-FGF-2 antibody. As a positive control, exogenous human recombinant FGF-2 (10 ng/ml, Upstate Biotechnology Inc.) was added to the culture media of control smooth muscle cell-gels either in the presence or absence of the anti-FGF-2 antibody.

4.3.6 Measurement of FGF-2 and Lactate Dehydrogenase Activity.

Serum-free media conditioned for 12 hours by transiently compressed and control gels were harvested and assayed for FGF-2 with a quantitative enzyme immunoassay (R&D Systems, Quantikine Human FGF basic Immunoassay). To assess cell injury, lactate dehydrogenase (LDH) activity in the media was measured with a quantitative, colorimetric assay (Sigma). The lower limit sensitivity of this assay was 40 units/ml.

Parallel media, conditioned by gel cultures subjected to three cycles of freeze-thaw, were used as positive controls.

4.3.7 Measurement of Total DNA Content.

To further assess cell injury, total DNA in smooth muscle cell-gel cultures was measured at 12 hours following transient compression (65%) and compared with that in uncompressed gel cultures. Smooth muscle cell-gel cultures were frozen, lyophilized, and digested in 1 ml/gel papain (Sigma, 125 mg/ml) for 24 hours at 60° C. Hoechst 33258 dye solution was added to digest aliquots in an acrylic cuvet, and DNA content was measured fluorometrically, using calf thymus DNA as a standard.¹⁴⁷

4.3.8 Measurement of FGF-2 mRNA.

Total cellular RNA in smooth muscle cell-gel cultures was isolated by guanidine isothiocyanate extraction at 0, 0.5, 1, 2, 3, and 12 hours following compression; RNA extracted from smooth muscle cells treated for 30 min. with either IL-1 or 10% fetal calf serum was used as positive controls. Total RNA (7.5 µg) of each sample was electrophoresed in the presence of ethidium bromide on 1.4% agarose gels containing formaldehyde and transferred to nylon hybridization membranes. Blots were photographed under UV illumination to verify evenness of loading and transfer, UV immobilized, and then hybridized to a 1.2 kb cDNA probe (gift of Prof. M. Klagsbrun, Children's Hospital, Boston) for FGF-2 which was labeled with ³²P-dCTP using the random primers method. Blots were washed and autoradiographed with x-ray film for 3 days at -80° C.

4.3.9 Statistics.

All data are presented as mean \pm one standard deviation for $n = 3$ or 4 measurements. For comparison between specific groups of continuous variables, the two-sample Student's *t* test was used. A p value < 0.05 was considered statistically significant.

The findings reported below are representative of results of at least two independent experiments.

4.4 Results

4.4.1 DNA Synthesis Following Transient Strain.

In serum-supplemented conditions, transient compression (5 min) led to an increase in ^3H -thymidine incorporation by vascular smooth muscle cells in collagen gels, following an initial period of decreased incorporation (Figure 4.2). From 12 to 24 hours after release of compression of 60% or 80% strain, there were no differences in ^3H -thymidine incorporation relative to control; from 24 to 36 hours, there was a 1.6 ± 0.4 ($p < 0.05$ vs. control) and a 2.4 ± 0.6 ($p < 0.005$ vs. control) fold increase in ^3H -thymidine incorporation for 60% and 80% strain, respectively.

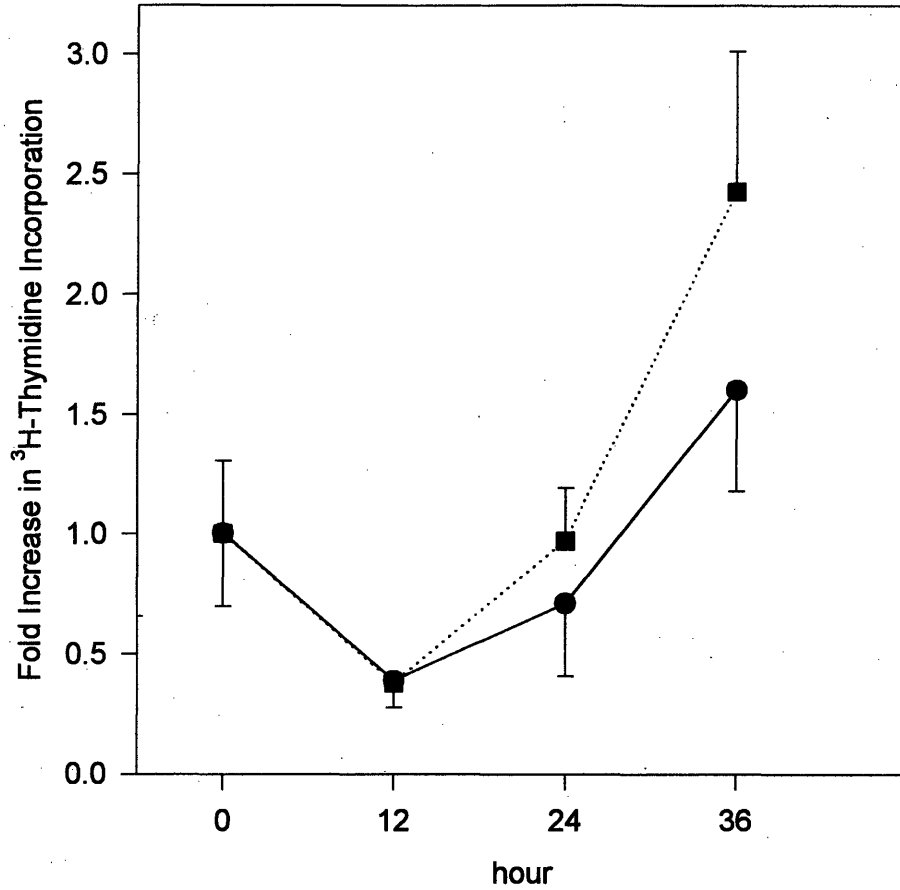


Figure 4.2. Increase in ^3H -thymidine incorporation by human vascular smooth muscle cells following a 5 min compression at time 0 in the presence of 10% fetal calf serum at strains of 60% (●) or 80% (■). Control 12-hour incorporated counts were 710 ± 220 , 560 ± 210 , 1290 ± 207 , and 930 ± 140 cpm, at 0, 12, 24, and 36 hours following compression. $n = 3$ or 4 for each measurement, error bars denote one standard deviation.

Exogenous serum-associated growth factors were not required for the mechanical induction of DNA synthesis. In defined serum-free medium, transient compression of gel cultures again led to a delayed increase in ^3H -thymidine incorporation (Figure 4.3). From

12 to 24 hours after release of compression, there was a 3.3 ± 0.5 ($p < 0.001$ vs. control) and 3.0 ± 0.6 ($p < 0.002$ vs. control) fold increase in ^3H -thymidine incorporation for 60% or 80% strain, respectively; from 24 to 36 hours, there was a 1.8 ± 0.5 ($p < 0.05$ vs. control) and a 4.3 ± 0.8 ($p < 0.001$ vs. control) fold increase in ^3H -thymidine incorporation for 60% and 80% strain, respectively. Cumulative incorporated counts during the 36-hour period following compression were 1670 ± 120 , 2730 ± 440 , and 3960 ± 470 cpm, for 0%, 60%, and 80% compressions, respectively ($p < 0.001$ by analysis of variance). Maximum inductions of ^3H -thymidine incorporation by strains of 60-65% in different experiments ranged from 1.6 to 3.0-fold in the presence of serum (five experiments), and from 1.8 to 10-fold in the absence of serum (seven experiments).

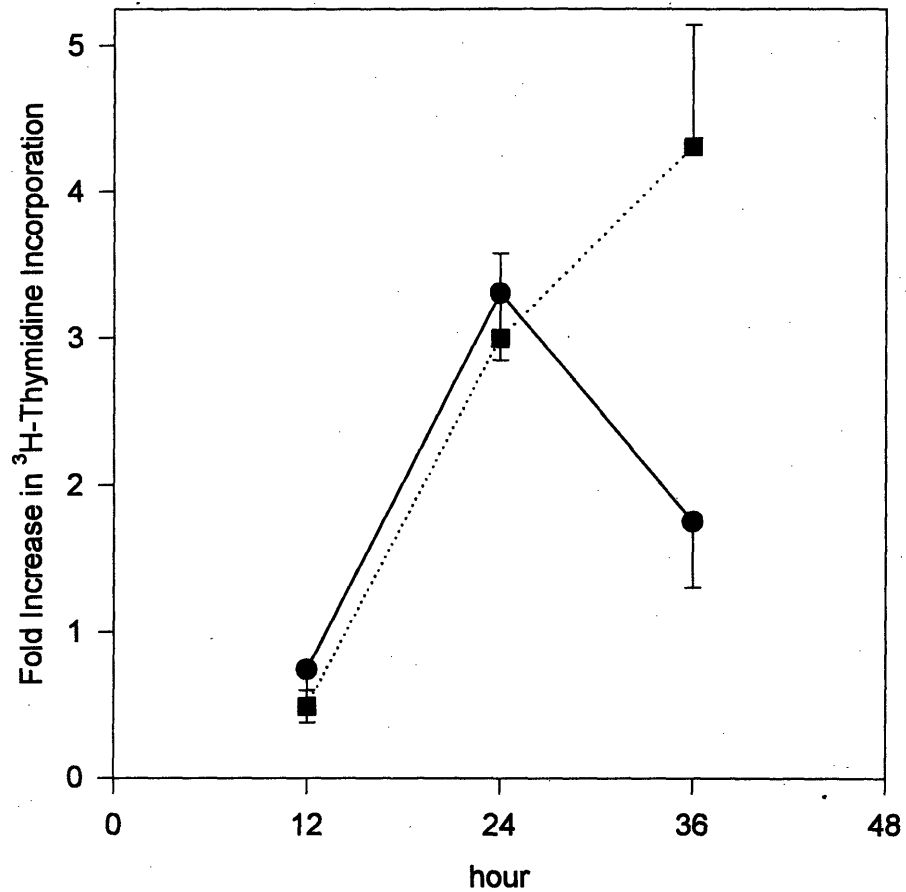


Figure 4.3. Increase in ^3H -thymidine incorporation by human vascular smooth muscle cells following a 5 min compression at time 0 in defined serum-free conditions at strains of 60% (●) or 80% (■). Control 12-hour incorporated counts were 730 ± 200 , 350 ± 70 , and 590 ± 120 cpm, at 12, 24, and 36 hours following compression. $n = 4$ for each measurement, error bars denote one standard deviation.

To minimize potential effects of exogenous mitogens and other serum constituents, further characterization of this induction of ^3H -thymidine incorporation was performed under serum-free conditions. Defined serum-free media conditioned for 12 hours by

transiently compressed gels increased ^3H -thymidine incorporation in target control (unstimulated) gels by 2.5 ± 0.5 fold over control media ($p < 0.005$). Conversely, transiently compressed gels whose media were replaced with control media demonstrated no induction in DNA synthesis. These data suggested the release of autocrine growth factor(s) by transient compression of the smooth muscle cell-gels.

4.4.2 Autocrine Growth Factor Studies.

Antibody neutralization experiments were performed under serum-free conditions to study the possible role of specific endogenous growth factors. Neutralizing antibodies against either PDGF-A (Figure 4.4A) or PDGF-B (Figure 4.4B) chain did not inhibit induction of ^3H -thymidine incorporation by transient compression. In parallel control experiments, neutralizing antibodies to PDGF were able to block the induction of ^3H -thymidine incorporation by the appropriate exogenous PDGF homodimers. However, a monoclonal anti-FGF-2 neutralizing antibody inhibited strain-induced ^3H -thymidine incorporation in a dose-dependent manner, achieving 89% inhibition ($p < 0.01$ vs. compressed) at $10 \mu\text{g/ml}$ (Figure 4.5), while the non-immune IgG antibody at that concentration had no effect. In control experiments, the monoclonal anti-FGF-2 antibody also completely blocked the induction of ^3H -thymidine incorporation by exogenous FGF-2. Although nearly complete inhibition of compression-induced ^3H -thymidine incorporation was achieved in this experiment, inhibition by the monoclonal anti-FGF-2 antibody ($10 \mu\text{g/ml}$) ranged from 65-89% in four independent experiments using a strain of 60 - 65%. Additionally, compression-conditioned media significantly induced ^3H -thymidine incorporation in target gel cultures by 1.7 ± 0.2 fold over control-conditioned

media ($p < 0.001$), and this induction was completely blocked by the monoclonal anti-FGF-2 antibody (Figure 4.6).

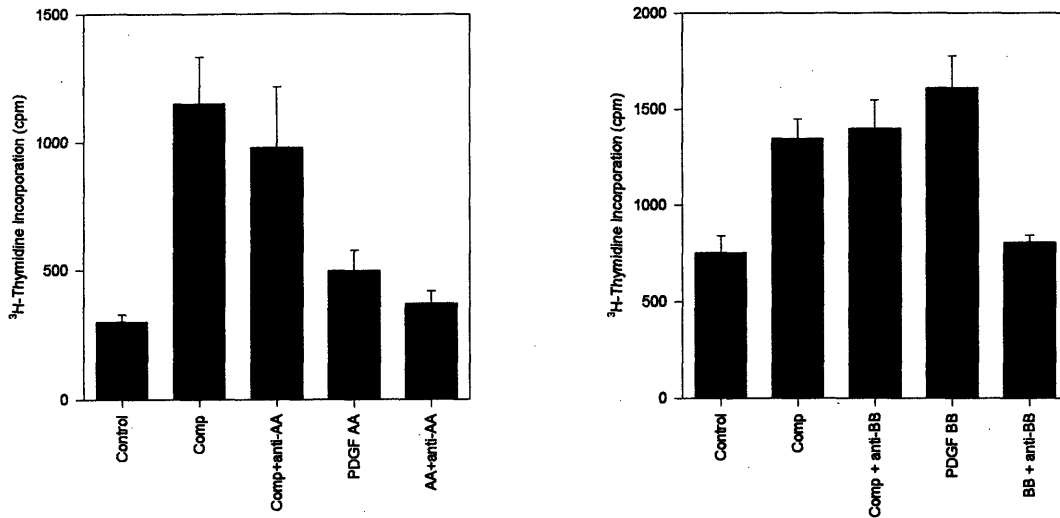


Figure 4.4. ³H-thymidine incorporation by human vascular smooth muscle cells 12-24 hr following a 5 min, 60% compression (Comp) in serum-free conditions. Control cell-gels received no stimulation. (A) Addition of a neutralizing polyclonal antibody to PDGF-A immediately following compression (Comp+anti-AA) did not inhibit the effect of transient compression (Comp) ($p = ns$). Addition of PDGF-AA in the absence of compression led to an increase in ³H-thymidine incorporation (PDGF-AA) that was inhibited by the polyclonal antibody (AA+anti-AA). (B) Addition of a neutralizing polyclonal antibody to PDGF-B immediately following compression (Comp+anti-BB) did not inhibit the effect of transient compression (Comp) ($p = ns$). Addition of PDGF-BB in the absence of compression led to an increase in ³H-thymidine incorporation (PDGF-BB) that was inhibited by the polyclonal antibody (BB+anti-BB). $n = 3$ or 4 for each measurement, error bars denote one standard deviation.

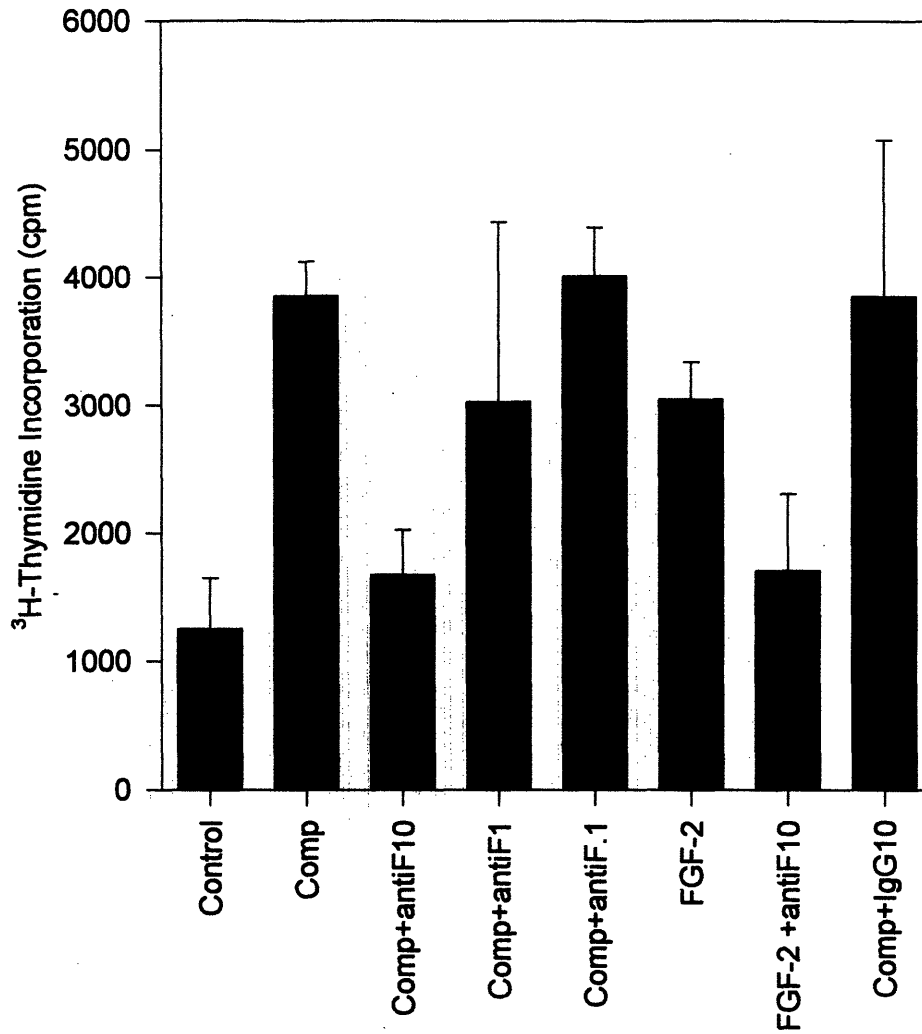


Figure 4.5. ³H-thymidine incorporation by human vascular smooth muscle cells 12-24 hr following a 5 min, 65% compression (Comp) in serum-free conditions. Control cell-gels received no stimulation. The effect of transient compression was inhibited by a neutralizing monoclonal antibody to FGF-2 (10 μg/ml, $p < 0.005$) added immediately following compression (Comp+antiF10), but was unaffected by a mouse non-immune IgG (10 μg/ml) (Comp+IgG10). Nonsignificant inhibitory effects of lower concentrations of antibody to FGF-2 are shown (comp+antiF1, 1 μg/ml; comp+antiF.1, 0.1 μg/ml). Addition of FGF-2 in the absence of compression led to an increase in ³H-thymidine incorporation (FGF-2) that was inhibited by the monoclonal antibody (FGF-2+anti-F10). $n = 3$ or 4 for each measurement, error bars denote one standard deviation.

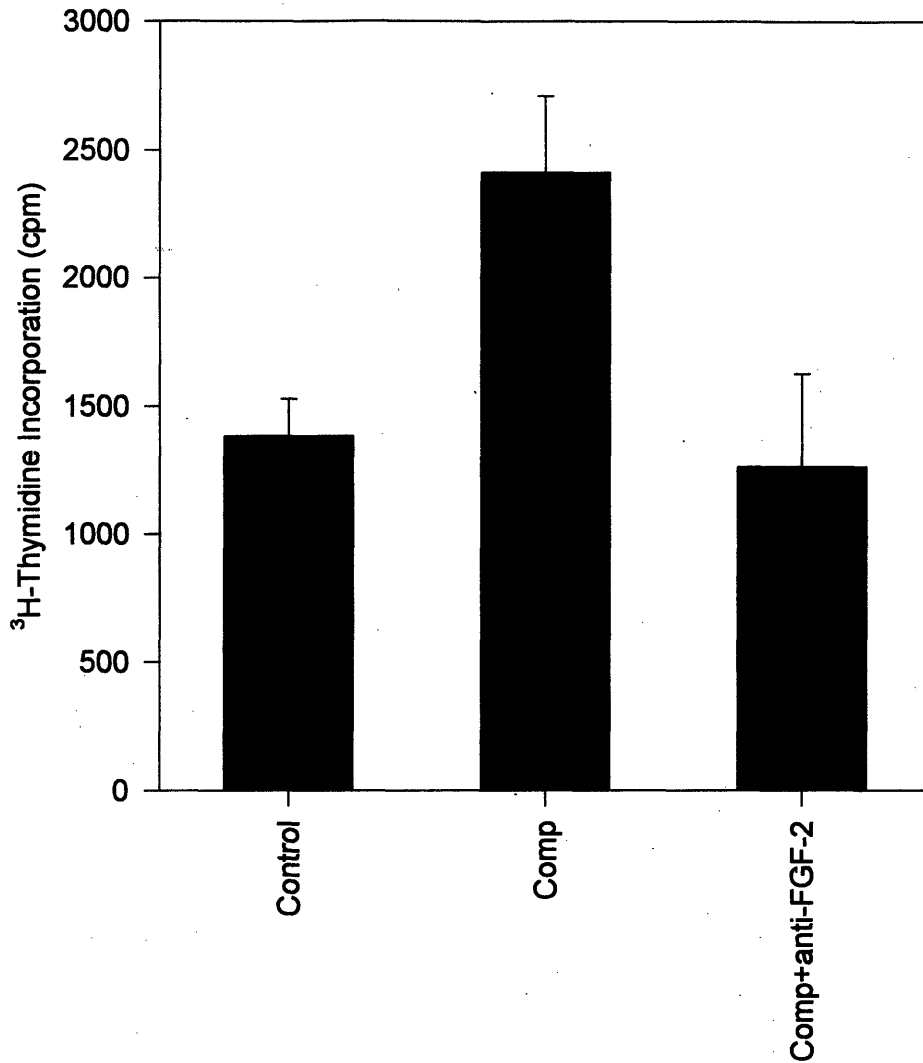


Figure 4.6. Ability of conditioned media from transiently compressed vascular smooth muscle cell-gel cultures to increase ³H-thymidine incorporation by unstimulated gel cultures. Media harvested 12 hr following a 5 min, 60% compression (Comp) or no compression (Control) were transferred to unstimulated gel cultures, and ³H-thymidine incorporation was measured from 12-36 hr later. The stimulatory effect of the compression-conditioned media was reversed by a neutralizing monoclonal antibody to FGF-2 (Comp+anti-FGF-2) ($p < 0.001$ vs. Comp). $n = 4$ for each measurement, error bars denote one standard deviation.

To assess the release of FGF-2 in response to transient compression, culture media were analyzed by a quantitative immunoassay. Increased levels of FGF-2 were found in serum-free media 12 hours after transient compression (Table 4.1). Analysis of media following freeze-thawing of the gel cultures demonstrated that the released FGF-2 represented only a small component (< 3%) of total available FGF-2. There was no significant increase in LDH release following the transient compression stimulus. In another experiment, DNA content in compressed gels ($3.71 \pm 0.08 \mu\text{g/gel}$) was no different from that in control gels ($3.63 \pm 0.07 \mu\text{g/gel}$) at 12 hours after mechanical stimulation, suggesting that the FGF-2 release occurs without widespread cell death. In addition, Northern analysis demonstrated no differences in FGF-2 mRNA levels at 0, 0.5, 1, 2, 3, and 12 hours after compression, and these levels were low compared to those in cells stimulated with IL-1 or serum (data not shown).

	Control	Compressed	Freeze-Thaw
FGF-2 (pg/ml)	2 ± 2	$17 \pm 5 *$	$725 \pm 47 *$
LDH (units/ml)	< assay	< assay	$1040 \pm 300 *$

Table 4.1 FGF-2 and LDH in culture media 12 hr following 5 min, 60% compression of the three-dimensional smooth muscle cell gel cultures in serum-free condition. Parallel gel cultures were subjected to three cycles of freezing and thawing without compression. The lower limit sensitivity of the LDH assay was 40 units/ml. * $p < 0.005$ vs. control, $n = 4$.

4.5 Discussion

A cascade model for restenosis is emerging in which mechanical strain, as well as acute local thrombosis, may trigger the early expression of cytokines and growth factors

by smooth muscle cells and macrophages.¹⁴⁸ These mediators stimulate multiple cell types in paracrine and autocrine fashions to regulate their own expression or induce one another. Amplification feedback loops and redundant pathways may be ushered in, circumventing therapeutic modalities intended to block a specific growth factor or cytokine. Thus, understanding the initial cellular responses to mechanical strain may be important for identifying rational therapeutic targets early in the cascade.

The previous chapter demonstrated that smooth muscle cells in a collagen matrix respond biologically to both static and transient compression. In this chapter we further characterized the induction of DNA synthesis in response to transient compression of the matrix. Transient compression of human vascular smooth muscle cell-collagen gel cultures increased DNA synthesis in a delayed, strain-dependent fashion, without exogenous serum-associated mitogens. Conditioned-media experiments demonstrated that DNA synthetic induction was not solely mediated by an intracellular mechanism. Although antibodies against PDGF-A or PDGF-B chain had no effect on the DNA synthetic response, a monoclonal antibody against FGF-2 inhibited the mechanical induction of DNA synthesis. In addition, increased levels of FGF-2 in the culture media after compression were measured by a quantitative immunoassay. Taken together, these data strongly suggest that transient mechanical strain of *in vitro* vascular smooth muscle cells stimulates DNA synthesis, in part by autocrine release of FGF-2.

In a series of experimental restenosis studies, Reidy and colleagues made the important observation that early smooth muscle cell proliferation in response to vascular injury is probably mediated not by PDGF from platelets, but instead by FGF-2 released from injured medial smooth muscle cells.⁴³ However, given the potential dual roles of

FGF-2 and PDGF in promoting migration and proliferation of smooth muscle cells,^{42,167-170} and the multiple sources of these factors,^{153,157,158} *in vivo* experiments have not directly assessed the ability of isolated vascular smooth muscle cells to proliferate in direct response to a transient mechanical strain. The present study offers direct evidence for autocrine FGF-2 in mediating the induction of DNA synthesis by transient mechanical stimulation of these cells.

Following transient compression, FGF-2 was released presumably from pre-existing stores without increased FGF-2 gene expression; while FGF-2 mRNA levels in the compressed gel cultures did not change during the 12 hour period following compression, FGF-2 levels in conditioned media increased by several fold. FGF-2 lacks a leader sequence for the classical secretory pathway and is believed to be stored in the cytoplasm or nucleus and released upon disruption of the cell membrane or by a novel uncharacterized secretory mechanism.^{161,171,172} In our experimental model, FGF-2 release was not accompanied by lethal smooth muscle cell injury, as assessed by LDH activity and total gel DNA content; however, these parameters may be insensitive to minor cell injury. Such injury might account for the observed initial period of decreased DNA synthesis following compression. Although the amount of FGF-2 released was less than 3% of the total presynthesized pool, it should be noted that measurements of FGF-2 in the media may underestimate local concentrations, since FGF-2 is selectively bound to heparan sulfate proteoglycans and sequestered from the high-affinity cell surface receptors.¹⁷³ Thus, we do not know whether FGF-2 is being released from smooth muscle cells undergoing minor focal injury, from extracellular matrix sites disrupted by the mechanical

strain, or from both; further study with this system may elucidate mechanisms of strain-induced FGF-2 release.

Although autocrine FGF-2 may be critical to the mechanical induction of DNA synthesis, additional mechanisms are likely. First, inhibition of strain-induced DNA synthesis by the neutralizing anti-FGF-2 monoclonal antibody was incomplete, suggesting the existence of FGF-2-independent autocrine and/or intracellular mechanisms. Second, while conditioned-media treatment led to increased DNA synthesis which could be blocked by the neutralizing antibody, the concentration of FGF-2 measured in this conditioned media was lower than exogenous FGF-2 concentrations (> 1 ng/ml) needed to induce DNA synthesis in these serum-deprived gel cultures. Thus, mechanically induced DNA synthesis may depend on the release of additional factors. Under certain conditions, the mitogenic effects of FGF-2 on vascular smooth muscle cells can be potentiated by other growth factors such as PDGF,¹⁷⁴ and an autocrine PDGF-dependent growth response to continuous cyclic strain has been described in cultured neonatal rat vascular smooth muscle cells.⁷¹ However, a similar role for PDGF in our transient strain system was not observed, reflecting possible dependence of cellular responses on the nature of the mechanical strain (transient vs. dynamic) or on culture configuration (three-dimensional vs. monolayer).

The relationship between gel deformation and the associated cellular strains may lend insight to the mechanotransduction mechanism(s). Biosynthesis in the experiments of this and the previous chapter appear to be regulated by the imposed gel strain, suggesting that cellular deformation determines the magnitude of these responses. Although the three-dimensional culture used in this thesis has the potential advantage of providing a

mechanical environment for the cell that is more similar to the in vivo situation, the cellular strain within the compressed gel may be spatially variable and difficult to assess. In the next chapter, the relationship between cellular and culture substrate strain is discussed and a device is developed to impose homogeneous and uniform strain to cells grown in a monolayer configuration.

The DNA synthetic response we have observed may have implications not only for restenosis, but for development and progression of atherosclerosis, in general. Although atherosclerosis is multifactorial,¹⁷⁵ vascular insult from mechanical and/or biochemical sources is believed to be a major predisposing factor.²⁰ These data indicate that vascular smooth muscle cells may be sensitive to brief, sublethal variations in mechanical strain, and further emphasize the potential influence of mechanical forces on vascular cell biology. Additional study of the early smooth muscle cell responses to mechanical stimuli may reveal promising therapeutic targets for vascular diseases.

Development of Membrane Strain Device: Preliminary Assessment of FGF-2 and IL-1 α Release by Cellular Strain

5.1 Abstract

The previous chapters characterized the capacity of mechanical loading to control cellular function within a three-dimensional matrix. Static compression of smooth muscle cell-collagen gel cultures decreased DNA and glycosaminoglycan synthesis, while transient compression led to a delayed induction of DNA synthesis by autocrine FGF-2 release. An advantage to using the three-dimensional culture over a two-dimensional configuration is that it may more closely simulate certain cell-matrix interactions. A disadvantage to the gel compression experiment, however, is that cellular strains are potentially variable and cannot generally be interpolated from the imposed gel strain. To characterize the specific dependence of cell function on cellular strain, a prototype device previously used to apply homogeneous and equi-biaxial strains to cells in monolayer was re-designed and constructed. Strains were found to be homogeneous and uniformly biaxial under 1) static static deformation for the membrane, the matrix-coated membrane, and cells adhered to the matrix-coated membrane; and 2) oscillatory deformation for the membrane alone. In preliminary experiments, a single, rapid strain impulse (15% to 55% amplitude) induced the release of FGF-2 in a strain amplitude-dependent fashion. In addition, human keratinocytes released IL-1 α after an impulsive strain (40%, < 1 sec duration), but not

after sustained oscillatory strain (1 Hz, 15%, 1 hr duration). Thus, certain cellular functions may be tightly regulated by cellular strain.

5.2 Introduction

The experiments of the two previous chapters demonstrate the metabolic responsiveness of a three-dimensional smooth muscle cell-matrix culture to mechanical loading. Static, uniaxial, unconfined compression of cylindrical collagen gel cultures decreased DNA and glycosaminoglycan synthesis by human vascular smooth muscle cells, but a transient compression induced DNA synthesis by autocrine release of FGF-2. The imposed matrix strain, rather than the applied stress, appeared to regulate the response; biosynthesis decreased linearly with gel compression over a wide range of strain (0-80%) but due to the compliance of the gel, the range of associated stresses (0 - 1 kPa) was extremely narrow compared to the range typically experienced by the normal vessel wall. These observations suggest that a cell responds specifically to its own deformation, and thus its ability to sense a globally applied stress depends largely on the stiffness of its surrounding extracellular matrix. This is not surprising since it is difficult to imagine how a cell embedded in a matrix of hypothetically infinite stiffness would sense a finite external stress at all. Thus, while signal transduction mechanisms that mediate cellular responses to mechanical loading may be diverse, cellular strain could be a unifying early regulatory parameter.

For several reasons, gel compression may not be the ideal method for assessing the role of cellular strain in the regulation of cellular function. First, compression of the gel culture may exert functional control not only through cellular deformation but also

through changes in matrix concentration, particularly for high strains (See Chapter 3). Thus, it may be difficult to dissect the effect of cellular strain from that of modulating the matrix environment. In addition, cellular strains cannot be precisely interpolated from the imposed matrix strain. Although cellular deformation under uniaxial gel compression would be expected to increase generally with the imposed matrix strain, individual cell strains may be variable.

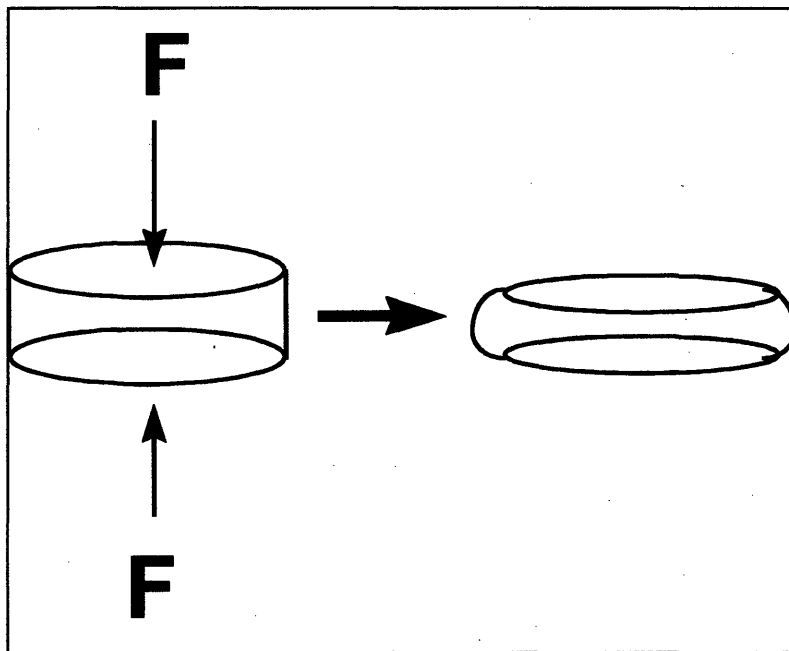


Figure 5.1 Uniaxial unconfined compression of cylindrical gel. Macroscopic strain profile is complicated by friction at the top and bottom surfaces of the gel, but these edge effects could be minimized by confined compression.

At the macroscopic level, material isotropy and homogeneity, as well as the axisymmetric loading, suggest that the strain profile may be predicted (Figure 5.1). However, this analysis would be limited by structural heterogeneity at the microscopic level. In the vicinity of a given cell, the gel culture is a heterogeneous, anisotropic

network of cell and matrix elements forming a structure similar to an engineering truss. As is the case for truss elements, the strain in a given cell may vary from that of neighboring cells, depending on its own orientation, and the orientation and elastic moduli of its neighboring cell and matrix elements. The strains in the individual elastic elements of this simple mechanical model (Figure 5.2) depend on the relative arrangements and stiffnesses of those elements. Similarly, in the gel culture, differing orientations of cells and matrix fibrils may lead to a spectrum of normal and shear cellular strains.

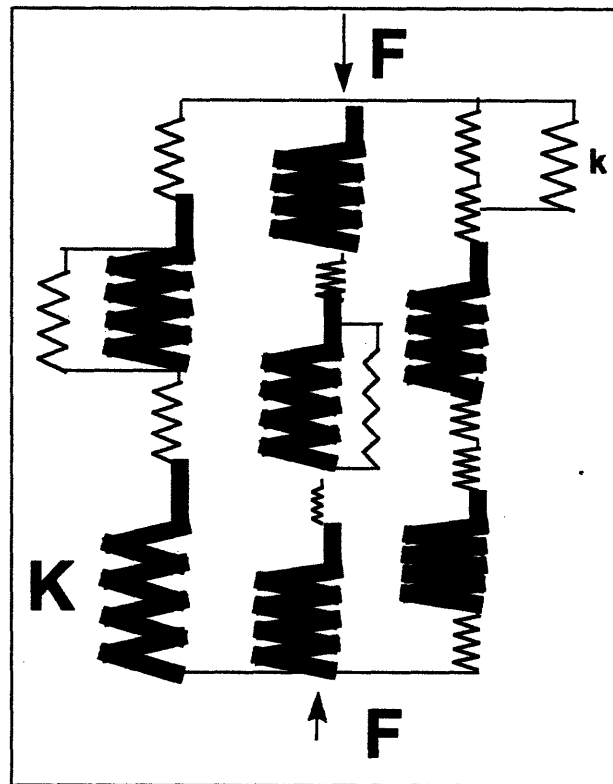


Figure 5.2 One-dimensional lumped-parameter mechanical model of cells (thin springs, k) and matrix elements (thick springs, K) bearing compressive force embedded in series and parallel orientations. Although overall gel strain is constrained by the platen displacement, the strains of the individual internal components may be spatially variable due to random density and orientation of these elements. In reality, both tension and compression-bearing elements resist the compression of the gel.

Another limitation of the gel culture compression configuration is the inability to apply oscillatory matrix strain at a moderate amplitude (e.g. 5%) and frequency (e.g. 1 Hz) such as that found in the arterial wall *in vivo*. The response of gel thickness following release of compression of 50% magnitude has a time constant on the order of an hour (Figure 5.3). Cyclic compression at 1 Hz, 10% amplitude would require forced oscillation of the upper and lower gel boundaries, in both compression and tension, to entrain the gel deformation to the desired frequency. Continuous contact between the platen and gel would be difficult to maintain or verify throughout the loading period.

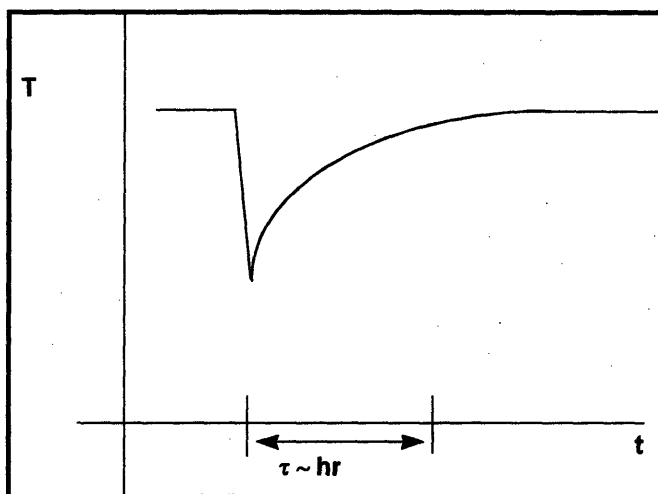


Figure 5.3 Viscoelastic response of gel culture after brief transient compression and release. Thickness (T) returns to 90 % of its initial value after $t \sim 1$ hr.

A fourth limitation of the gel culture is the relative inability to detect cell injury. In the transient compression-induced release of FGF-2 (Chapter 4), cell injury was not detected by measurement of lactate dehydrogenase. More sensitive markers for injury rely on cell visualization. Because the smooth muscle cell-collagen gel cultures are optically

opaque at the time of compression, visualization of cells is restricted to those at the surface of the gel.

Thus, the three-dimensional collagen gel culture that was useful for assessing smooth muscle cell contraction and reorganization of matrix (Chapter 2) and metabolic responsiveness to general mechanical loading (Chapter 3 and 4), presents several limitations to characterizing the role of cellular strain. Although a suitable form of mechanical loading could be developed for the three-dimensional matrix, the application of strain to cells on a matrix-coated elastic membrane may offer several advantages. First, the effect of cellular strain may be more effectively isolated from a matrix concentration effect. Second, the strain profile in a thin membrane, under certain mechanical conditions, can be theoretically modeled and experimentally verified. Third, because the extracellular matrix coating is typically much thinner than either the cell layer or membrane, the compliance of the matrix can be neglected in the assessment of cellular strain; given that the cell-matrix and matrix-membrane interfaces remain rigidly intact, the cell focal adhesions are constrained to move with the membrane. In addition, because the membrane is much stiffer than the cells in parallel, the overall deformation is dominated by the membrane (Figures 5.4 and 5.5), and the ability to perform oscillatory deformation would be limited only by the membrane's material properties. Finally, cell injury/morphology can be assessed microscopically if the membrane is optically transparent.

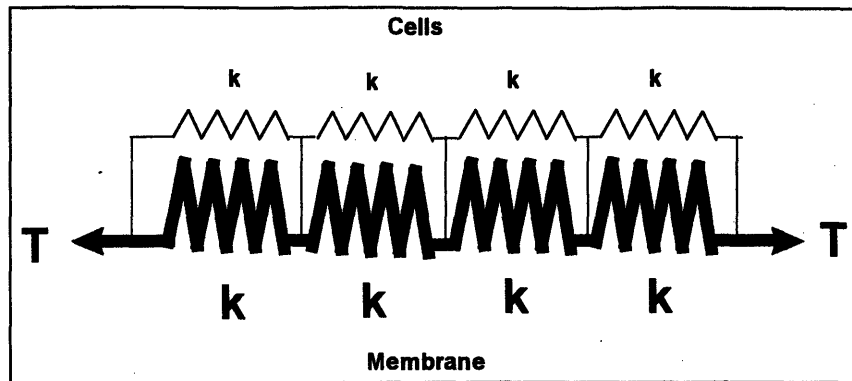


Figure 5.4 One-dimensional lumped-parameter mechanical model of cells (thin springs, k) and membrane (thick springs, K) under tensile force T . Assuming cells are rigidly constrained to the membrane through a thin matrix coating, the deformation of the ensemble is dominated by the membrane because it is much stiffer than the cell layer.

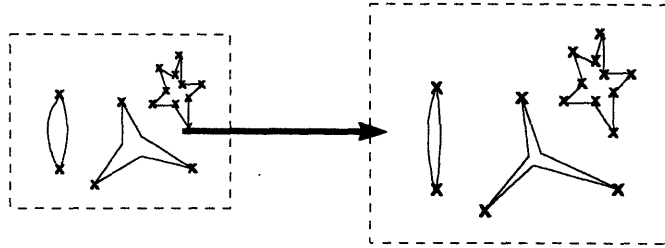


Figure 5.5 Schematic diagram of cellular deformation under tensile deformation of membrane (dotted boundary). Focal adhesions (x) move with membrane displacement, so that average cell strain is determined by membrane strain.

In this chapter a prototype device, used previously to impose homogeneous and uniform biaxial strain to cultured cells, was re-designed and constructed. Strains were experimentally verified to be homogeneous and biaxially uniform under 1) static deformation in the membrane, matrix-coated membrane, and cells adhered to the matrix-coated membrane; and 2) oscillatory deformation in the membrane. With this device, the cellular release of FGF-2 and interleukin-1 α (IL-1 α) in response to cellular strain was assessed in preliminary experiments. Like FGF-2, IL-1 is an ubiquitous cytokine which is synthesized by a number of cells, including vascular smooth muscle cells,^{36,176} and exerts numerous effects on various target cells.¹⁷⁷ The mechanism of IL-1 secretion is incompletely understood; however, structural similarities between FGF-2 and IL-1 suggest that these molecules share a common release mechanism: both are ~17 kDa, have similar three-dimensional structure by crystallography,¹⁷⁸ and lack a hydrophobic secretory leader sequence.¹⁷⁹ We found that FGF-2 was released from human vascular smooth muscle cells in response to either continuous cyclic strain of moderate frequency (1 Hz) and magnitude (15%) or a single strain impulse. Conversely, IL-1 α was rapidly released from

human keratinocytes after a single strain impulse, but was not released by continuous cyclic strain of moderate frequency and magnitude. The preliminary data suggest that FGF-2 and IL-1 molecules can be liberated by cellular deformation, but that release is dependent on certain characteristics of the imposed strain.

5.3 Materials and Methods

5.3.1 Prototype Device Modifications.

The prototype device designed by Prof. Martha Gray ² has been used previously to impose homogenous and uniform biaxial strain to cultured cells (Figure 5.6). Cells are cultured on a thin circular, matrix-coated elastic membrane which is deformed from below by a slightly smaller circular platen. The platen assembly moves vertically in a sinusoidal fashion as its center shaft rides on a rotating cam shaft driven by a feedback-controlled gear motor; at the lowest position on the cam, the membranes are in slight contact with the platens but remain undeformed. The following modifications to the prototype design were made to simplify operation and improve performance.

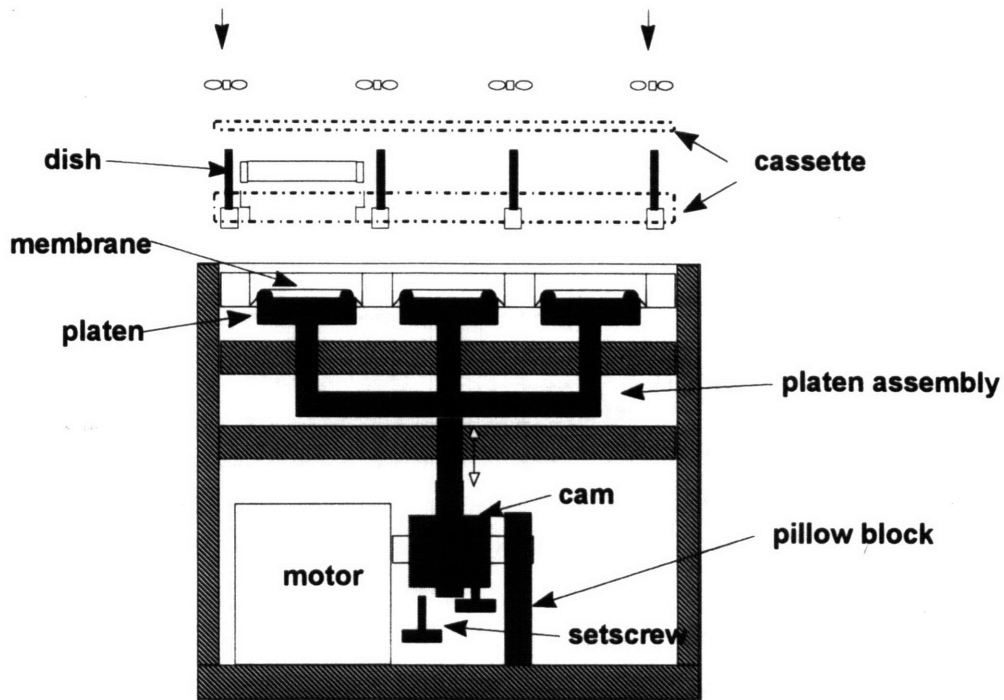


Figure 5.6 Side view of the prototype device to impose homogeneous and equi-biaxial strain to cells growth on a circular membrane.

Dishes and cassette. Access to dishes in the prototype device required the dismounting and disassembly of a cassette (Figure 5.6). The cassette and dish designs were modified so that each of four dishes was independently accessible (Figure 5.7). The dish sits in a bottomless well of the cassette, and a locking collar sits on a ledge near the base of the dish. The collar is rotated to engage three screws in the cassette which are tightened to secure the dish. With this design, dishes can be loaded or removed in less than 10 seconds. The dish height was also increased to simplify manipulation.

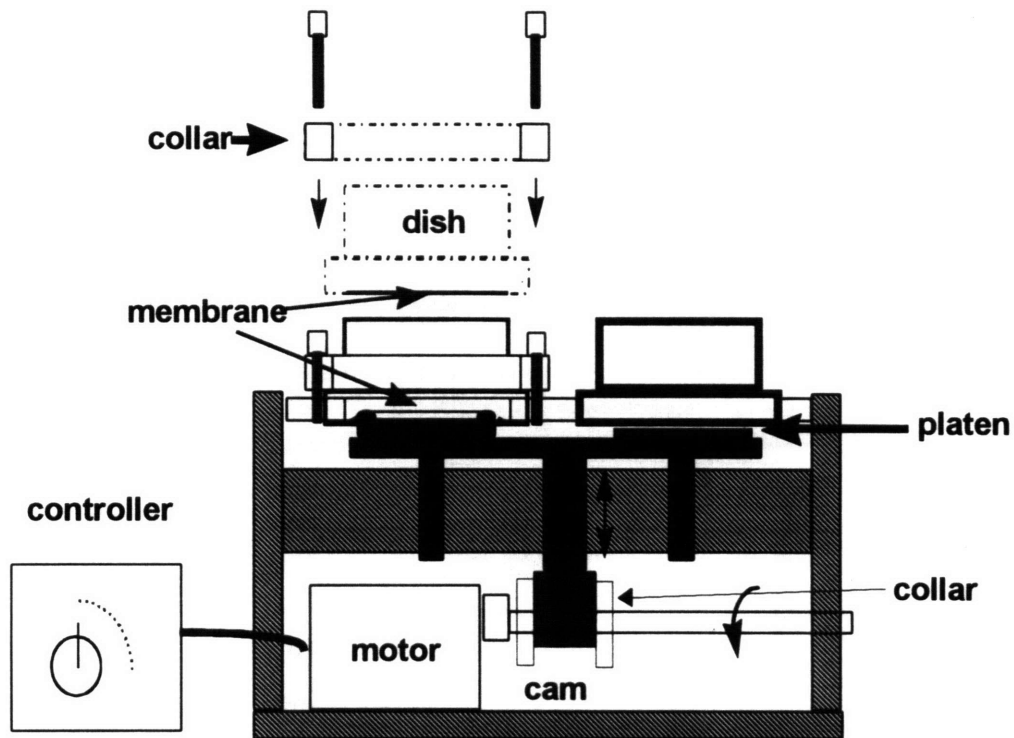


Figure 5.7 Side view of current device illustrating modifications made to simplify operation and improve performance.

Platen assembly. Due to its material (Teflon) compliance and number of kinematic degrees of freedom, the prototype platen assembly potentially contributed to variability in membrane strain (Figure 5.6). The current platen assembly consists of four aluminum or Delrin platens secured to a single aluminum platform (Figure 5.7). The platform thickness (0.50”) was selected to minimize bending during the loading cycle. The platform was secured directly to a single drive shaft, and two lateral guide shafts each made of stainless steel. These shafts were guided through an aluminum support beam by glass-filled Teflon bearings (BOStonE F-1, Boston Gear) with a clearance of 0.001”. With these modifications, the weight of the platen assembly is sufficient to overcome friction in the bearings and spring assistance is not required. The current device provides noticeably

smoother vertical translation with less rotation and horizontal translation than achieved with the prototype.

Cam and motor shaft. With the prototype device, cam changes required turning the entire device on its side and removing a pillow block to release the cam shaft (Figure 5.6). The setscrews securing the cam to the shaft could then be loosened and the cam released. Over time, the setscrew threads in the cam were observed to degrade. To simplify cam changes, the shaft was lengthened to rotate in a bearing within the side wall of the device, thereby eliminating the need for the pillow block (Figure 5.7). The cam was rotationally constrained to the shaft with a key, and horizontal displacement of the cam was constrained by two stainless steel collars. The cam could thus be removed by loosening the cam shaft from the motor shaft, sliding the former off the latter, loosening the inside collar, and sliding the cam off the end of the shaft. Cams were designed to produce platen displacement amplitudes of 3.1, 5.4, 7.3, 9.4, and 17 mm and can be changed in less than 30 seconds.

Motor, controller, and power supply- The previous motor was a 24 volt direct current motor requiring separate transformer power supply and controller units connected through extensive wiring. This motor was replaced with a 120V alternating current motor (Bodine Electric Company) with a combined power supply and speed feedback-controller connected by a single umbilical. The motor speed can be varied within a continuous frequency range of 0 to 1 Hz.

5.3.2 Cell Culture on Matrix-Coated Membranes.

Human vascular smooth muscle cells were derived from explants of discarded portions of saphenous veins obtained during coronary bypass surgery performed at Brigham and Women's Hospital. Smooth muscle cells were cultured in DMEM with 10% FCS at 37°C and 5% CO₂. These conditions are selective for growth of smooth muscle cells over endothelial cells.¹⁴³ The explant and culture methods were identical to those used in previous studies of cultured vascular smooth muscle cells.^{144,145} Cells were cultured through passages 3 through 5 before transfer to membrane dishes for use in mechanical strain experiments. Human keratinocytes and dermal fibroblasts were provided by Prof. Thomas Kupper and maintained as previously described.¹⁸⁰

Silicone elastomeric sheeting, Silastic, (0.005" thick, gloss/gloss, Specialty Manufacturing) was prepared for cell culture by coating with either human plasma fibronectin (Sigma) or Vitrogen 100 collagen (Celtrix Pharmaceutical). A silicone membrane pre-treated with a surface coating of type I collagen (0.020", thickness Flexcell Corp) was also tested. Cells were plated at a density of 5 - 15 x 10³/cm² in DMEM supplemented with 10% fetal calf serum and were trypsinized at various times to assess proliferation.

5.3.3 Compatibility of Lubricant.

A well-lubricated interface between platen and membrane is critical for achieving a uniform strain profile in this configuration (see next section). Prior to their mechanical evaluation, lubricants were tested for their ability to diffuse across the membrane and affect cellular function. Several lubricants were obtained, including the partially hydrogenated oil, Crisco, which had been previously used with the prototype device,² and

Braycote 804 (Castrol), a grease designed to be impermeant to silicone and chemically and biologically inert. Cells were cultured on the matrix-coated membrane, the underside of which was coated with lubricant.

5.3.4 Displacement of Platen (oscillatory, impulse, or step)

For many experiments oscillatory platen displacement was performed with the motor set at a desired frequency. In some experiments it was desired to apply a rapid and large magnitude displacement which exceeded the capabilities of the motor. A single impulse or step of strain was applied by manually raising the platen assembly to a displacement constrained by a rigid spacer inserted between the platen assembly platform and the cassette. For an impulse, the platen was raised, held briefly, and then released. Durations for the three stages of impulses performed by the author were assessed by video analysis (Table 5.1); the total duration of the impulse for all displacements was < 1 sec. For a step, the platen was raised and maintained at the desired displacement with another spacer inserted between the assembly platform and the underlying support beam.

Platen displacement (mm)	Raise (msec)	Hold (msec)	Lower (msec)
9.4	66 ± 9.7	642 ± 27	62 ± 6
13.5	92 ± 10	600 ± 53	78 ± 6
19.3	130 ± 11	570 ± 15	86 ± 10
25.4	140 ± 19	560 ± 46	100 ± 6

Table 5.1 Duration of three impulse stages for various platen displacements performed manually. Data represent mean ± sd for n = 10 measurements.

5.3.5 Estimation of Strain Distribution

The strain distribution within a circular membrane, deformed by the displacement of a concentric circular platen, can be predicted geometrically from the relative dimensions of the platen and dish, assuming a frictionless membrane-platen interface. Axisymmetric deformation yields a condition of two-dimensional hydrostatic stress within the membrane:

$$\sigma_r = \sigma_\theta \quad (5.1)$$

$$\sigma_{r\theta} = 0. \quad (5.2)$$

For a homogeneous, isotropic, linear elastic material,

$$e_r = \frac{1}{E} \left(\sigma_r - \frac{1}{\nu} \sigma_\theta \right) \quad (5.3)$$

$$e_\theta = \frac{1}{E} \left(\sigma_\theta - \frac{1}{\nu} \sigma_r \right) \quad (5.4)$$

where E = Young's Modulus and ν = Poisson's Ratio.

Combining these equations, yields

$$e_r = e_\theta \quad (5.5)$$

The strain component e_r may be derived geometrically. For a platen of diameter r and a membrane of diameter R , the membrane elongation in the radial direction (Figure 5.8) is

$$\Delta = \frac{r - R + \sqrt{(R - r)^2 + x^2}}{R} \quad (5.6)$$

where x is the vertical platen displacement. Assuming a frictionless membrane-platen interface,

$$e_r = \Delta \quad (5.7)$$

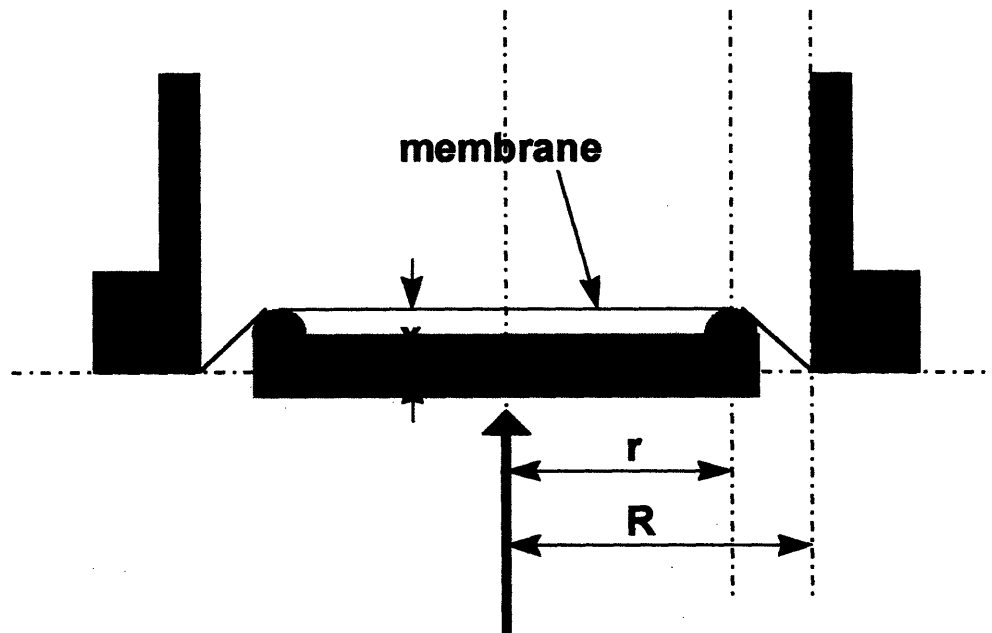


Figure 5.8 Side view of deformation of circular membrane by circular platen displacement, x .

Using equation 5.6, strain amplitudes for various platen displacements with $r = 31.1$ mm and $R = 36.5$ mm were predicted (Figure 5.9).

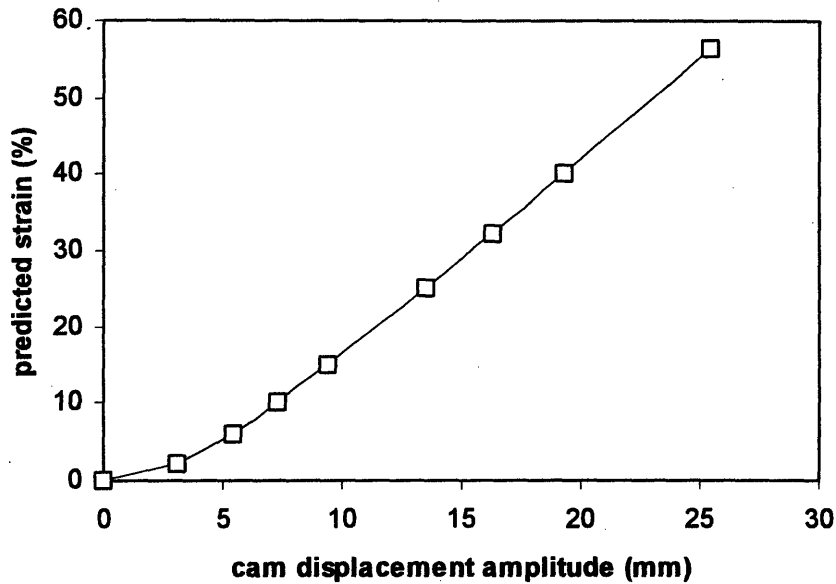


Figure 5.9 Predicted membrane strain amplitudes for various cam displacement amplitudes.

5.3.6 Dependence of Strain Magnitude on Oscillatory Platen Displacement

Although the circular cams displace the platen assembly in a sinusoidally time varying manner, the difference between platen and membrane radii ($R - r$) contributes to a skewing of the membrane strain-time relationship. Differentiating equation 5.6 with respect to x demonstrates that the nonlinear relationship between strain and platen displacement is diminished when $x \gg (R - r)$:

$$\frac{de}{dx} = \frac{x}{R\sqrt{x^2 + (R-r)^2}} \quad (5.8)$$

The time variation of strain was computed for various cam sizes relative to the hypothetical condition $R = r$ (Figure 5.10).

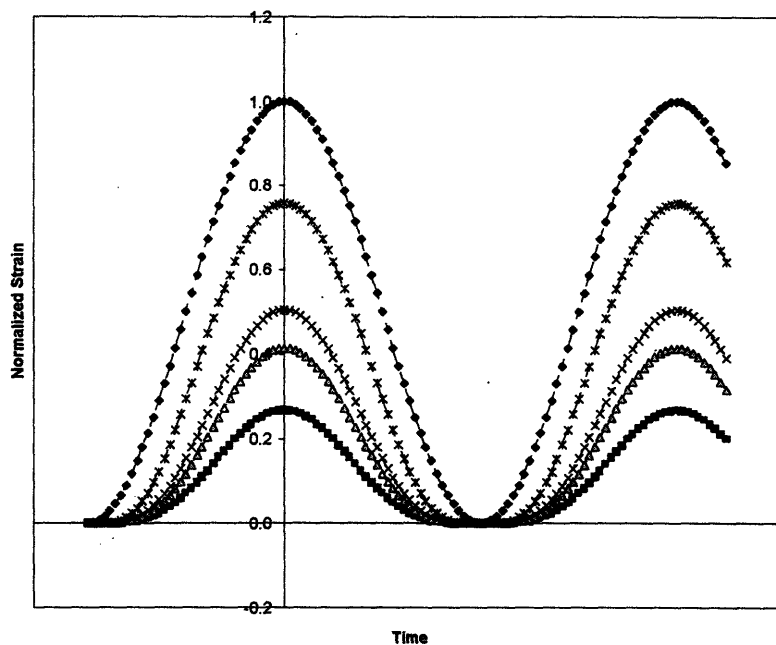


Figure 5.10 Time course of membrane strain for cam displacement amplitudes of 3.1 mm (■), 5.4 mm (▲), 7.3 mm (×), 19.3 mm (*). For each cam, data are normalized to the maximum strain yielded for the hypothetical condition $R = r$ (◆).

5.3.7 Measurement of Strain Distribution.

The relationship between strain distribution and platen displacement was assessed experimentally for both static and dynamic membrane deformations. For static deformation, evaluation was performed using an open platen, identical in dimensions to that in the strain device, which was mounted onto a microscope stage (Figure 5.11). Thus, relative membrane displacements could be visualized both microscopically and

macroscopically. Strains were assessed for static deformation of the membrane alone, the matrix-coated membrane, and for cells grown on the membrane. For dynamic deformation, membrane displacements were measured macroscopically only using a video acquisition system capable of capturing 10 moving objects at a frequency of 10 images/sec.

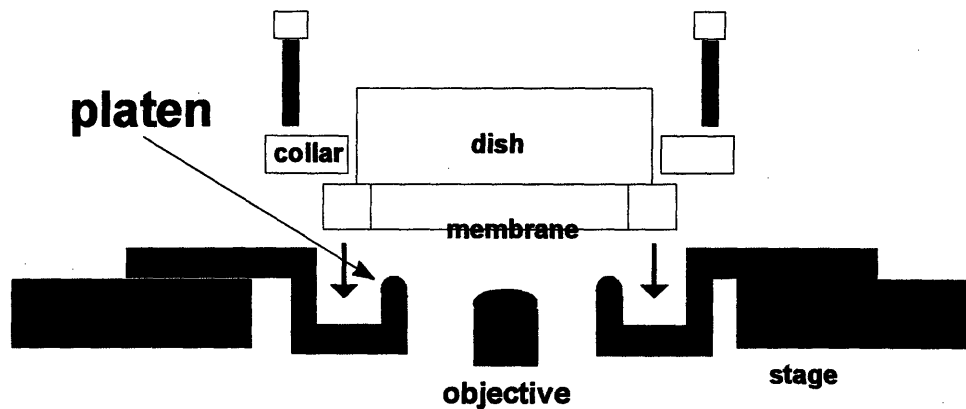


Figure 5.11 Side view of platen for viewing cells microscopically under static strain. Membrane is deformed as dish is lowered manually into well and secured with locking collar.

For macroscopic measurement of membrane strain, dots were marked in ink on the membrane in radial and concentric patterns. Relative membrane displacements were obtained from photographs of the ink markings taken before deformation and in the deformed configuration. For assessing microscopic strains, either on the matrix coating or on the cells, fluorescent microspheres (Fluoresbrite, 1 μm diameter, Polysciences) were suspended in culture media and allowed to settle onto the matrix or cell surface for 30 min. Unbound microspheres were eluted to leave a random array of microspheres. The

microsphere displacements were derived from fluorescence photomicrographs taken before deformation and in the deformed configuration; ink dot markings were used as landmarks so that the identical aggregates of microspheres were photographed.

The membrane plane strain components were computed from either the dot or microsphere displacements using the strain tensor (Figure 5.12). Consider a triad of points (p_1 , p_2 , and p_3) on a solid body constrained to deform in one plane. In the undeformed configuration the point locations are described in the a_1 - a_2 rectangular coordinate system, while in the deformed configuration these locations are represented in the x_1 - x_2 coordinate system. By the geometric definition of distance, the change in distance between two (p_1 , p_2) of the three points is

$$dS^2 - dS_o^2 = dx_i dx_i - da_j da_j \quad (5.9)$$

in summation indicial notation. Expressing this equation in terms of the undeformed coordinate system a_1 - a_2 ,

$$dS^2 - dS_o^2 = 2e_{ij} da_i da_j \quad (5.10)$$

where

$$e_{ij} = \frac{1}{2} (\delta_{\alpha\beta} \frac{\partial x_\alpha}{\partial a_i} \frac{\partial x_\beta}{\partial a_j} - \delta_{ij}) \quad (5.11)$$

For computing the average strain based on markers a finite distance apart, the differentials are approximated so that equation 5.9 becomes:

$$\begin{aligned} \Delta S^2 - \Delta S_o^2 &= 2e_{ij} \Delta a_i \Delta a_j \\ &= 2(e_{11} \Delta a_1 \Delta a_1 + 2e_{12} \Delta a_1 \Delta a_2 + e_{22} \Delta a_2 \Delta a_2) \end{aligned} \quad (5.12)$$

Thus the three independent plane strain components e_{11} , e_{12} , and e_{22} , may be derived from the three linearly independent equations from a triad of points.

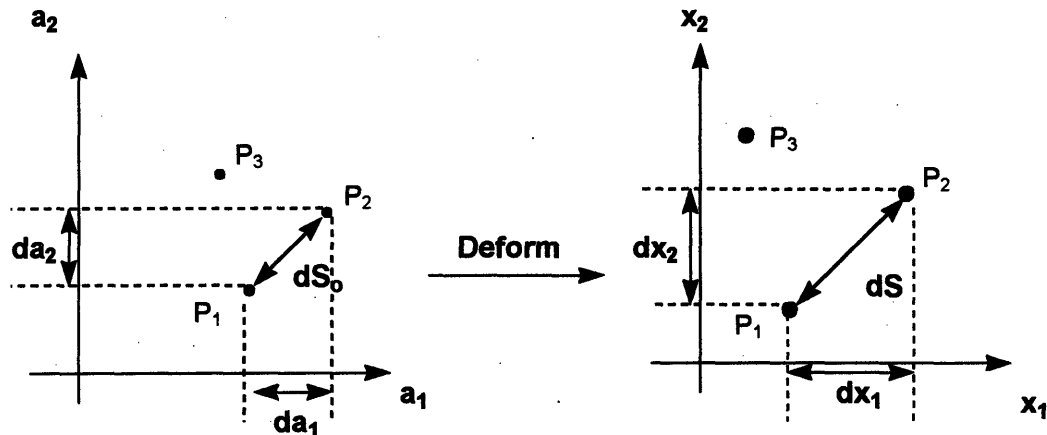


Figure 5.12 Method used to compute strain components from the relative planar displacements of a triad of points.

5.3.8 Measurement of FGF-2 and IL-1 α .

The release of FGF-2 or IL-1 α into the media was assessed quantitative immunoassays (Quantikine Human FGF basic or Human IL-1 α Immunoassay, R&D Systems). Cell layers were subjected to three cycles of freezing and thawing to assess the FGF-2 or IL-1 α remaining at the end of the experiment.

5.4 Results

5.4.1 Cellular Growth on Matrix-Coated Membrane.

Growth of human vascular smooth muscle cells and human dermal fibroblasts on membrane was assessed for various concentrations of matrix coating. In initial experiments, dissolved matrix was distributed on to the membrane and evaporated overnight in a sterile hood. Membranes were coated with collagen at a density ranging

from 0 to 100 $\mu\text{g}/\text{cm}^2$, or with fibronectin at a density ranging from 0 to 10 $\mu\text{g}/\text{cm}^2$. For collagen and fibronectin, respectively, 20 $\mu\text{g}/\text{cm}^2$ and 2.5 $\mu\text{g}/\text{cm}^2$ coating densities were optimal for adhesion, spreading, and growth of cells. Cell adhesion and spreading were attenuated on matrix below these densities. Cells grew in overlapping sheets on matrix coated at above the optimal densities, which would potentially create deviations between membrane deformation and the actual deformation experienced by some cells.

Cells grew comparably on collagen-coated membrane, fibronectin-coated membrane, or tissue culture plastic, but grew less efficiently on the collagen surface-treated membrane from Flexcell (Figure 5.13). Although initial mechanical strain experiments were performed with collagen-coated membranes, a rapid onset of retraction and peeling of cells from the membrane was observed occasionally within two days of plating. The process appeared similar to collagen gel contraction by smooth muscle characterized in Chapter 2 and suggested that focal regions of the matrix-membrane interface were disrupted by cellular contractile forces. Coating the membrane with fibronectin overnight at 4° C, followed by aspiration, was found to be the most reliable method for achieving cell anchorage. With this protocol, growth was dependent on the coating density of fibronectin, reaching a maximum for 0.6 μg fibronecting/ cm^2 .

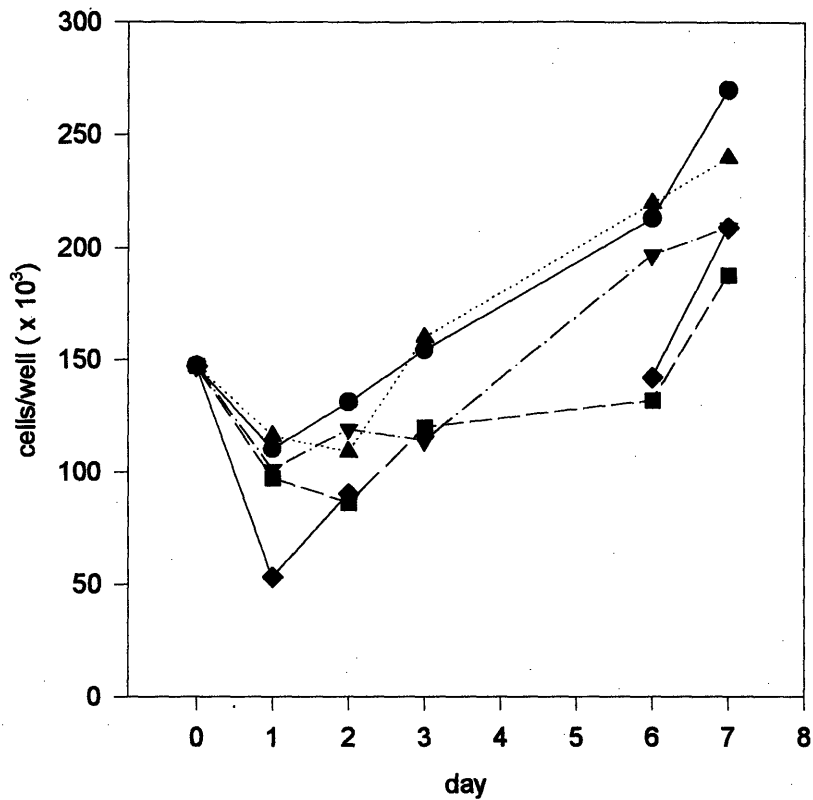


Figure 5.13 Growth of human vascular smooth muscle cells on plastic (●), Silastic (■), Vitrogen-coated Silastic (▲), fibronectin-coated Silastic (▼), and silicone membrane pre-coated with collagen (◆). Cells were plated on day 0 and media were changed on days 1, 2, and 3.

5.4.2 Sterilization of Membrane Dishes.

Although sterilization of membrane dishes with ethylene oxide gas did not initially reveal toxicity, later experiments demonstrated cell death within days of plating. Eventually, cell death occurred within 24 hours of plating and strongly suggested a toxic process. Ethylene oxide can diffuse into and be adsorbed by certain plastics, and complete liberation of the substance requires a long aeration period. Frequent gas sterilization of

these dishes apparently increased the latent concentration of ethylene oxide in the plastic which presented a larger dose to the cultured cells. Although extending the aeration period between sterilization and cell culture culture was a possible solution, the need for ethylene oxide was eliminated altogether by machining new dishes out of the autoclavable materials, polysulfone or Kynar.

5.4.3 Effect of Lubricant on Cell Morphology and FGF-2 Release.

In addition to the ethylene oxide sterilization, the lubricant used for the platen-membrane interface was considered potentially toxic to cells. In preliminary experiments FGF-2 was rapidly released from cells under mild mechanical strain; however, further control experiments demonstrated the response to be induced primarily by Crisco. To characterize this effect, Crisco was applied to half of the under surface of the membrane, and cells were cultured on both halves of the top surface. Within 24 hours, cells on the Crisco-coated half of the membrane became thinner and retracted relative to cells on the control half. Media from cells on membrane coated with Crisco contained elevated amounts of FGF-2 relative to media from cells grown on membrane without lubricant. These observations strongly suggested that Crisco was diffusing across the membrane and inducing morphological changes and release of FGF-2.

After screening several lubricants, Braycote 804 was found to be well suited both biologically and mechanically (see next section). Cellular morphology was not affected by Braycote 804 placed directly in the culture media. In addition, Braycote 804 on the

undersurface of the membrane did not by itself induce FGF-2 release from cells (Figure 5.14).

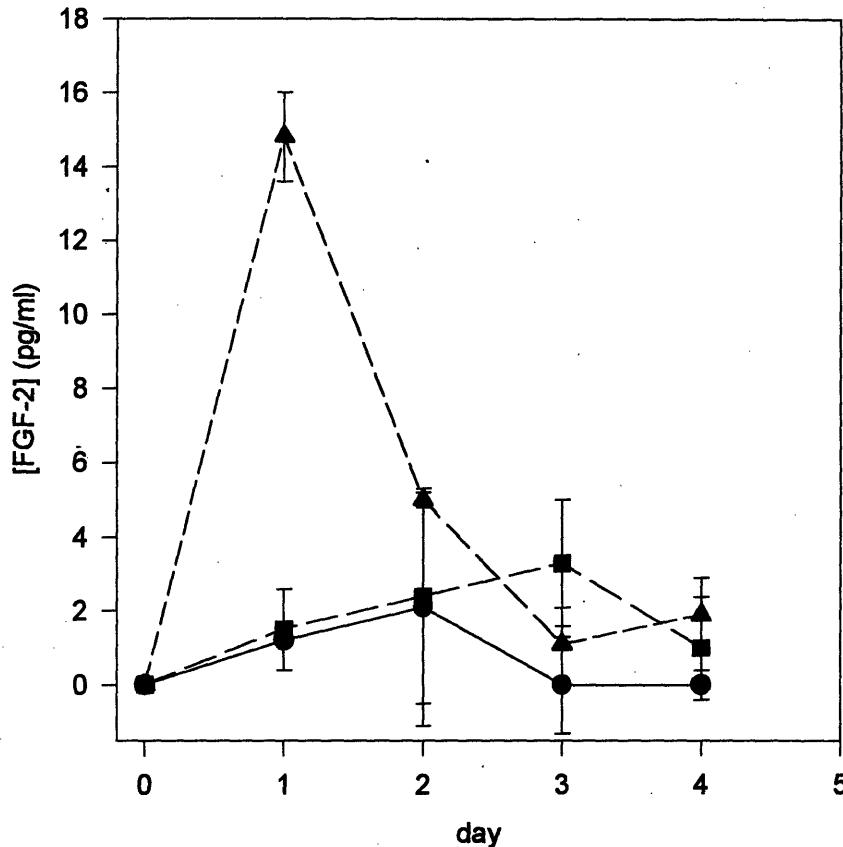


Figure 5.14 Effect of lubricants on the release of FGF-2 by human vascular smooth muscle cells. Cells growing on membrane with an undercoating of Crisco (▲) released FGF-2 during the first day, while cells growing on membrane with Braycote 804 (■) or without lubricant (●) released no growth factor during the four days. Error bars denote one standard deviation; $n = 3$ for each measurement.

5.4.4 Strain Distribution.

The normal and shear strain components were assessed for the membrane under static platen displacement of 5.4 mm. The normal strains, e_{11} and e_{22} , were approximately equal to 6%, while the shear strain e_{12} was approximately equal to zero; strains were

insensitive to either radial position (Figure 5.15A) or angular position (Figure 5.15B) on the membrane. Thus deformation of the circular membrane by the circular platen was associated with homogeneous and equi-biaxial strain, as predicted.

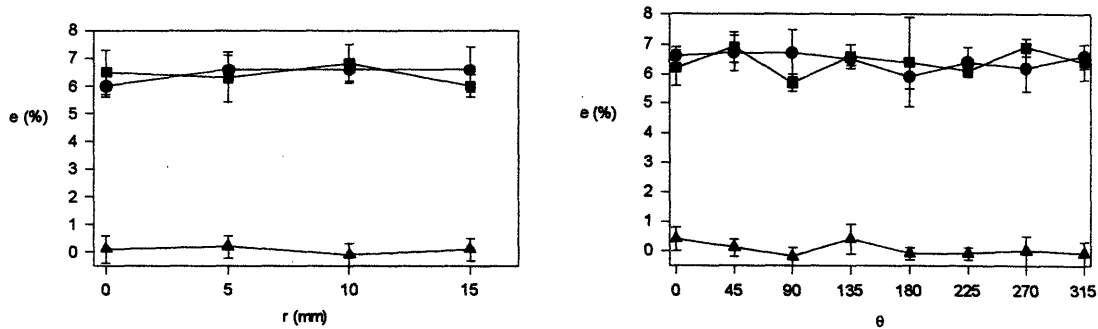


Figure 5.15 The dependence of strain components e_{11} (●), e_{12} (■), and e_{22} (▲) on radial (A) and angular (B) location on membrane during static deformation (5.4 mm platen displacement). Data represent mean \pm sd for $n = 4$ to 6.

To assess the potential disruption of the matrix coating and/or disruption of cell adhesion by dynamic deformation, the strain distribution was assessed for the collagen on membrane, for the fibronectin on membrane, and for cells adhered to the collagen-coated membrane. Membranes were first subjected to dynamic platen displacement of 5.4 mm at 1 Hz for 24 hrs. in an attempt to disrupt the membrane-matrix and/or matrix-cell interfaces. Fluorescent microspheres were laid down on the membrane and photographed in the undeformed state. The membrane was then statically deformed by a platen displacement of 5.4 mm and then photographed at the previous locations. Strain components derived from microspheres (Figure 5.16) on collagen (A), on fibronectin (B), and on cells (C) were similar to those derived from ink markings on the membrane (Figure

5.15A), and were independent of the radial position. Thus, no discontinuity in deformation related to disruption of the membrane-matrix and matrix-to-cell interfaces was observed. In addition, there were no obvious differences in cell morphology before and after mechanical strain (5%, 1 Hz, 24 hr).

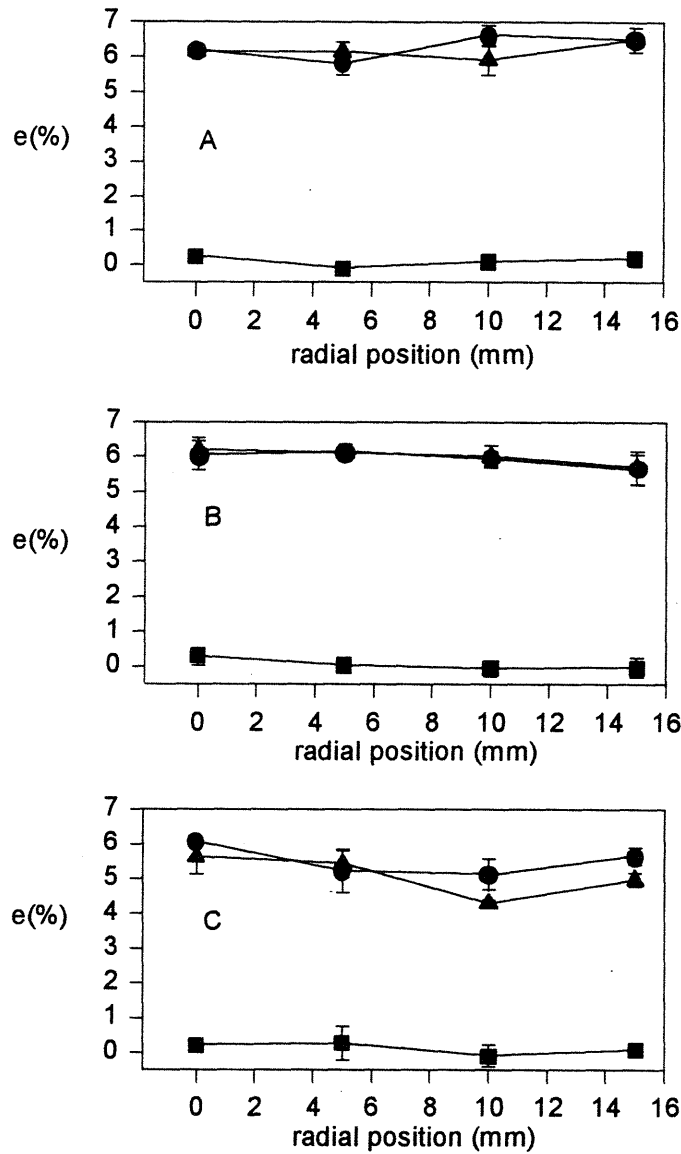


Figure 5.16 The dependence of strain components e_{11} (●), e_{12} (■), and e_{22} (▲) on radial location, computed from the displacements of microspheres adhered to the collagen coating (A), the fibronectin coating (B), and to cells on collagen-coated membrane (C) under static deformation (5.4 mm platen displacement). Data represent mean \pm sd for $n = 4$ to 6.

Strain distribution in the membrane was also assessed for dynamic platen displacement of different amplitudes. Strain components at maximum platen displacement were independent of radial or angular membrane position, with equal normal strains and shear strain equal to zero (Figure 5.17).

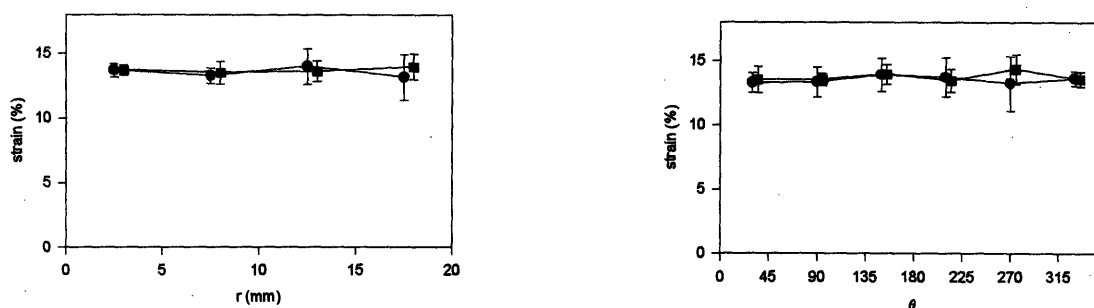


Figure 5.17 The dependence of strain components e_{11} (●) and e_{22} (■) on radial (A) and angular (B) membrane location computed from the displacements of ink markings on membrane under dynamic deformation (9.7 mm platen displacement amplitude). Data represent mean \pm sd for $n = 4$ to 6.

5.4.5 Clearance Between Dish Lid and Dish.

The membrane culture dish is essentially a vented chamber whose volume is regulated by the membrane deformation. When the vent is small (lid sitting on dish), deformation of the membrane increases the chamber pressure and expels a fraction of the gas inside the chamber; upon relaxation of the membrane, the internal pressure decreases relative to the atmosphere which causes the dish lid to sit firmly on the dish. This seal prolongs the pressure decrease and delays the elastic recoil of the membrane. When an offset clearance is maintained between dish lid and dish, the oscillatory circulation of the humid gas in the boundary layer and the drier gas outside the dish may lead to convective

loss of culture medium, particularly if the incubator is not saturated. When the incubator environment ranged between 50-75% saturation due to routine opening (Figure 5.18), media volume decreased with dynamic strain (10% amplitude, 1 Hz) dependent on the lid configuration; after 8 hrs., media volume (15 ml initial volume) was greatest in a covered control dish and lowest in an uncovered strained dish. The media loss relative to the uncovered strained condition was decreased by maintaining a 0.1" spacer clearance between the dish and lid, or by propping the lid on the adjacent collar screw, but was the same as the loss from the closed, strained condition. The uncovered, control condition was also associated a large loss of media. When the incubator door remained closed and the humidity level was allowed to attain saturation (Figure 5.18, 8 - 24 hrs.), the rates of evaporative loss decreased. Additional experiments performed for 24 hrs. with humidity sustained > 85% demonstrated no significant evaporation of media (Figure 5.19). Thus, saturated conditions should be maintained for dynamic strain experiments of longer than 1-2 hrs. duration.

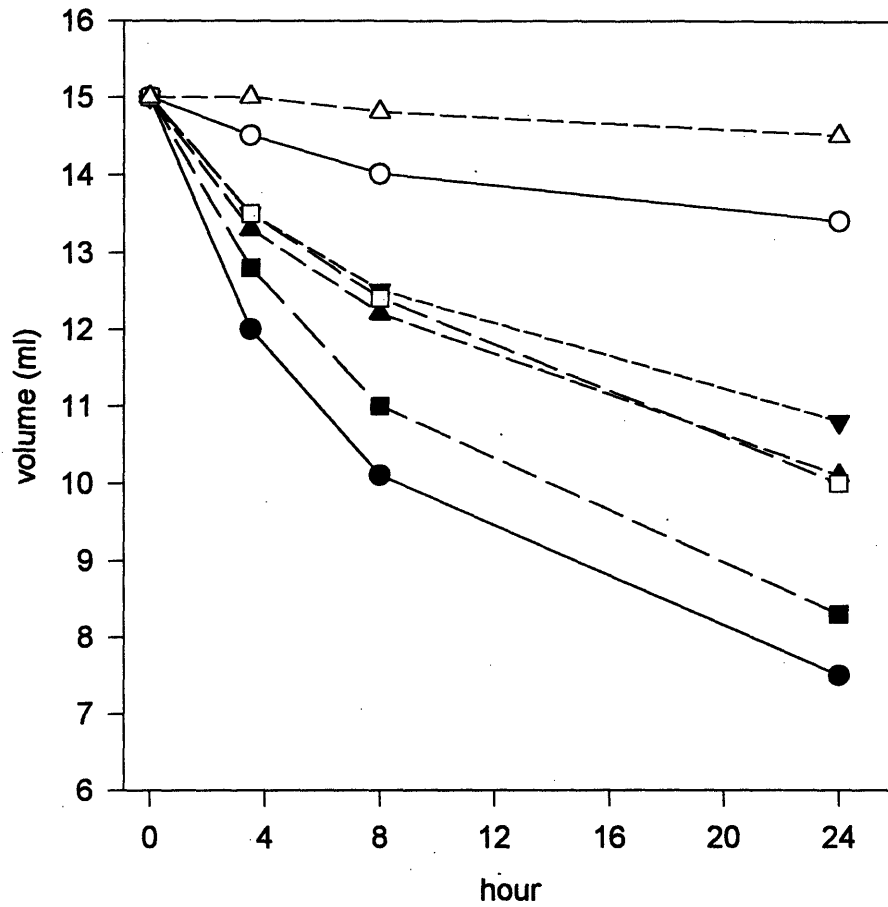


Figure 5.18 Evaporation of culture media from dishes with different lid configurations with or without membrane strain (1 Hz, 15%) as follows: uncovered + strain (●), uncovered - strain (■), propped lid + strain (▲), 0.1" lid clearance + strain (▼), 0.1" lid clearance - strain (○), covered + strain (□), and covered - strain (open ▲). Data represent mean for n = 2.

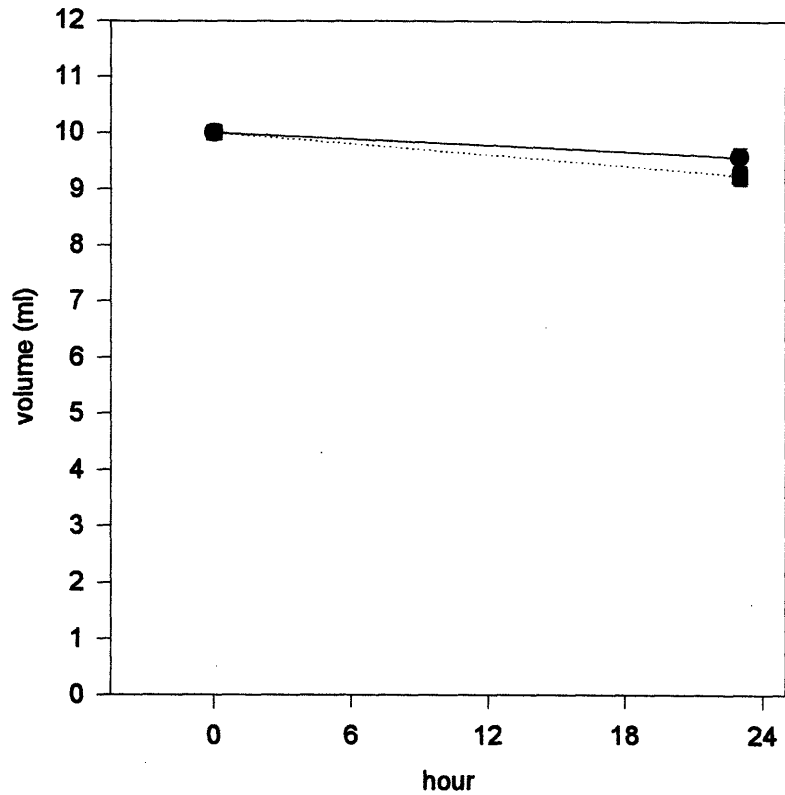


Figure 5.19 Maintenance of media volume under dynamic membrane strain (15%, 0.5Hz, ■) relative to control (●) when incubator humidity is maintained > 85%. Data represent mean for n = 2.

5.4.6 Release of FGF-2 From Human Vascular Smooth Muscle Cells.

Mechanical strain induced the rapid release of FGF-2 in a strain magnitude-dependent fashion (Figure 5.20). One hour after a single step or 10 impulses of strain (55% amplitude), respectively, media contained 930 ± 690 and 1100 ± 330 pg/dish FGF-2 (vs. 60 ± 40 pg/dish for control, $p < 0.05$); at 24 hours after the step and 10 impulse strains respectively, media (A) contained 420 ± 30 and 180 ± 30 pg/dish FGF-2 (vs. 0 ± 5 pg/dish for control), and the cell layers (B) contained 3440 ± 370 and 6260 ± 1180

pg/dish FGF-2 (compared to 8450 ± 2520 pg/dish for control). The decrease in media FGF-2 with time suggests degradation and/or cellular re-uptake and metabolism of the growth factor after mechanical release.

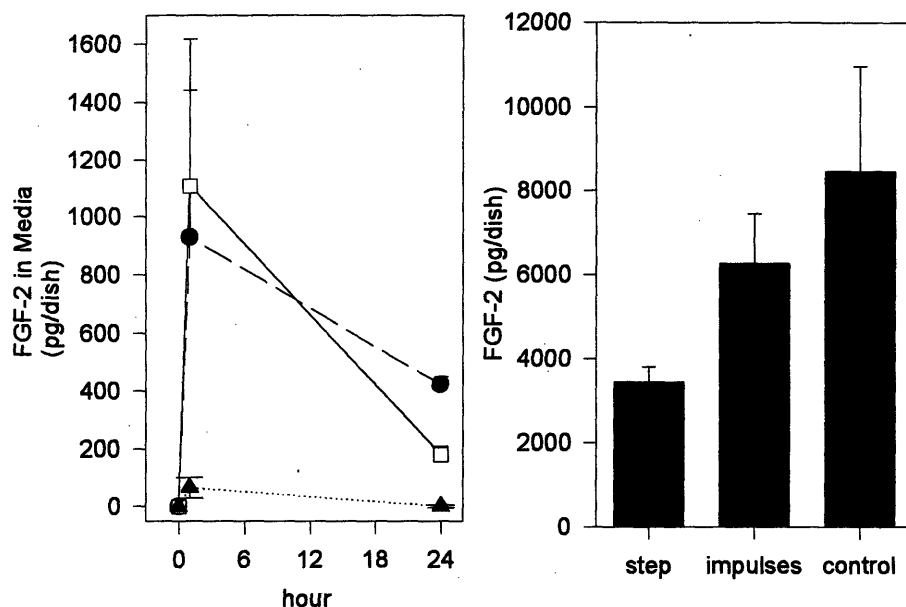


Figure 5.20 A) Time course of FGF-2 in media. FGF-2 is released by human vascular smooth muscle cells in response to a sustained step (●) and to 10 impulses (■) of strain at 55% magnitude relative to control (▲). B) FGF-2 remaining in the cell layers at 24 hours. Data represent mean + sd for n = 3 per measurement.

FGF-2 was rapidly released also to a single impulsive strain, increasing with the magnitude of strain (Figure 5.21); at 4 hr after strain of 15%, 25%, 40%, and 55% magnitudes, respectively, media contained 440, 650, 1110, and 1580 pg/dish FGF-2 (compared to 10 pg/dish for control). Thus 15% amplitude impulse strain was sufficient to induce release of the growth factor. Another experiment was performed to assess whether impulsive strain at a lower amplitude, or cyclic dynamic strain at a lower frequency, could also induce FGF-2 release (Figure 5.22). At 60 min. after a single strain

impulse of 5% and 15% amplitudes, and dynamic strain (1 Hz) of 15% amplitude, respectively, media contained 6 ± 25 , 260 ± 30 , and 240 ± 30 pg/dish FGF-2 (compared to 0 ± 36 pg/dish for control). Thus, FGF-2 was not released by 5% strain, but was released equally by 15% strain, either as a single rapid (< 150 msec, strain rate $\sim 100\%/sec$) impulse or as ~ 3600 cycles of lower frequency (strain rate $\sim 30\%/sec$) strain.

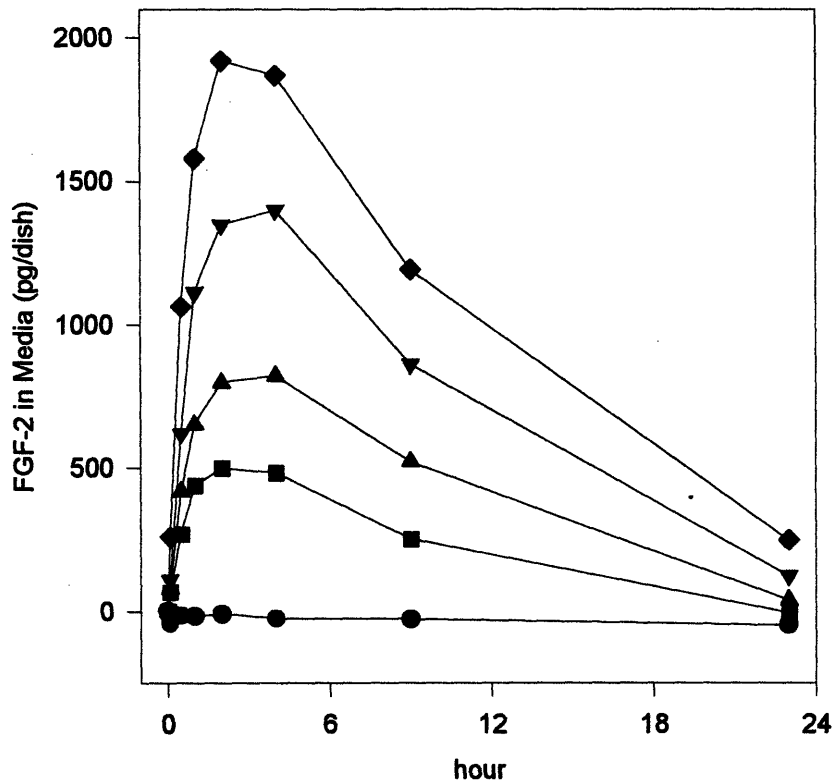


Figure 5.21 Time course of FGF-2 in media. FGF-2 is released by human vascular smooth muscle cells in response to a single strain impulse of 15% (■), 25% (▲), 40% (▼), and 55% (◆) magnitude relative to control (●). Data represent measurement of $n = 2$ pooled samples.

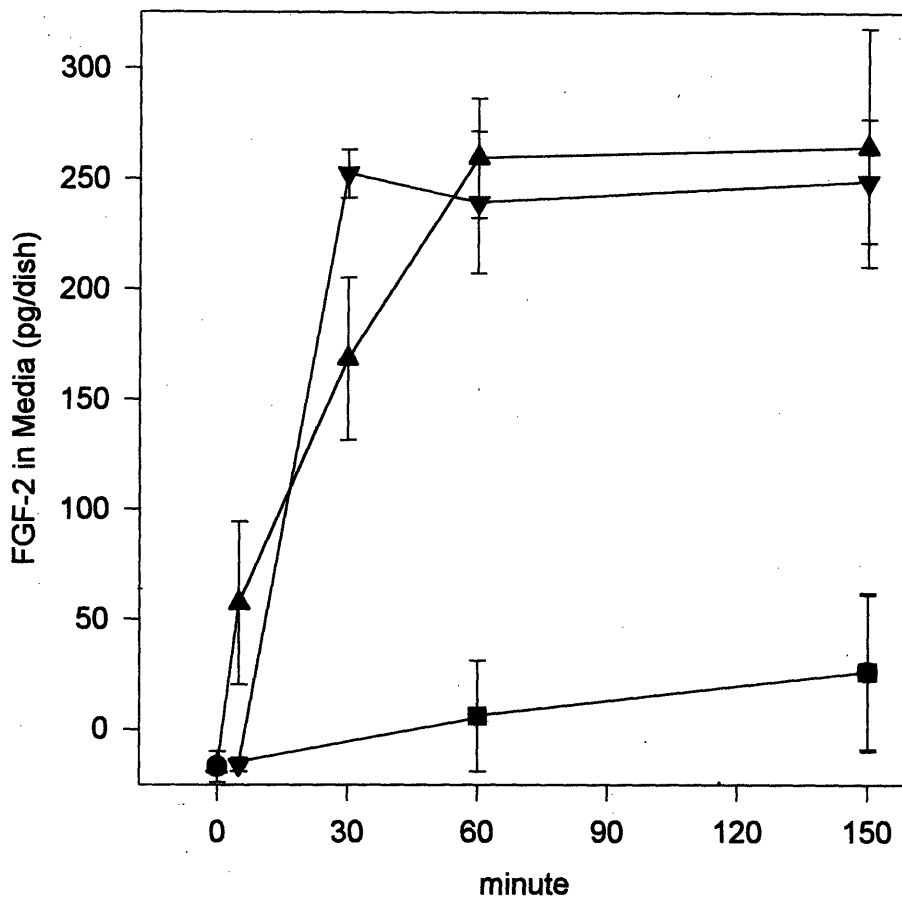


Figure 5.22 Time course of FGF-2 in media. FGF-2 is released by human vascular smooth muscle cells in response to single strain impulses of 5% (■) and 15% (▲), and to continuous cyclic strain of 15% (▼), relative to control (●). Data represent mean \pm sd for n = 4.

5.4.7 Release of IL-1 α from Human Keratinocytes.

A similar experiment was performed to assess the potential release of IL-1 α by cyclic dynamic or impulsive strain (Figure 5.20). At 60 min. after a single strain impulse of 40% impulse and after beginning cyclic strain (1 Hz) of 15% amplitude, respectively, media (A) contained 3170 and 110 pg/dish IL-1 α (compared to 68 pg/dish for control);

90 min. later, the cell layers (B) contained 3290 and 20,500 pg/dish IL-1 α (compared to 20,100 pg/dish for control). Thus, IL-1 α was released in response to a single high frequency, large amplitude strain, but not in response to sustained dynamic strain of lower frequency and amplitude.

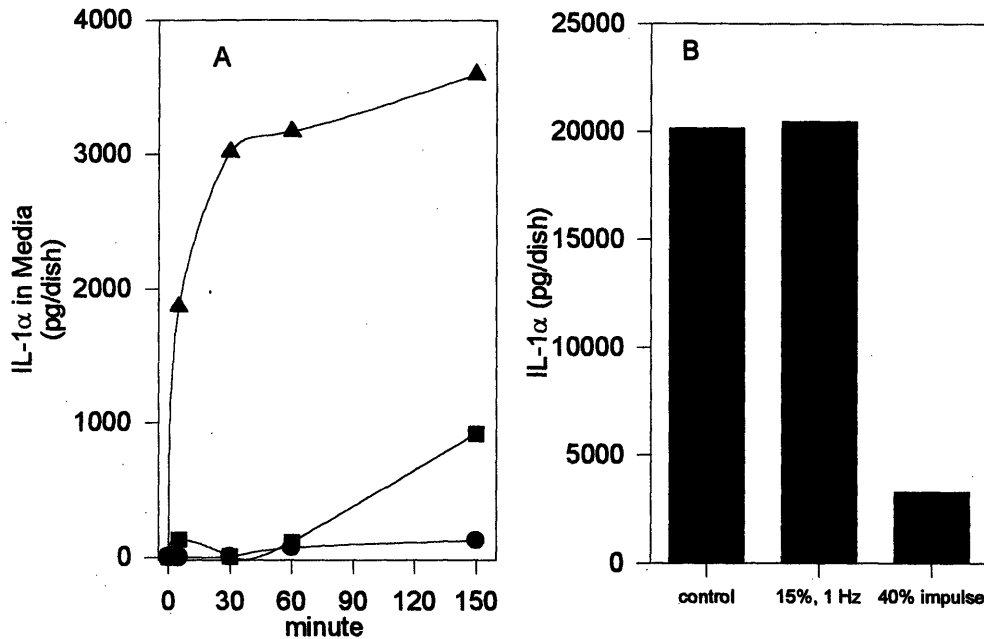


Figure 5.23 A) Time course of IL-1 α in media. IL-1 α is released from human keratinocytes in response to a single impulse of 40% strain (\blacktriangle) and to continuous cyclic strain of 15% magnitude (\blacksquare), relative to control (\bullet). B) IL-1 α remaining in cell layer after 150 min. Data represent measurement of $n = 3$ pooled samples.

5.5 Discussion

Although smooth muscle cells within a three-dimensional matrix culture were shown in previous chapters to be metabolically responsive to mechanical loading, the cellular strains in these experiments were unknown and presumably non-uniform. Most two-dimensional membrane “stretch” devices, while offering the advantage of cell visualization, do not deliver spatially uniform strains.^{2,181} Frequency of oscillation can be controlled with these devices, but as will be discussed in Chapter 6 (Discussion), both

strain amplitude and strain rate vary with position on the membrane. Thus, a device was developed to apply homogeneous and uniform biaxial strain to all cells on a flexible membrane substrate. Design modifications to a previously used prototype device were made to improve its operation, and technical obstacles related to sterilization, membrane lubrication, and cell culture were addressed. In addition, membrane, matrix, and cellular strains were verified to be homogeneous and biaxially uniform under static deformation. In preliminary experiments, a single strain impulse induced the rapid release of FGF-2 from human vascular smooth muscle cells in a strain amplitude-dependent fashion. Oscillatory strain (1 Hz, 150 min. duration) and impulsive strain (< 1 sec. Duration) of 15% amplitude induced comparable cellular FGF-2 release; however, FGF-2 was not released during 5% oscillatory strain (1 Hz, 150 min. duration). In addition, impulsive strain (40%, < 1 sec duration) induced the rapid release of IL-1 α from human keratinocytes, but IL-1 α was not released in response to sustained oscillatory strain (1 Hz, 15%, 1 hr duration). Thus, certain features of cellular strain such as amplitude and rate may control certain cellular responses.

Characterization of FGF-2 Release in Response to Oscillatory Cellular Strain

6.1 Abstract

Although FGF-2 was released from cells in response to mechanical loading (Chapter 4), the specific role of cellular deformation in FGF-2 release was not characterized. To test the hypothesis that release of FGF-2 may be tightly regulated by cellular strain, the device developed in the previous chapter was used to impose controlled, homogeneous and uniform biaxial strain to human vascular smooth muscle cells. Release of FGF-2 increased with the number of cycles of strain (15%, 1 Hz); 1, 9, and 90 cycles of strain, respectively, released $0.55 \pm 0.06\%$, $2.9 \pm 0.3\%$, and $5.5 \pm 1.3\%$ of the total cellular FGF-2 (vs. $0.00 \pm 0.40\%$ for control, $p < 0.05$ by ANOVA), but release was not further increased for strain of 90 - 90,000 cycles. Mechanical release of FGF-2 was dependent on the frequency of deformation; strain (90 cycles, 15%) at 0.25 Hz, 0.5 Hz, and 1 Hz, respectively, released $4.8 \pm 0.8\%$, $10.0 \pm 0.8\%$, and $14.0 \pm 1.2\%$ of the total FGF-2. Release was controlled also by the amplitude of deformation; strain (90 cycles, 1 Hz) at 5% amplitude released only $0.1 \pm 0.1\%$ of the FGF-2, but strain at 15% and 30% amplitudes, respectively, released $5.7 \pm 0.5\%$ and $19.0 \pm 3.0\%$ of the initial growth factor (vs. $0.0 \pm 0.3\%$ for control, $p < 0.05$), suggesting a strain amplitude threshold for FGF-2 release. Injury to a sub-population of cells increased with the frequency and amplitude of strain, as detected by propidium iodide or fluoresceinated

dextran, but cells were not injured by strain below 10% amplitude. Strain following heparin treatment released $12.6 \pm 1.6\%$ of the total FGF-2 (vs. $15.8 \pm 0.9\%$ for strain alone, $p < 0.05$), suggesting that most FGF-2 was liberated from the nuclear or cytoplasmic pools. Conversely, strain (15%, 1 Hz) in the presence of heparin released $25.2 \pm 3.5\%$ of the total FGF-2 (vs. $15.6 \pm 2.6\%$ for strain alone, $p < 0.05$). These data suggest that the frequency and amplitude of cellular strain tightly regulate the release of intracellular FGF-2. In addition, mechanical strain causes a transfer of intracellular FGF-2 to the extracellular low-affinity receptors.

6.2 Introduction

Mechanical forces may regulate cellular function in physiological and pathological states. Vascular cells are subjected to a dynamic mechanical environment modulated by pulsatile pressure and oscillatory shear forces. The accompanying stresses may regulate normal vascular tone¹⁸² and contribute to atherogenesis,¹⁸³ the vascular hypertrophy associated with hypertension,¹⁸⁴ and the acute rupture of atherosclerotic lesions.^{37,185} The mechanical forces associated with certain therapeutic interventions also may induce important biological responses. Coronary balloon angioplasty, a common treatment for occlusive vascular disease, imposes extreme vessel wall strains which may play a major role in triggering restenosis.^{130,186}

Fibroblast growth factor-2 (FGF-2) may participate in the early smooth muscle cell migratory and proliferative responses of restenosis.⁴⁸ FGF-2 is a potent mitogen and chemotactic factor for endothelial cells and vascular smooth muscle cells, and is synthesized by these and a variety of other cells.^{43,166,167,187} FGF-2 may be synthesized in

multiple forms^{188,189} which are differentially distributed in the cytoplasm and nucleus.¹⁹⁰⁻¹⁹³ FGF-2 may bind to receptors on a broad range of target cells to regulate growth, differentiation, tissue regeneration, and angiogenesis. However, despite its apparent extracellular mode of action, FGF-2 is not found in vesicles¹⁸⁷ and does not have a classical hydrophobic leader sequence for secretion by the exocytotic pathway.¹⁷²

FGF-2 has been shown to be released from cells *in vitro* by cytosolic leakage through injured cell membranes.^{160,194-196} Biochemical stimuli^{197,198} and also mechanical trauma, such as scraping¹⁶⁰ and crushing¹⁹⁹ have been shown to induce FGF-2 release from cultured cells. Wounding by needle puncture causes skeletal myofibers to release a variable amount of FGF-2 which correlates with the frequency of membrane disruptions.¹⁶² However, healthy cells under little or no mechanical stimulus also may release FGF-2. In cultured endothelial cells, basal levels of protease production and DNA synthesis are inhibited by neutralizing antibodies to FGF-2. Physiological activities such as contraction of cardiac myocytes¹¹ and migration of endothelial cells²⁰⁰ induce FGF-2 release, suggesting that neither cell death nor extreme injury is a prerequisite for release.

Once released, FGF-2 may bind not only to specific cell surface receptors, but also with lower affinity to heparan sulfate proteoglycans and other pericellular matrix components.^{173,201} These low-affinity, non-signaling receptors are thought to enhance growth factor activity²⁰² by raising local growth factor concentrations, promoting receptor binding²⁰³, or by other mechanisms. The matrix may also serve as a FGF-2 reservoir which may be released rapidly under certain conditions²⁰⁴⁻²⁰⁷.

Although FGF-2 can modulate a variety of cellular functions in vitro, the function of this growth factor in physiological and pathological states is unclear, in part, because the regulation of its release is incompletely understood. The ability of a broad range of mechanical stimuli to induce release of FGF-2 in vitro suggests that FGF-2's release and function in vivo may vary with local mechanical conditions. Many cells that synthesize FGF-2 also experience strain in vivo; depending on the type of cell and anatomic location, these strains may be cyclical or intermittent, short or long in duration, rapid or slow in onset. In addition, as discussed in Chapters 1 and 3, strains in neighboring cells may be widely variable depending on their orientation. Thus, understanding the specific role of mechanical strain in FGF-2 release may help elucidate the function of this growth factor. Additionally, the relative roles of the matrix and intracellular reservoirs of FGF-2 have not been characterized for a mechanical stimulus. In the experiments of Chapter 4, the release of FGF-2 was observed in response to a transient mechanical compression of a three-dimensional smooth muscle cell-collagen matrix culture.²⁰⁸ The induction of DNA synthesis was dependent on the magnitude of the compressive strain, but the dependence of FGF-2 release on cellular deformation, the extent of cellular injury, and the role of extracellular FGF-2 binding could not be readily assessed.

The preliminary experiments in Chapter 5 demonstrate the release of FGF-2 following either oscillatory strain of moderate frequency and magnitude or a single impulsive strain; mechanical release to the latter stimulus was also amplitude-dependent. In this chapter, human vascular smooth muscle cells cultured in monolayer were subjected to uniform biaxial mechanical strain to address the following hypotheses: 1) brief oscillatory mechanical strain induces rapid release of FGF-2; 2) release of FGF-2 and

cellular injury depend on the amplitude, frequency, and the number of cycles of the mechanical strain; 3) FGF-2 is released primarily from the intracellular pool; and 4) once released, part of the FGF-2 is sequestered by the extracellular receptor compartment.

6.3 Materials and Methods

6.3.1 Cell Culture.

Human vascular smooth muscle cells were derived from explants of discarded portions of saphenous veins obtained during coronary bypass surgery performed at Brigham and Women's Hospital. Smooth muscle cells were cultured in DMEM with 10% FCS at 37°C and 5% CO₂. These conditions are selective for growth of smooth muscle cells over endothelial cells.¹⁴³ The explant and culture methods were identical to those used in previous studies of cultured vascular smooth muscle cells.^{144,145} Cells were cultured through passages 3 through 5 before transfer to membrane dishes for use in mechanical strain experiments. Sterilized membrane dishes were coated with human plasma fibronectin (Gibco) overnight, washed with PBS, and plated with cells at a density of 5×10^3 cells / cm². Cells were incubated overnight in DMEM supplemented with 10% FCS to permit adhesion and spreading. For serum-free conditions, cells were washed twice with DMEM and cultured for ~24 hours in defined, serum-free IT medium (equal volumes of DMEM and Ham's F-12 supplemented with 1 μmol / L insulin and 5 μg / mL transferrin). Before the experiment, serum-free medium was again changed to minimize residual growth factors.

6.3.2 Application of Mechanical Strain.

Oscillatory, homogeneous and equibiaxial strain was applied to cells on fibronectin-coated membranes at frequencies ranging from 0.1 to 1 Hz and at amplitudes of ~ 5%, 10%, 15%, and 30%. The design of the membrane strain device, theoretical relationships between platen displacement and membrane strain, and experimental strain validations obtained for the membrane, matrix, and cells are presented in the previous chapter. Control parallel dishes received no mechanical strain but were otherwise treated in identical fashions.

6.3.3 Measurement of FGF-2.

To evaluate the time course of FGF-2 release, media aliquots were collected at various times after beginning strain. At the end of the experiment, the combined intracellular and receptor-bound FGF-2 was harvested with 2 M NaCl, pH 7.5 and three cycles of freeze/thaw. In some experiments, the cell layer was eluted with 2M NaCl, pH 7.5 and 2M NaCl, pH 4.0 to harvest FGF-2 bound to the low- and high-affinity receptors, respectively.²⁰⁹⁻²¹¹ Alternatively, FGF-2 bound to the low-affinity receptors was harvested by treatment with heparan sulfate, heparitinase,¹⁷³ or heparin²¹² Media, elutions, and cell lysates were assayed for FGF-2 with a quantitative enzyme immunoassay (Quantikine Human FGF basic Immunoassay, R&D Systems).

6.3.4 Measurement of Cellular Injury.

To evaluate the acute detachment of cells from the culture substrate, cell adhesion was measured before and immediately after strain. Cellular nuclei were stained with acridine orange (2 µg/mL, Sigma) and photographed under fluorescence microscopy at

random locations marked on the underside of the membrane. Cells were subjected to mechanical strain and re-photographed at the identical locations.

To assess plasma membrane integrity, cells were subjected to mechanical strain and stained with propidium iodide and fluorescein diacetate (10 $\mu\text{g}/\text{mL}$, Sigma) for several minutes. Propidium iodide and fluorescein diacetate staining has been used previously to identify injured cells and are more sensitive markers than lactate dehydrogenase release.^{213,214} Alternatively, plasma membrane disruption was detected by fluorescein dextran uptake, which has been used previously to assess cell injury in the context of FGF-2 release.^{160,162,195} Before mechanical strain, cells were changed to serum-free media with fluoresceinated dextran (10,000 MW, 2.5 mg/mL, Sigma). Cells were subjected to mechanical strain, incubated for 10 minutes, and washed twice with PBS. After labeling with either method, cells were photographed under fluorescence microscopy at several random membrane locations.

6.3.5 Immunofluorescence.

Cells were washed with PBS, fixed with 2% paraformaldehyde for 10 minutes, and permeabilized with 0.1% Triton X-100 for 2 minutes. They were incubated in blocking buffer (20% goat serum) and then changed to the primary anti-human FGF-2 antibody (10 $\mu\text{g}/\text{ml}$, Upstate Biotechnology) for 1 hr. Cells were washed with PBS and incubated with the secondary, anti-mouse IgG antibody conjugated to Rhodamine (Sigma) for 1 hr. After washes in PBS, cells were rinsed and allowed to air dry.

6.3.6 Statistics.

Data are presented as mean \pm one standard deviation or are measurements of pooled samples. Comparison among several groups of continuous variables was performed using analysis of variance. For comparison between specific groups of continuous variables, the two-sample Student's t test was used. A p value < 0.05 was considered statistically significant. The findings reported below are representative of results of at least two independent experiments.

6.4 Results

6.4.1 Release of FGF-2 During Dynamic Strain.

Continuous, oscillatory mechanical strain (1 Hz, 15%) of human vascular smooth muscle cells induced the rapid release of FGF-2 (Figure 6.1); after 10 min. of strain, media contained $3.2 \pm 0.2\%$ of the total initial cellular FGF-2 (vs. $0.3 \pm 0.2\%$ for unstrained control, $p < 0.005$); after 30 min, media contained $3.5 \pm 1.2\%$ of the total FGF-2 (vs. $0.4 \pm 0.2\%$ for control, $p < 0.005$); and after 60 min., media contained $3.8 \pm 1.1\%$ of the total FGF-2 (vs. $0.3 \pm 0.3\%$ for control, $p < 0.001$). The total initial cellular FGF-2 in each dish was estimated as the combined media and cell-associated (intracellular and receptor-bound) FGF-2 at the end of the experiment. Additional experiments were performed to assess the dependence of release on components of the mechanical strain.

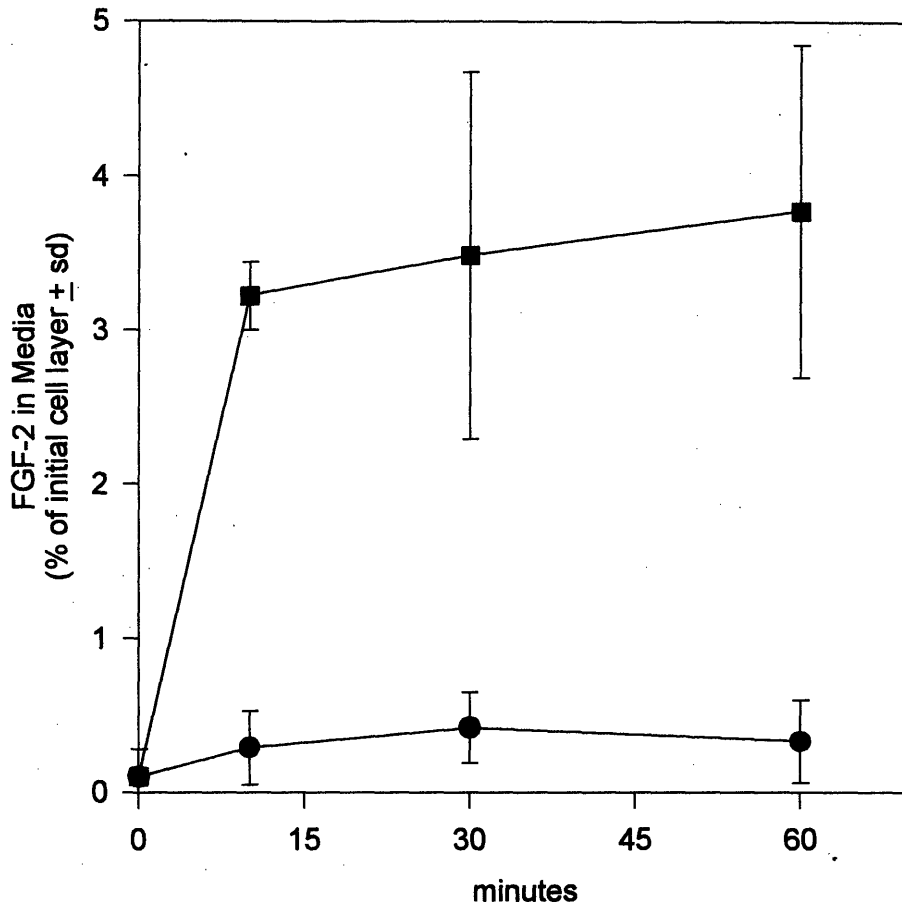


Figure 6.1. Cumulative FGF-2 in culture media during continuous oscillatory strain (1 Hz, 15% amplitude, ■) of human vascular smooth muscle cells, relative to control (●). Data represent mean \pm sd for n=3 to 7.

6.4.2 Dependence of FGF-2 Release on Characteristics of Strain.

Release of FGF-2 increased with the number of cycles of mechanical strain (Figure 6.2); 60 min. after one cycle of strain (1 Hz, 15% amplitude), media contained $2.9 \pm 1.5\%$ of the total initial cellular FGF-2 (vs. $0.9 \pm 0.4\%$ for unstrained control, $p = \text{NS}$ by

ANOVA); for 9 cycles of strain, media contained $4.8 \pm 0.4\%$ of the total FGF-2 ($p < 0.05$ vs. control); for 90 cycles, media contained $7.8 \pm 0.7\%$ of the total FGF-2 ($p < 0.005$ vs. one cycle). Mechanical strain of greater than 90 cycles released no additional FGF-2; after 900 cycles and 3600 cycles of strain, respectively, media contained $7.2 \pm 1.2\%$ and $6.2 \pm 0.9\%$ ($p = \text{NS}$ vs. 90 cycles) of the initial total cellular FGF-2, suggesting a limited releasable FGF-2 pool for a given combination of strain frequency and amplitude. In a separate experiment, cells were exposed to strain (1 Hz, 15% amplitude) of either 90 cycles or $\sim 90,000$ cycles and were changed to fresh media at 150 min. after beginning strain (Figure 6.3); cumulative FGF-2 in the media increased with time before the media change, but decreased to baseline control thereafter. Thus, FGF-2 was rapidly released to either brief (~ 1 min) or sustained (~ 24 hr) oscillatory strain, but release did not continue after 150 min. Thus, further characterization of FGF-2 release was performed primarily for 90 cycles of strain.

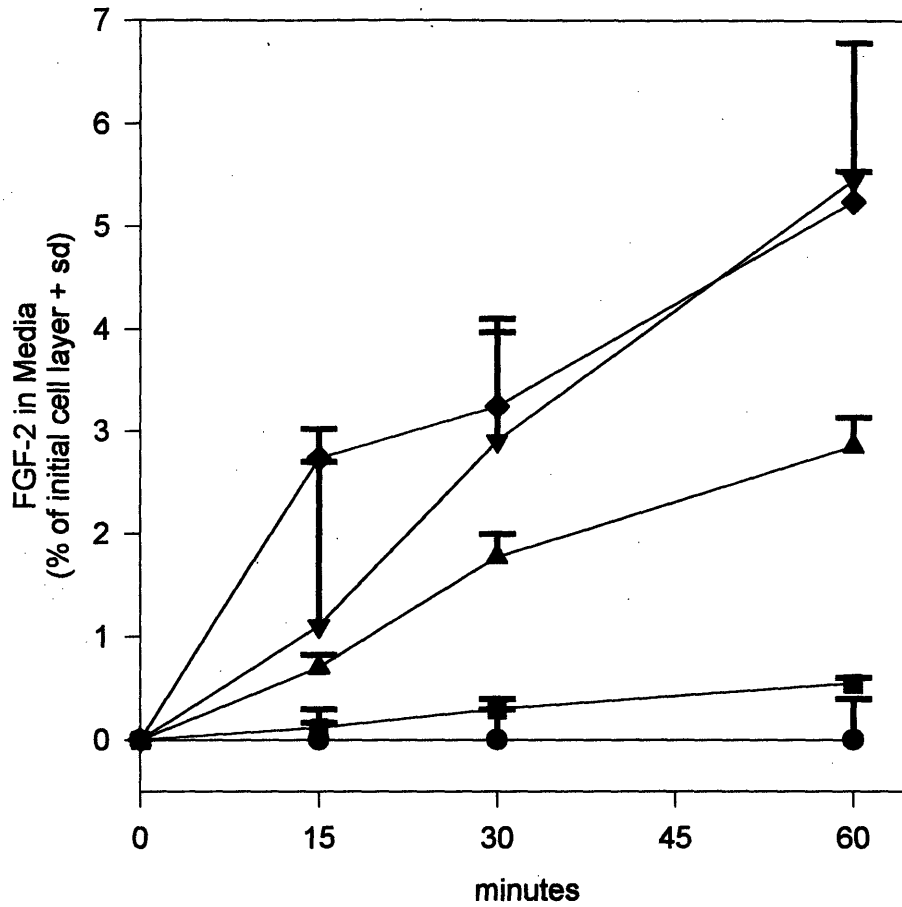


Figure 6.2. Dependence of FGF-2 release from human vascular smooth muscle cells on the number of cycles of mechanical strain (1 Hz, 15% amplitude). Relative to control (●), cumulative FGF-2 in the media increased with cycle number for 1 cycle (■), 9 cycles (▲), and 90 cycles (▼) of strain (1 Hz, 15% amplitude); however, FGF-2 was not further increased for 900 cycles (◆). Data represent mean \pm sd for $n=3$.

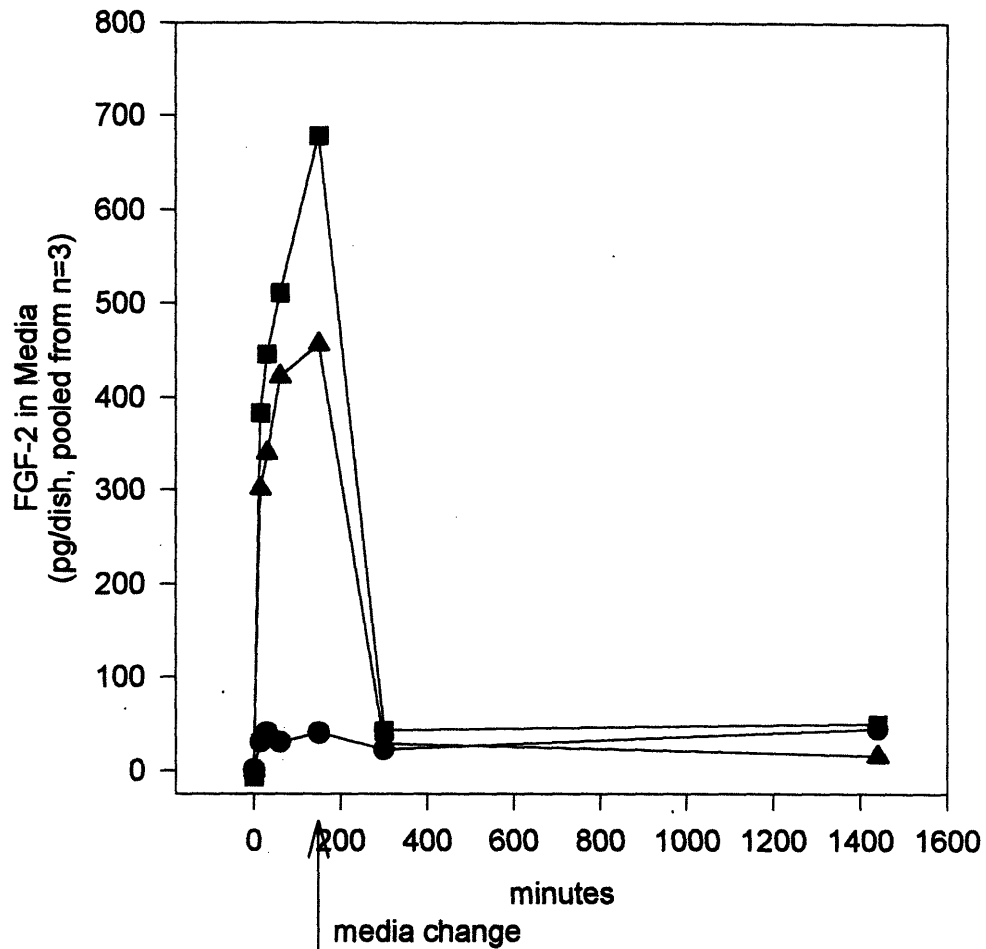


Figure 6.3. Acute FGF-2 release from human vascular smooth muscle cells in response to both brief and prolonged dynamic strain. Relative to control (●), strain (1 Hz, 15%) of 90 cycles (■) and 90,000 cycles (▲) initiated at t=0 min. were associated with rapid increases in FGF-2 in the media; however, FGF-2 was not further released after change to fresh media at t=150 min. Data represents measurement of n = 3 pooled samples.

Cyclic strain at 15% amplitude induced FGF-2 release in a frequency-dependent fashion (Figure 6.4); 60 min. after beginning strain (90 cycles, 0.25 Hz), media contained 4.8 ± 0.8 % of the total initial cellular FGF-2 (vs. $0.4 \pm 0.6\%$ for control, $p < 0.01$ by ANOVA); for strain at 0.5 Hz, media contained $10.4 \pm 0.8\%$ of the total FGF-2 ($p <$

0.001 vs. 0.25 Hz); for strain at 1 Hz, media contained $13.8 \pm 1.2\%$ of the total FGF-2 ($p < 0.05$ vs. 0.5 Hz). Mechanical release of FGF-2 was also dependent on the amplitude of strain (1 Hz) (Figure 6.5); 60 min. after beginning strain (90 cycles, 5%) amplitude, media contained $0.1 \pm 0.1\%$ (vs. $0.0 \pm 0.1\%$ for control, $p = \text{NS}$) of the total initial cellular FGF-2; for strain at 15% amplitude, media contained $5.7 \pm 0.5\%$ ($p < 0.05$ vs. 5% amplitude); for strain of 30% amplitude, media contained $18.9 \pm 2.7\%$ ($p < 0.001$ vs. 15% amplitude). Another experiment was performed to characterize the apparent amplitude threshold for FGF-2 release (Figure 6.6); 90 cycles (1 Hz) at 15% amplitude strain induced rapid release of FGF-2 within 150 min., while 90,000 cycles at 5% amplitude induced little release throughout the 24-hr period.

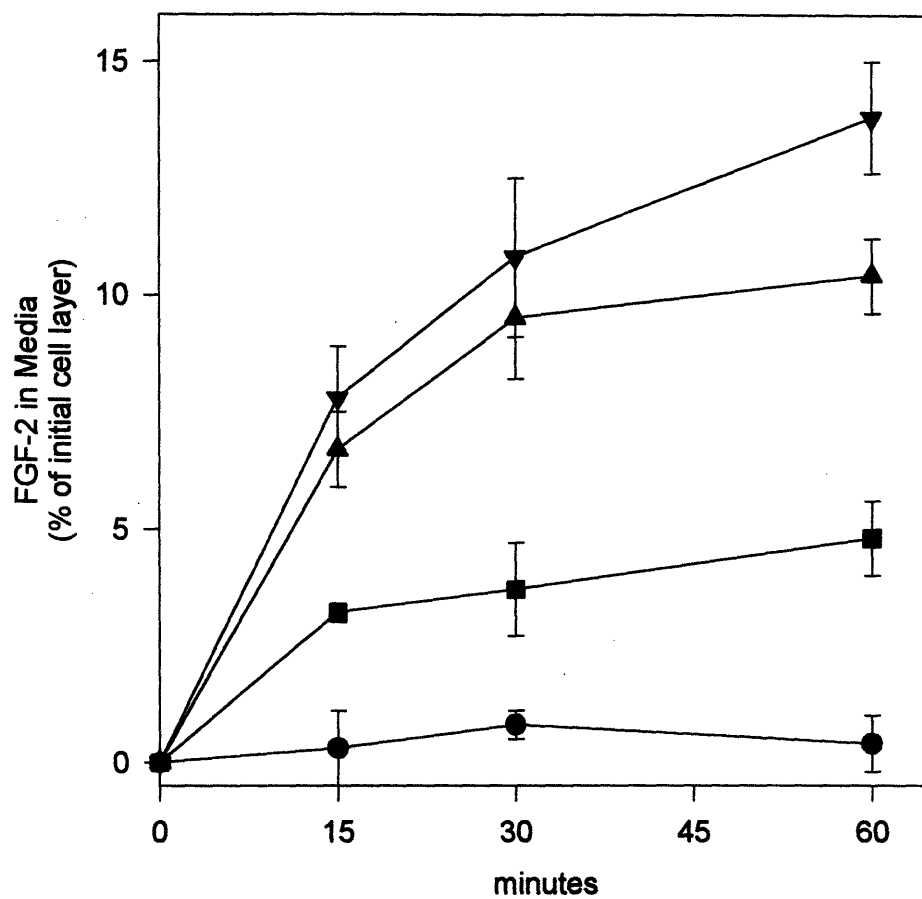


Figure 6.4. The dependence of release of FGF-2 from human vascular smooth muscle cells on the frequency of mechanical strain (90 cycles, 15% amplitude). Relative to control (●), cumulative FGF-2 in media increased with frequency for 0.25 Hz (■), 0.5 Hz (▲), and 1 Hz (▼). Data represent mean \pm sd for n=3.

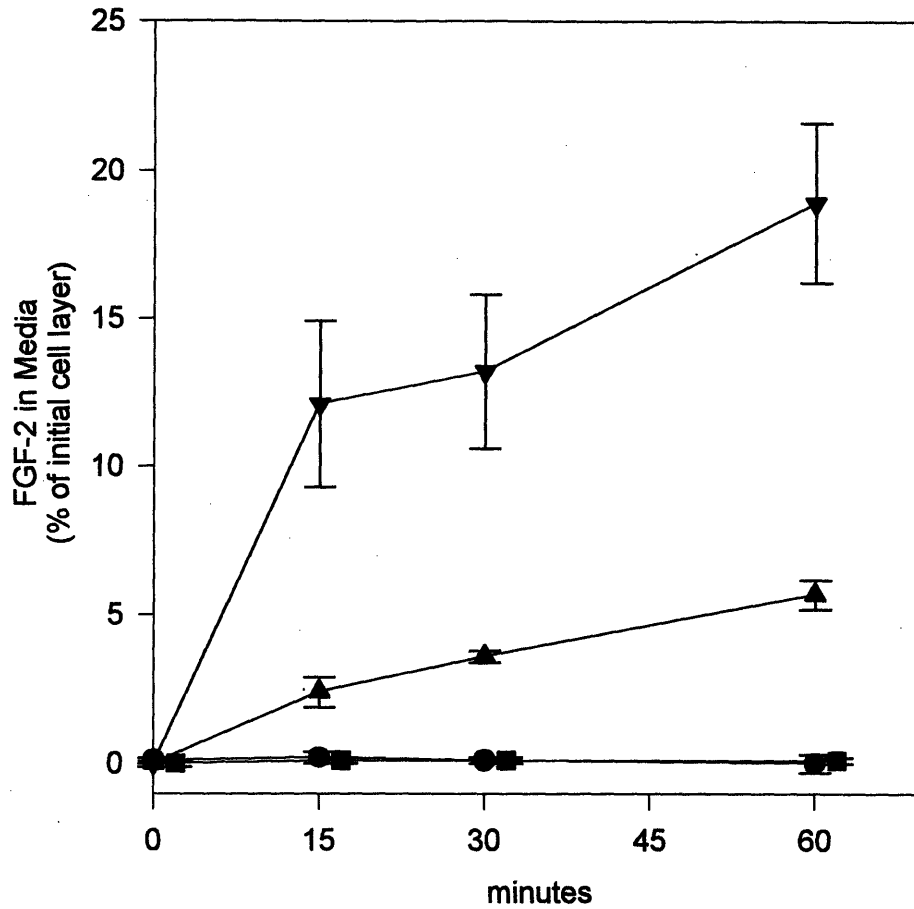


Figure 6.5. The dependence of FGF-2 release from human vascular smooth muscle cells on the amplitude of mechanical strain (90 cycles, 1 Hz). Relative to control (●), cumulative FGF-2 in media did not increase for 5% amplitude strain (■) but increased with amplitude for 15% (▲) and 30% (▼) strain. Data represent mean \pm sd for n = 3.

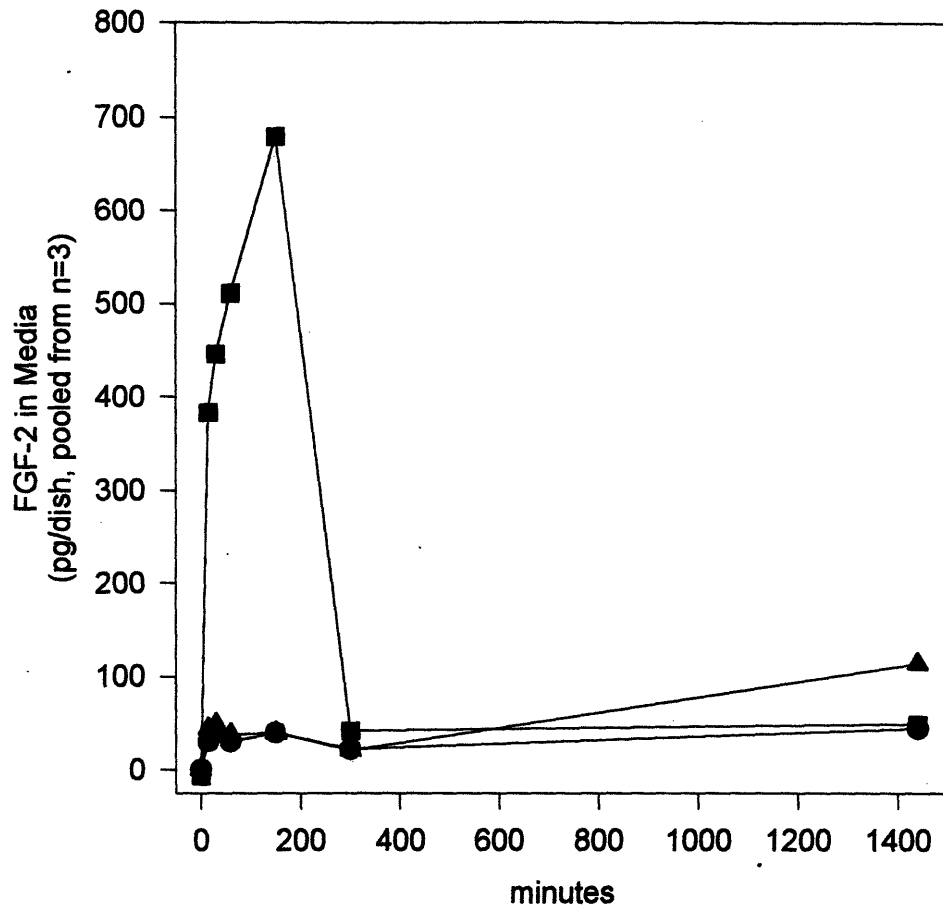


Figure 6.6. The release of FGF-2 from human vascular smooth muscle cells by mechanical strain above and below 10% amplitude. Relative to control (●), 90 cycles of 15% strain (■) induced rapid release of FGF-2, but 90,000 cycles of 5% strain (▲) caused no release. Data represents measurement of n = 3 pooled samples.

6.4.3 Cellular Injury.

To evaluate the possibility that the increase in FGF-2 in the media was caused simply by acute detachment of cells from the membrane during the mechanical strain, cell detachment was compared to the percentage of total cellular FGF-2 released. After mechanical strain (90 cycles, 1 Hz, 15%), the fraction of cells that had detached ($0.7 \pm 1.1\%$) was small compared to the fraction of FGF-2 released ($11.5 \pm 0.6\%$, $p < 0.001$). Thus, approximately 90% of the FGF-2 in the media was derived from the intact cell layer.

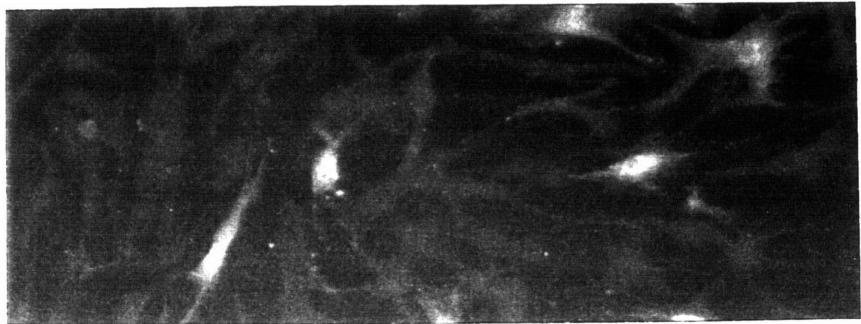
In the experiments of Chapter 4, cellular injury was not detectable by lactate dehydrogenase or total DNA. In this study, cellular injury by mechanical strain was detected by dual staining with fluorescein diacetate and propidium iodide. Propidium iodide stains the nuclei of injured cells by diffusing through disrupted plasma membranes, while fluorescein diacetate stains intact plasma membranes of healthy cells; together, these markers have been shown to be more reliable than either lactate dehydrogenase or trypan blue exclusion in the assessment of cell injury.^{214,215} Mechanical strain led to increased propidium iodide staining of a sub-population of cells distributed diffusely on the culture membrane. The percentage of propidium iodide-stained cells increased with the frequency of mechanical strain (90 cycles, 30%) and with the amplitude of strain (90 cycles, 1 Hz) (Data not shown). This amplitude-dependence of cellular injury was also detected by dextran uptake (Figure 6.7); because dextran is retained only by cells whose membranes have resealed,^{160,162,216} these observations suggest transient, sublethal injury to cellular strain.

Figure 6.7. Dependence of cellular injury on mechanical strain. Fluoresceinated dextran uptake by cells for control and after 15%, and 30% amplitude strain (90 cycles, 1 Hz).

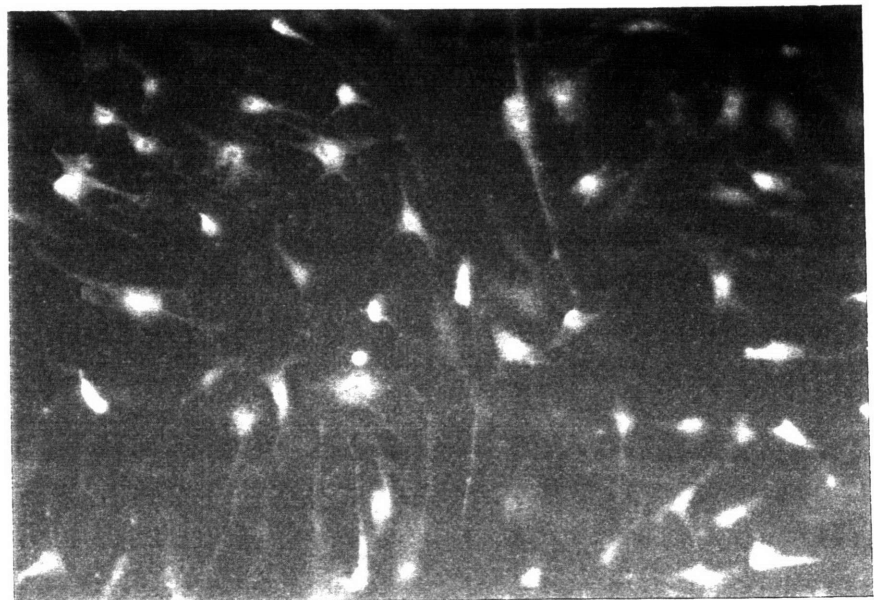
Control



15%



30%



6.4.4 Role of Matrix Reservoir in FGF-2 Release.

Heparin-like molecules and certain matrix degradative enzymes have been shown to either release FGF-2 pre-bound to the low-affinity receptors or compete with these receptors for binding of free FGF-2¹⁷³; in control experiments, treatment of quiescent smooth muscle cells by heparin, heparitinase, or heparan sulfate caused comparable release of FGF-2 (~ 1% of the total) into the media (data not shown). To evaluate the relative contributions by the intracellular and the low-affinity receptor FGF-2 pools to the mechanical release of FGF-2, cells were pretreated with heparin (5 µg/ml) before mechanical strain. Heparin treatment released less than 1% of the total cellular FGF-2 (Figure 6.8). Mechanical strain (90 cycles, 30%, 1 Hz) after heparin treatment released $12.6 \pm 1.6\%$ of the total initial cellular FGF-2 (vs. $15.8 \pm 0.9\%$ for strain alone, $p < 0.05$). Thus, most FGF-2 was released into the media from the nuclear or cytoplasmic pools and not from the low-affinity receptors.

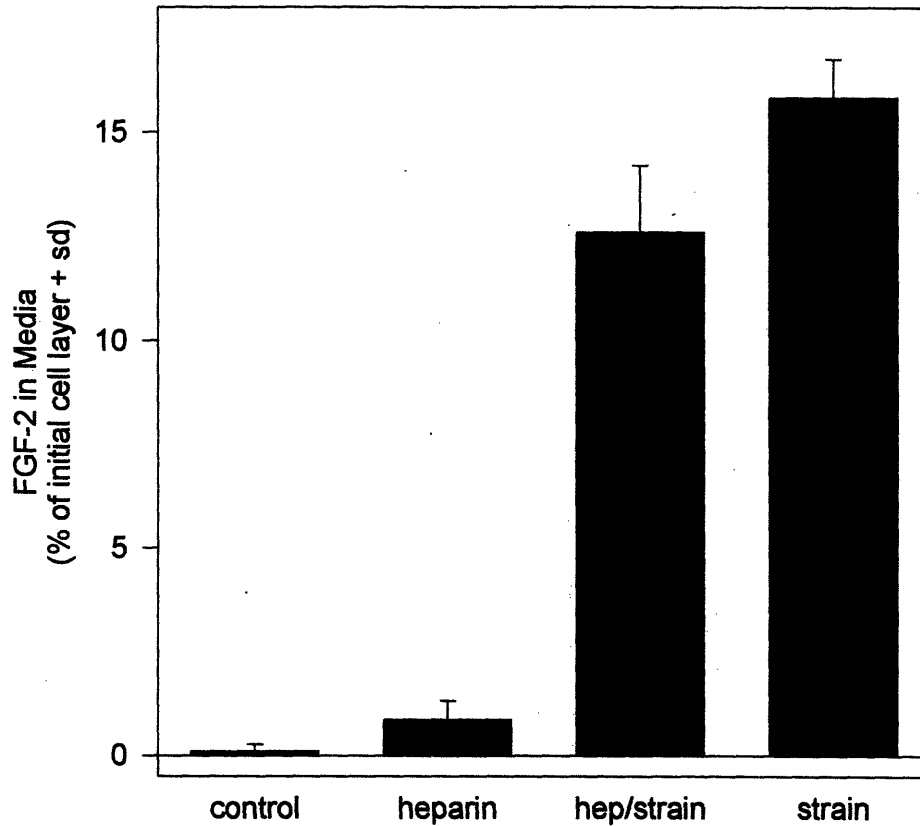


Figure 6.8. Effect of pre-treatment with heparin on FGF-2 release from human vascular smooth muscle cells in response to mechanical strain. FGF-2 in the media is increased in media by heparin treatment (second column). Strain (90 cycles, 1 Hz, 30%) after heparin pre-treatment caused release of FGF-2 (third column) that was less than that caused by strain alone (fourth column).

To assess the amount of FGF-2 that is sequestered by the low-affinity receptors after mechanical release, cells were exposed to strain (90 cycles, 30%, 1 Hz) and incubated with heparin (5 $\mu\text{g/ml}$) to block receptor binding of the FGF-2 as it was being released. After 60 min., media with and without heparin, respectively, contained $25.2 \pm$

3.5% and $15.6 \pm 2.6\%$ ($p < 0.05$) of the total initial cellular FGF-2 (Figure 6.9). Conversely, parallel cells were exposed to strain, incubated for one hour, and treated with fresh, heparin-supplemented media to liberate any FGF-2 that was potentially transferred by mechanical strain to the low-affinity receptors. Media with and without heparin, respectively, contained 11.0 ± 0.7 and $4.2 \pm 0.1\%$ ($p < 0.001$) of the total initial cellular FGF-2. Thus, approximately one-third of the mechanically released FGF-2 was subsequently bound to the low-affinity receptors. In addition, the relative distribution of released FGF-2 to the extracellular media and receptor pools was dependent on the amplitude of strain (90 cycles, 1 Hz); mechanical strain of 5% amplitude transferred no intracellular FGF-2 to either the media or receptors (Figure 6.10); 15% strain released FGF-2 that was distributed approximately equally to the media and receptors; 30% strain led to a three-fold increase in media FGF-2 with no additional transfer to the receptors beyond that associated with 15% strain, suggesting saturation of the receptor pool by 15% strain.

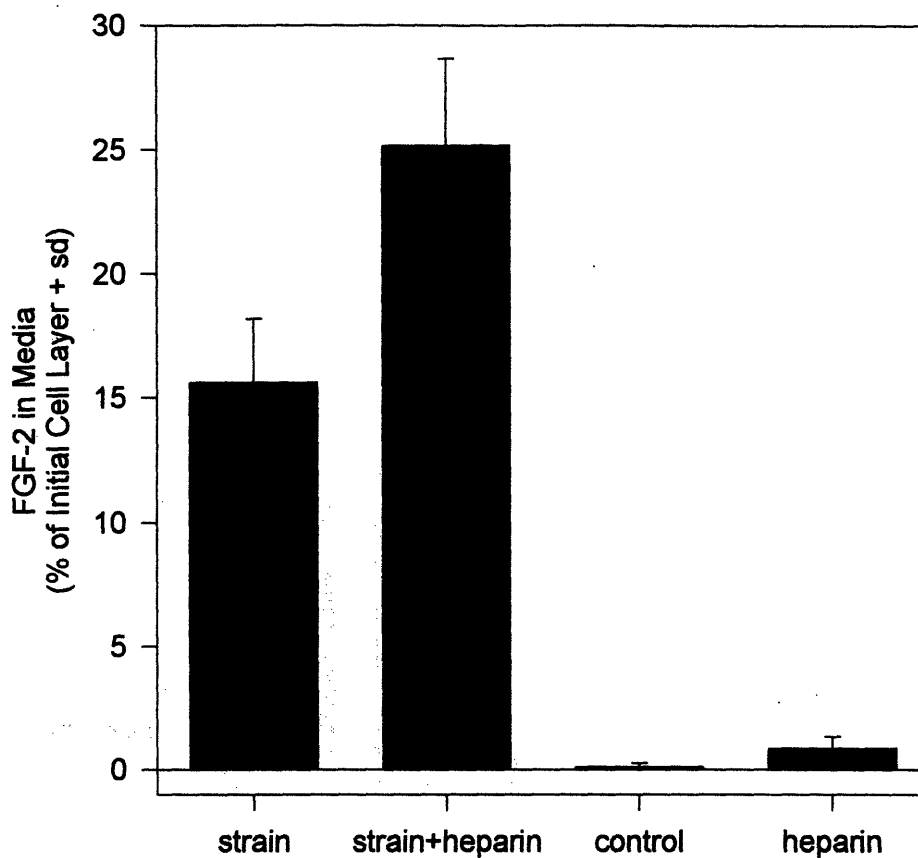


Figure 6.9. Ability of heparin to increase FGF-2 in the culture media after mechanical strain. Human vascular smooth muscle cells were subjected to strain (90 cycles, 1 Hz, 30%) or received no mechanical strain and further incubated in the presence or absence of heparin (5 $\mu\text{g}/\text{mL}$). After 60 min. FGF-2 in the media was increased by heparin treatment (column 2). Strain in the presence of heparin (column 4) released a greater amount of FGF-2 than strain alone (column 3). Data represent mean + sd for $n = 3$.

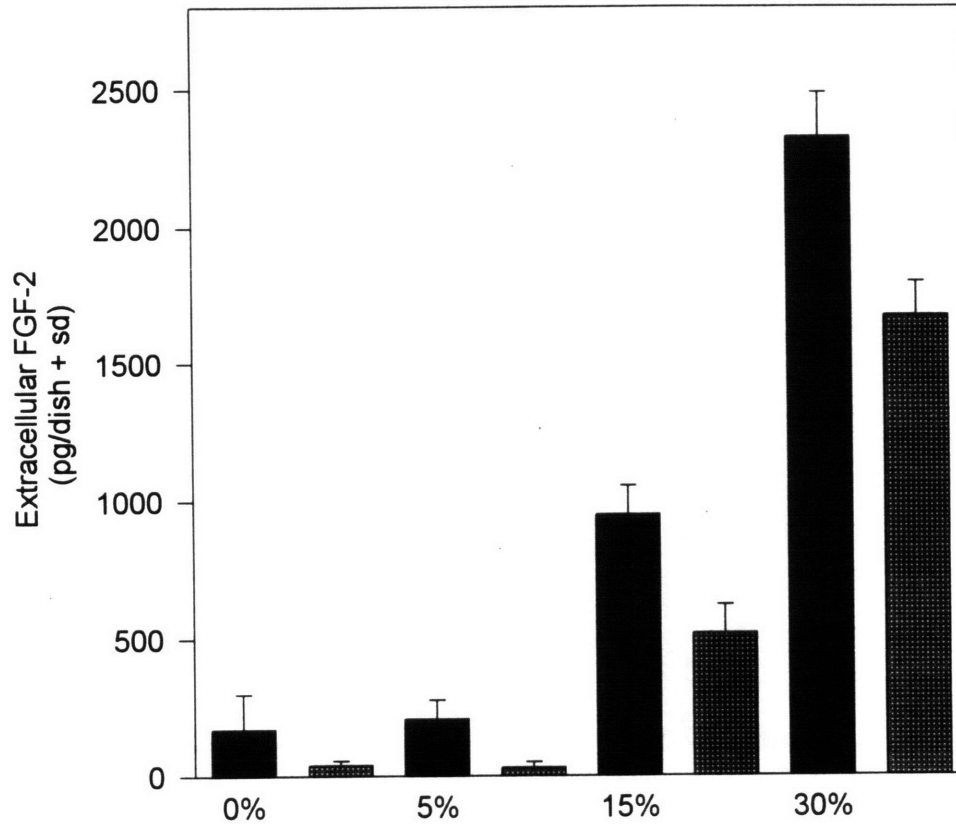


Figure 6.10. Transfer of FGF-2 to media and low-affinity receptors by mechanical strain of 5%, 15%, and 30% amplitude. FGF-2 in the media 60 min. after mechanical strain (90 cycles, 1 Hz) in the presence (black column) or absence (gray) of heparin (5 $\mu\text{g}/\text{ml}$). After 5% strain (second pair of columns), FGF-2 was not increased in the media (gray column) or low-affinity receptor pool (difference between gray and black columns). Strain of 15% amplitude (third pair of columns) increased FGF-2 in both the media and receptor pool; however strain of 30% amplitude (fourth pair of columns) caused further increase of FGF-2 in the media only. Data represent mean + sd for $n = 3$.

6.4.5 Localization of Release.

Immunofluorescence staining for FGF-2 in basal control human vascular smooth muscle cells revealed nuclear and cytoplasmic FGF-2 pools; control staining conditions

demonstrated the nuclear staining was specific. Although, staining of the nucleus was more intense than of the cytoplasm, the relative intracellular distributions are difficult to assess from staining intensity. To localize the mechanical release of intracellular FGF-2, cells were stained for FGF-2 after strain (90 cycles, 1 Hz, 15%) and incubated for 60 min. with heparin. FGF-2 staining was less intense in the strained cells, particularly in the nuclei, than in the unstrained control cells; however, staining intensity was consistent among neighboring cells on the same membrane. Thus, mechanical release of FGF-2 may involve a transfer of FGF-2 both from nucleus to cytoplasm and from cytoplasm to the extracellular pools. Although the staining is consistent with FGF-2 being released uniformly from cells (in contrast to the cell injury distribution), the localization of release can only be assessed with more accurate quantification of the nuclear and cytoplasmic FGF-2 pools before and after strain.

6.5 Discussion

Although FGF-2 is an ubiquitous cytokine which can mediate a variety of cellular responses *in vitro*, the regulation of its release and thus the importance of this angiogenic growth factor *in vivo* is incompletely understood. FGF-2 has been referred to as a "wound hormone" by McNeil and colleagues, who made the important observation that FGF-2 is released by mechanical injury to cells. Studies by that group^{11,161,162} and others demonstrate cellular release of FGF-2 by both overt trauma and mild mechanical stimuli, suggesting that FGF-2 may serve important but potentially different roles in physiologic and pathologic states.

The present data demonstrate tight control of FGF-2 release by cellular strain and are summarized as follows. First, release of FGF-2 was regulated by a strain-amplitude threshold. At amplitudes below 10%, prolonged ($\sim 10^5$ cycles at 1 Hz) oscillatory strain did not cause release of FGF-2; however, brief ($\sim 10^2$ cycles) oscillatory strain above 10% amplitude induced rapid release of the growth factor. Second, when strain exceeded 10% amplitude, FGF-2 release increased with the amplitude. Third, release of FGF-2 increased with the frequency of strain. Fourth, release increased with the number of cycles of strain but was maximal for a relatively brief stimulus (10^2 cycles, 1 Hz). FGF-2 release began within 5 minutes of the onset of strain and was complete within ~ 150 minutes even for prolonged (10^5 cycles) of oscillatory strain. Taken together, these data suggest that sustained oscillatory cellular strain above an amplitude threshold induces an acute FGF-2 release response. Additionally, FGF-2 release does not continue with repeated cycles of strain, but rather the response is finite and determined specifically by the frequency and amplitude of the early (10^2 cycles) mechanical stimulus.

The rapid and finite nature of the FGF-2 release response to cellular strain is consistent with a cell injury-mediated mechanism. Cellular injury occurred in parallel with FGF-2 release; a sub-population of cells was injured for strain above an amplitude threshold of 10%, and increased with the amplitude and frequency of strain. One interpretation of these observations is that cellular injury is determined independently by the strain amplitude and frequency. Alternatively, cellular injury may be determined by a single parameter, the strain rate. It is important to distinguish frequency of strain from strain-rate; for sinusoidal strain oscillation ($e = e \sin \omega t$), the strain rate is a sinusoidal function whose amplitude depends on both frequency and the amplitude of strain ($de/dt =$

$\epsilon \cos \omega t$). Thus, in the experiments assessing amplitude dependence, the strain amplitude was not changed without also changing strain rate; amplitude dependence could be tested by adjusting the frequency accordingly to maintain a constant strain rate amplitude. Injury to astrocytes by a single strain impulse of constant magnitude increases with the strain rate.²¹³ Mechanical failure of engineering construction materials is typically a function of the amplitude, strain rate, and number of cycles of strain.

Cells subjected to external mechanical manipulation, such as scraping^{161,195} or puncture,¹⁶² suffer transient resealable cell membrane disruptions through which FGF-2 may be released. Our experiments demonstrate that cellular perturbation via the underlying culture substrate induces a transient increase in cell membrane permeability.^{162,217} Although plasma membrane disruptions were not localized, one possible scenario is that mechanical failure occurs near integrins at focal adhesions as they transmit forces from the underlying matrix.^{82,218,219} The process may be similar to the disruption and detachment of focal adhesions observed at the trailing edge of migrating cells;²²⁰ migration is associated with release of intracellular FGF-2 possibly through permeabilized cell membranes.²⁰⁰

In addition to the intracellular FGF-2 pool, the extracellular receptor-bound FGF-2 also was hypothesized to be a potential source of mechanically releasable growth factor. FGF-2 binds to both high affinity signaling receptors and with lower affinity to heparan sulfate and other cell surface proteoglycans^{201,202} These low-affinity receptors may serve potentially as a high capacity reservoir for FGF-2 which may be released by enzymatic degradation^{204,207}. Binding of the low-affinity receptors to free FGF-2 may be competitively inhibited by heparin and heparin-like molecules. In these experiments,

treatment with heparin, heparan sulfate, or heparitinase demonstrated release of FGF-2 primarily from the intracellular compartment, with only a small fraction arising from the low-affinity receptor binding. It is important to note that the relative baseline intracellular and extracellular distributions of FGF-2 may be altered by cell density or other culture conditions.²¹² In addition, the monolayer cell culture may not adequately simulate FGF-2 binding to and potential mechanical release from a three-dimensional matrix *in vivo*.

The low-affinity receptors are required for some FGF-induced biological responses and may help stabilize,²²¹ present, and promote binding of the growth factor to the high-affinity signaling receptors.²⁰³ Subsequent dimerization of the high-affinity receptors may also depend on interactions with these proteoglycans.²²² Another function of the low-affinity receptors may be to minimize FGF-2 diffusion away from the site of release.²⁰² Previous studies suggest the potential for the level of FGF-2 in the culture medium to underestimate total FGF release.^{200,208} In this study, mechanical strain induced the transfer of FGF-2 from the intracellular cytoplasmic pool to the extracellular receptors. In response to mechanical strain of 15% amplitude, the majority of the released FGF-2 was distributed to the receptors; FGF-2 released by 30% strain saturated the receptors and was partially distributed to the culture medium. Thus, the low-affinity receptors can increase the effective concentration of the growth factor near the site of release, presumably enhancing the probability of interactions with the high affinity receptors. The role of cell surface proteoglycans in concentrating FGF-2 near the site of injury may be particularly important for targeting appropriate angiogenic responses.²²³ In addition, the properties of the mechanical strain may determine the extent to which the released FGF-2 may diffuse to more distant target cells.

The dependence of FGF-2 release on mechanical strain suggests a potential model for the regulation of FGF-2 release in physiologic and pathophysiologic vascular states. Under long-term, oscillatory deformation, vascular smooth muscle cells may synthesize and maintain an intracellular FGF-2 pool of which little is released. This reservoir remains intact and is depleted only when cellular strain exceeds an amplitude threshold. Under conditions of elevated heart rate or of mechanical stress such as hypertension or at focal regions of atherosclerotic plaque,^{37,46,47} the strain rate may be sufficient to injure a subset of cells which then rapidly release FGF-2. Under conditions of extremely high mechanical strain such as during balloon angioplasty, a majority of cells may be injured, releasing a large amount of FGF-2.

Interestingly, neighboring cells exposed to nearly identical membrane substrate strain were nonuniformly injured, reflecting possible differences in *intracellular* strains. Vascular smooth muscle exposed to biaxial deformation experience higher local strains in the pseudopods than in the cell body.²²⁴ Because the strain profile in a given cell under these experimental conditions may depend on its particular cytoskeletal arrangement and focal adhesion distribution, sensitivity to injury may be variable within a population of cells. The sensitivity to injury and the potential release of FGF-2 by mechanical strain may also be cell type-specific. Additional studies with other cell types may further clarify the functions of FGF-2 in different conditions in vivo.

Responses to mechanical loading have been studied in vascular smooth muscle and other types of cells using a variety of devices. Mediated by various signal transduction mechanisms,^{54,149,182,225} the observed responses include early gene induction,^{151,226} proliferation,^{71,227,228} morphologic changes,^{229,230} matrix metabolism,^{73,74} and release of

growth factors and other cytokines.¹⁹⁹ Despite the diversity of these responses, the experiments of this chapter imposing a homogeneous and uniform biaxial strain to all cells within a culture well suggest that specific components of the applied strain may be critical regulatory parameters. Previous studies that apply an oscillatory but spatially nonhomogeneous cellular strain, while precisely controlling the frequency of oscillation, do not control either the strain amplitude or the strain rate. Under such conditions, the precise mechanical control of a cellular response may be difficult to discern if the response is strain amplitude- or strain rate-dependent. In addition, the observed response may not be directly controlled by mechanical strain but may be modulated in a paracrine fashion by a second co-existing strain amplitude- or strain rate-dependent response such as FGF-2 release. Thus, the application of uniform mechanical stimulation may be critical for understanding the regulation of certain mechanoresponses.

This study may have potential implications for the clinical management of atheroma. Current treatment of atherosclerotic lesions by balloon angioplasty is often followed by late restenosis,^{130,231} and animal models of vascular injury suggest that intimal thickening is dependent on the severity of vascular injury and the magnitude of FGF-2 release.⁴⁸ The amplitude and frequency-dependence we have observed suggest that smooth muscle cell injury and FGF-2 release after angioplasty may be regulated by the rate and magnitude of vascular dilation. Thus, further understanding the dependence of injury on the rate and number of inflations as well as the balloon size may help improve angioplasty strategies.

In conclusion, this chapter summarizes experiments performed to further characterize FGF-2 release by human vascular smooth muscle cells under mechanical

deformation and addresses some of the questions raised in Chapter 4. FGF-2 release was dependent on the frequency, amplitude, and number of cycles of mechanical strain. Injury to a sub-population of cells randomly distributed on the membrane was detected immediately after brief dynamic strain using methods more sensitive than those used in the previous chapter. Although the extracellular low-affinity receptors were not a major source of mechanically released FGF-2, these receptors effectively sequestered growth factor after release.

Conclusions

7.1 Summary of Experiments: Relevance to Disease

7.1.1 Reorganization of Matrix.

The experiments of Chapter 2 assessed the mechanical influence of vascular smooth muscle cells on their surrounding matrix. While adhesion to collagen was mediated by two ($\alpha^1\beta_1$, $\alpha^2\beta_1$) of the four β_1 integrins expressed by these cells. However, contraction and reorganization of a three-dimensional collagen matrix depended on only the $\alpha^2\beta_1$ integrin. In addition, an anti- β_1 antibody known for its stimulatory effect on collagen adhesion was found to inhibit gel contraction, suggesting that reorganization of matrix involves a dynamic cycling of integrin-matrix interactions, perhaps similar to integrin-mediated cell migration.^{220,232} These results suggest that smooth muscle cells *in vivo* participate in tissue remodeling through the function of specific integrins. Selective targeting of integrin-matrix interactions, through local delivery of antibodies or peptides, may be a useful strategy for modulating early remodeling activities in atherosclerosis and other diseases.^{233,234}

7.1.2 Mechanical Response in Three-dimensional Matrix.

In addition to mechanically altering the collagen matrix, vascular smooth muscle cells were also metabolically responsive to mechanical loading of the matrix. Static compression of vascular smooth muscle cell-collagen gel cultures decreased DNA and

glycosaminoglycan synthesis. Although the mechanism for decreased biosynthesis was not assessed, one possibility may be related to the general inhibition of cellular activity by a three-dimensional matrix.^{38,88,92,93,100,235} Gel compression in these experiments may have decreased the cellular responsiveness to growth factors by increasing the matrix concentration.⁹⁴ In addition, these data suggest that elevated arterial pressure would inhibit cellular proliferation and matrix synthesis, despite the accelerated medial hypertrophy observed with hypertension. This apparent discrepancy might be accounted for by numerous factors, including the absence of a superimposed oscillatory deformation in the compression experiment.

A single, brief transient compression of the gel cultures caused an FGF-2-mediated, delayed induction of DNA synthesis that was dependent on the magnitude of imposed gel strain. This mechanical loading is qualitatively similar to vessel dilation during balloon angioplasty. Although the participation of FGF-2 in intimal smooth muscle hyperplasia has been demonstrated in vivo, this thesis assessed the specific role of smooth muscle cell responses to mechanical strain. Interestingly, only part of the DNA synthetic response appeared to be mediated by FGF-2. There was a dose-dependent inhibition of compression-induced DNA synthesis by a monoclonal antibody against FGF-2, but only partial inhibition was achieved. In addition, the concentration of FGF-2 measured in conditioned media after compression was not sufficient to induce a DNA synthetic response when added exogenously to control cells. PDGF has been shown to participate in growth responses to mechanical loading,^{71,199} but was not found to play a role in our experiments.

Surprisingly, cellular injury was not detected in association with transient compression. Previous studies have demonstrated FGF-2 release by cellular injury; FGF-2 lacks a secretory leader sequence and is distributed diffusely in the cytoplasm, and a cell injury-release model is consistent with the vascular injury associated with restenosis models. However, due to a number of factors, the possibility of cell injury by transient gel culture compression could not be excluded. Lactate dehydrogenase and total DNA content were, at best, crude markers of cell death. Thus, focal cell death or generalized sublethal cell injury, as has been associated with FGF-2 release,^{160,195} might not be detected by these methods. The presence of the three-dimensional matrix created a couple obstacles. The potential for matrix to bind FGF-2 suggested that the level of FGF-2 measured in the media might underestimate the magnitude of FGF-2 released and the extent of cell injury. In addition, the optical opacity of the dense matrices prevented visual assessment of cell morphology.

7.1.3 Role of Cellular Strain.

The experiments of the Chapters 3 and 4 demonstrated a dependence of cellular responses on the matrix strain, suggesting functional control by cellular strain. In the experiments of Chapters 5 and 6, the tensile biaxial strain device was used instead of the gel culture compression configuration for several reasons. First, homogeneous and biaxially uniform strain could be applied to cells. Second, both static and oscillatory strains of varying frequencies were possible. Third, changes in morphology and cellular injury could be microscopically detected.

Preliminary experiments demonstrated that FGF-2 and IL-1 α , molecules which lack secretory leader sequences, are released by cellular strain of smooth muscle cells and

keratinocytes, respectively. The mechanical release of IL-1 α may be relevant to the pathophysiology of psoriasis. Psoriasis is manifested primarily in extensor joint surfaces of the extremities, and psoriatic symptoms are expressed by a transgenic mouse which over-expresses IL-1 α . Further characterization of the FGF-2 release response revealed a strain-amplitude threshold for both FGF-2 release and cell injury. *In vivo*, vessel wall dilation typically does not exceed 5-10% suggesting that the amplitude-threshold for FGF-2 release may be a stringent requirement satisfied only during balloon angioplasty; however, as discussed in Chapter 5, variations in tissue structure at the cellular level may result in a sub-population of cells receiving strains higher than the macroscopic tissue strain. In addition, structural heterogeneities in plaque may cause concentrations of strain. Furthermore, random variations in intraluminal pressure may momentarily increase the strains within some cells. As demonstrated by the experiments of Chapter 6, strain need only exceed the amplitude-threshold for ~ 1 minute to induce maximal FGF-2 release. In addition, FGF-2 release is limited and does not continue two hours after initiation of the elevated strain. Once released, FGF-2 may be sequestered near the release site by the low-affinity receptors. Thus, in certain vascular conditions, FGF-2 may be released from smooth muscle cells in a temporally and spatially targeted fashion.

7.2 Limitations and Future Work

7.2.1 Integrins in Cellular Responses.

Although Chapter 2 demonstrated the role of collagen-specific integrins in transmitting the forces from cell to matrix, force transmission and signal transduction from matrix to cell may rely on different integrins. The mechanical induction of DNA synthesis

via autocrine PDGF in vascular smooth muscle cells is mediated by fibronectin-specific integrins²¹⁸ even when the cells are grown on collagen. Experiments imposing mechanical strain to cells on various matrices in the presence of integrin-blocking antibodies and peptides may clarify the role of integrins in FGF-2 release as well as other responses to strain.

7.2.2 Growth Factor Responsiveness.

The experiments of Chapters 3 and 4 raise additional questions concerning the regulation of cellular responses by mechanical loading. Although static compression decreased DNA synthesis, and transient compression increased DNA synthesis, both forms of loading should have similar effects on FGF-2 release. Assuming that FGF-2 is released during sustained static compression, the differential response in DNA synthesis to static and transient compression may suggest regulation of growth factor responsiveness by strain. Experiments could be performed in both monolayer and three-dimensional matrix culture to assess whether changes in cellular strain and/or matrix concentration (through matrix compression) regulate cellular responses to exogenous growth factor.

7.2.3 Tissue Stress and Cellular Strain.

Although mechanical stress is commonly considered an important modulator of biological function, under certain conditions, stress applied to a tissue may be an insignificant parameter to a given cell. For example, dramatically elevated intravascular pressure might not affect vascular smooth muscle cell function if the vessel wall compliance is diminished. Interpretation of *in vivo* responses to mechanical stress might require not only careful control of the stress, but also a knowledge of the tissue compliance or the specific cellular strains. Altering the biaxial strain device to

dynamically modulate the pressure of the culture medium might further clarify whether bulk stress in addition to cellular strain independently regulates cell function. In the absence of cellular deformation, changes in cellular function with ambient fluid pressure would be surprising.

7.2.4 Substrate Deformation and Cellular Strain.

The monolayer biaxial strain device in Chapter 5 was used in part to impose more uniform cellular strains. Measured membrane strains were homogeneous and biaxially uniform for dynamic deformations, and average cellular strains under static deformation correlated with the predicted membrane strain. However, intracellular strains may deviate from that of the underlying culture substrate depending on the number and distribution of focal adhesions.²²⁴ Additionally, the cellular strain behavior under dynamic membrane deformation has yet to be characterized. The ability to continuously observe cell morphology during dynamic culture membrane deformation would be necessary to verify the presumed correspondence between cellular and membrane strains.

7.2.5 Improving the Three-Dimensional Configuration.

Ultimately, the presence of a three-dimensional matrix may be important for simulating certain in vivo cell-matrix interactions during mechanical loading. Compression of the collagen gel culture was useful for studying responses to static and transient loading, but was unsuitable for applying oscillatory deformations. In principle, the gel culture could be adapted to a different configuration of mechanical loading to achieve cyclic deformation.

7.2.6 Injury and IL-1 Release.

The experiments in Chapters 5 and 6 demonstrate the ability of mechanical strain to release molecules (FGF-2 and IL-1) which lack secretory leader sequences. The mature form of IL-1 is similar in size and tertiary structure to FGF-2, suggesting that both molecules may be released from cells in a similar manner. Mechanical strain experiments with other cells, particularly transfected cell lines with either the pro or mature forms of IL-1 may elucidate the mechanism of release. One possible scenario may be that the mature form of IL-1 is released preferentially over the pro-form due to size selection by cell membrane disruption.

7.2.7 Other Responses.

Many of the experiments in this thesis may have been performed in a “high” strain regime for these cells. Mechanical strain below the threshold for injury may control other functions besides FGF-2 release. Additional experiments at lower strain levels may elucidate the role of the mechanical environment in non-FGF-2-induced signal transduction events and expression of immediate-early genes,^{151,236} chemotactic factors,¹⁸ degradative enzymes,²³⁷ and other mediators of atherosclerotic remodeling.

References

1. Brighton CT, Straffort B, Gross SB, Leatherwood DF, Williams JL, Pollack S: Proliferative and synthetic response of isolated calvarial bone cells of rats to cyclic biaxial mechanical strain. *J Bone Joint Surg* 1991;73-A(3):320-331.
2. Schaffer JL, Rizen M, L'Italien GJL, Benbrahim A, Megerman J, Gerstenfeld LC, Gray ML: Device for the application of a dynamic biaxially uniform and isotropic strain to a flexible cell culture membrane. *J Ortho Res* 1993;12:709-719.
3. Neidlinger-Wilke C, Wilke Hans-J, Claes L: Cyclic stretching of human osteoblasts affects proliferation and metabolism: a new experimental method and its application. *J Ortho Res* 1994;12:70-78.
4. Carvalho RS, Scott JE, Yen EH: The effects of mechanical stimulation on the distribution of beta 1 integrin and expression of beta 1-integrin mRNA in TE-85 human osteosarcoma cells. *Archives of Oral Biology* 1995;40:257-264.
5. Sah RL-Y, Kim Young-J, Doong Joe-YH, Grodzinsky AJ, Plaas AHK, Sandy JD: Biosynthetic response of cartilage explants to dynamic compression. *J Ortho Res* 1989;7:619-636.
6. Buschmann MD, Gluzband YA, Grodzinsky AJ, Kimura JH, Hunziker EB: Chondrocytes in agarose culture synthesize a mechanically functional extracellular matrix. *J Ortho Res* 1992;10:745-758.
7. Kolpakov V, Rekhter MD, Gordon D, Wang WH, Kulik TJ: Effect of mechanical forces on growth and matrix protein synthesis in the in vitro pulmonary artery: analysis of the role of individual cell types. *Circ Res* 1995;77:823-831.
8. Pender N, McCulloch CA: Quantitation of actin polymerization in two human fibroblast sub-types responding to mechanical stretching. *J Cell Sci* 1991;100:187-193.
9. Lee TL, Lin YC, Mochitate K, Grinnell F: Stress-relaxation of fibroblasts in collagen matrices triggers ectocytosis of plasma membrane vesicles containing actin, annexins II and VI, and beta I integrin receptors. *J Cell Sci* 1993;105:167-177.
10. Sadoshima J, Jahn L, Takahashi T, Kulik TJ, Izumo S: Molecular characterization of the stretch-induced adaptation of cultured cardiac cells: an in vitro model of load-induced cardiac hypertrophy. *J Biol Chem* 1992;267:10551-10560.

11. Clarke MSF, Caldwell RW, Chiao H, Miyake K, McNeil PL: Contraction-induced cell wounding and release of fibroblast growth factor in heart. *Circ Res* 1995;76:927-934.
12. Kaye D, Pimental D, Prasad S, Mäki T, Berger Hans-J, McNeil PL, Kelly RA, Smith TW: Role of transiently altered sarcolemmal membrane permeability and bFGF release in the hypertrophic response of adult rat ventricular myocytes to increased mechanical activity in vitro. *J Clin Invest* 1995.
13. Yamazaki T, Komuro I, Kudoh S, Zou Y, Shiojima I, Mizuno T, Takano H, Hiroi Y, Ueki K, Tobe K, Kadowaki T, Nagai R, Yazaki Y: Angiotensin II partly mediates mechanical stress-induced cardiac hypertrophy. *Circ Res* 1995;77:258-265.
14. Cheng W, Li B, Kajstura J, Li P, Wolin MS, Sonnenblick EH, Hintze TH, Olivetti G, Anversa P: Stretch-induced programmed myocyte cell death. *J Clin Invest* 1995;96:2247-2259.
15. Perrone CE, Fenwick-Smith D, Vandeburgh HH: Collagen and stretch modulate autocrine secretion of insulin-like growth factor-1 and insulin-like growth factor binding proteins from differentiated skeletal muscle cells. *J Biol Chem* 1995;270:2099-2106.
16. Clarke MSF, Feedback DL: Mechanical load induces sarcoplasmic wounding and FGF release in differentiated human skeletal muscle cultures. *FASEB J* 1996;10:502-509.
17. Zhao S, Suci A, Ziegler T, Moore JE, Bürki E, Meister Jean-J, Brunner HR: Synergistic effects of fluid shear stress and cyclic circumferential stretch on vascular endothelial cell morphology and cytoskeleton. *Arterioscler Thromb Vasc Biol* 1995;15:1781-1786.
18. Wang DL, Wung BS, Shyy YJ, Lin CF, Chao YJ, Usami S, Chien S: Mechanical strain induces monocyte chemotactic protein-1 gene expression in endothelial cells. Effects of mechanical strain on monocyte adhesion to endothelial cells. *Circ Res* 1995;77:294-302.
19. Awolesi MA, Sessa WC, Sumpio BE: Cyclic strain upregulates nitric oxide synthase in cultured bovine aortic endothelial cells. *J Clin Invest* 1995;96:1449-1454.
20. Ross R: The pathogenesis of atherosclerosis: a perspective for the 1990s. *Nature* 1993;362:801-809.

21. Fuster V, Badimon L, Badimon JJ, Chesebro JH: The pathogenesis of coronary artery disease and the acute coronary syndromes. *N Engl J Med* 1992;326:242-250.
22. Chesebro JH, Zoldhelyi P, Fuster V: Plaque disruption and thrombosis in unstable angina pectoris. *Am J Cardiol* 1991;68:9C-15C.
23. Falk E: Why do plaques rupture. *Circulation* 1992;86:30-42.
24. Davies MJ, Thomas AC: Plaque fissuring: the cause of acute myocardial infarction, sudden ischaemic death, and crescendo angina. *Br Heart J* 1985;53:363-373.
25. Ambrose JA: Plaque disruption and the acute coronary syndromes of unstable angina and myocardial infarction: if the substrate is similar, why is the clinical presentation different? *J Am Coll Cardiol* 1992;19:1653-1658.
26. Sanders M: Molecular and cellular concepts in atherosclerosis. *Pharmacological Therapeutics* 1994;61:109-153.
27. Wight TN: Cell biology of arterial proteoglycans. *Arteriosclerosis* 1989;9:1-20.
28. Ylä-Herttuala S, Sumuvuori H, Karkola K, Möttönen M, Nikkari T: Glycosaminoglycans in normal and atherosclerotic human coronary arteries. *Lab Invest* 1986;54:402-407.
29. Hurt-Camejo E, Camejo G, Rosengren B, López F, Ahlström C, Fager G, Bondjers G: Effect of arterial proteoglycans and glycosaminoglycans on low density lipoprotein oxidation and its uptake by human macrophages and arterial smooth muscle cells. *Arterioscler Thromb* 1992;12:569-583.
30. Radhakrishnamurthy B, Srinivasan SR, Vijayagopal P, Berenson GS: Arterial wall proteoglycans--biological properties related to pathogenesis of atherosclerosis. *Eur Heart J* 1990;11:148-157.
31. Sperti G, van Leeuwen RTJ, Quax PHA, Maseri A, Kluft C: Cultured rat aortic vascular smooth muscle cells digest naturally produced extracellular matrix. *Circ Res* 1992;71:385-392.
32. Henney AM, Wakeley PR, Davies MJ, Foster K, Hembry R, Murphy G, Humphries S: Localization of stromelysin gene expression in atherosclerotic plaques by in situ hybridization. *Proc Natl Acad Sci USA* 1991;88:8154-8158.
33. Galis ZS, Sukhova GK, Lark MW, Libby P: Increased expression of matrix metalloproteinases and matrix degrading activity in vulnerable regions of human atherosclerotic plaques. *J Clin Invest* 1994;94:2493-2503.

34. Bendeck MP, Zempo N, Clowes AW, Galardy RE, Reidy MA: Smooth muscle cell migration and matrix metalloproteinase expression after arterial injury in the rat. *Circ Res* 1994;75:539-545.
35. Galis ZS, Sukhova GK, Kranzhöfer R, Clark S, Libby P: Macrophage foam cells from experimental atheroma constitutively produce matrix-degrading proteinases. *Proc Natl Acad Sci USA* 1994;92:402-406.
36. Libby P, Sukhova G, Lee RT, Galis Z: Cytokines regulate vascular functions related to stability of the atherosclerotic plaque. *J Card Pharm* 1994;in press.
37. Cheng GC, Loree HM, Kamm RD, Fishbein MC, Lee RT: Distribution of circumferential stress in ruptured and stable atherosclerotic lesions. *Circulation* 1993;87:1179-1187.
38. Schlumberger W, Thie M, Rauterberg J, Robenek H: Collagen synthesis in cultured aortic smooth muscle cells. Modulation by collagen lattice culture, transforming growth factor- β 1, and epidermal growth factor. *Arterioscler Thromb* 1991;11:1660-1666.
39. Amento EP, Ehsani N, Palmer H, Libby P: Cytokines and growth factors positively and negatively regulate interstitial collagen gene expression in human vascular smooth muscle cells. *Arterioscler Thromb* 1991;11:1223-1230.
40. Yanagi H, Sasaguri Y, Sugama K, Morimatsu M, Nagase H: Production of tissue collagenase (matrix metalloproteinase 1) by human aortic smooth muscle cells in response to platelet-derived growth factor. *Atherosclerosis* 1991;91:207-216.
41. Galis ZS, Muszynski M, Sukhova GK, Simon-Morrissey E, Unemori EN, Lark MW, Amento E, Libby P: Cytokine-stimulated vascular smooth muscle cells synthesize a complement of enzymes required for extracellular matrix digestion. *Circ Res* 1994;75:181-189.
42. Ross R: Polypeptide growth factors and atherosclerosis. *Trends Cardiovasc Med* 1991;1:277-282.
43. Reidy MA: Factors controlling smooth muscle cell proliferation. *Arch Pathol Lab Med* 1992;116:1276-1280.
44. Rollins BJ, Yoshimura T, Leonard EJ, Pober JS: Cytokine-activated human endothelial cells synthesize and secrete a monocyte chemoattractant, MCP-1/JE. *Am J Pathol* 1990;136:1229-1233.
45. Sumpio B: Mechanical stress and cell growth. *J Vasc Surg* 1989;10:570-571.
46. Gibbons GH, Dzau VJ: The emerging concept of vascular remodeling. *N Engl J Med* 1994;330:1431-1438.

47. Doyle AE: Hypertension and vascular disease. *J Card Pharm* 1992;19:S7-S10.
48. Clowes AW, Reidy MA, Clowes MM: Mechanisms of stenosis after arterial injury. *Lab Invest* 1983;49:208-215.
49. Foegh ML, Virmani R: Molecular biology of intimal proliferation. *Current Opinion in Cardiology* 1993;8:938-950.
50. Asakura T, Karino T: Flow patterns and spatial distribution of atherosclerotic lesions in human coronary arteries. *Circ Res* 1990;66:1045-1066.
51. Langille L, O'Donnell F: Reductions in arterial diameter produced by chronic decreases in blood flow are endothelium-dependent. *Science* 1986;231:405-407.
52. Lipke DW, Couchman JR: Increased proteoglycan synthesis by the cardiovascular system of coarctation hypertensive rats. *J Cell Physiol* 1991;147:479-486.
53. Reynertson RH, Oparil S, Rodén L: Proteoglycans and hypertension: III: aorta proteoglycans in Dahl salt-sensitive hypertensive rats. *Am J Med Sci* 1987;293:171-176.
54. Davies PF, Tripathi SC: Mechanical stress mechanisms and the cell: an endothelial paradigm. *Circ Res* 1993;72:239-245.
55. Barbee KA, Davies PF, Lal R: Shear stress-induced reorganization of the surface topography of living endothelial cells imaged by atomic force microscopy. *Circulation* 1994;74:168-171.
56. Remuzzi A, Dewey CFJ, Davies PF, Gimbrone MAJ: Orientation of endothelial cells in shear fields in vitro. *Biorheology* 1984;21:617-630.
57. Davies PF, Dewey CFJ, Bussolari SR, Gordon EJ, Gimbrone MAJ: Influence of hemodynamic forces on vascular endothelial function. In vitro studies of shear stress and pinocytosis in bovine aortic cells. *J Clin Invest* 1984;73:1121-1129.
58. Ives CL, Eskin SG, McIntire LV: Mechanical aspects of endothelial cell morphology: in vitro assessment. *In Vitro Cellular and Developmental Biology -- Animal* 1986;22:500-507.
59. Kanda K, Matsuda T: Behavior of arterial wall cells cultured on periodically stretched substrates. *Cell Transplantation* 1993;2:475-484.
60. Malek AM, Izumo S: Physiological fluid shear stress causes downregulation of endothelin-1 mRNA in bovine aortic endothelium. *Am J Physiol* 1992;263:C389-C396.

61. Malek AM, Jackman R, Rosenberg RD, Izumo S: Endothelial expression of thrombomodulin is reversibly regulated by fluid shear stress. *Circ Res* 1994;74:852-860.
62. Malek AM, Gibbons GH, Dzau VJ, Izumo S: Fluid shear stress differentially modulates expression of genes encoding basic fibroblast growth factor and platelet-derived growth factor B chain in vascular endothelium. *J Clin Invest* 1993;92:2013-2021.
63. Diamond SJ, Sharefkin JB, Dieffenbach C, Frazier-Scott K, McIntire LV, Eskin SG: Tissue plasminogen activator messenger RNA levels increase in cultured human endothelial cells exposed to laminar shear stress. *J Cell Physiol* 1990;143:364-371.
64. Resnick N, Collins T, Atkinson W, Bonthron DT, Dewey CFJ, Gimbrone MAJ: Platelet-derived growth factor B chain promoter contains a cis-acting fluid shear stress-responsive element. *Proc Natl Acad Sci USA* 1993;90:4591-4594.
65. Lan Q, Mercurius KO, Davies PF: Stimulation of transcription factors NF kappa B and AP1 in endothelial cells subjected to shear stress. *BioTech* 1994;201:950-956.
66. Malek AM, Greene AL, Izumo S: Regulation of endothelin-1 gene by fluid shear stress is transcriptionally mediated and independent of protein kinase C and cAMP. *Proc Natl Acad Sci USA* 1993;90:5999-6003.
67. Davies PF, Remuzzi A, Gordon EJ, Dewey CFJ, Gimbrone MAJ: Turbulent fluid shear stress induces vascular endothelial cell turnover in vitro. *Proc Natl Acad Sci USA* 1986;83:2114-2117.
68. Leung DYM, Glagov S, Mathews MB: Cyclic stretching stimulates synthesis of matrix components by arterial smooth muscle cells in vitro. *Science* 1976;191:475-477.
69. Buck RC: Behavior of vascular smooth muscle cells during repeated stretching of the substratum in vitro. *Atherosclerosis* 1983;46:217-223.
70. Sumpio BE, Banes AJ: Response of porcine smooth muscle cells to cyclic tensional deformation in culture. *J Surg Res* 1988;44:696-701.
71. Wilson E, Mai Q, Krishnankutty S, Weiss RH, Ives HE: Mechanical strain induces growth of vascular smooth muscle cells via autocrine action of PDGF. *J Cell Biol* 1993;123:741-747.
72. Predel Hans-G, Yang Z, von Segesser L, Turina M, Bühler FR, Lüscher TF: Implications of pulsatile stretch on growth of saphenous vein and mammary artery smooth muscle. *Lancet* 1992;340:878-879.

73. Kulik TJ, Alvarado SP: Effect of stretch on growth and collagen synthesis in cultured rat and lamb pulmonary arterial smooth muscle cells. *J Cell Physiol* 1993;157:615-624.
74. Kollros PR, Bates SR, Mathews MB, Horwitz AL, Glagov S: Cyclic AMP inhibits increased collagen production by cyclically stretched smooth muscle cells. *Lab Invest* 1987;:410-417.
75. Sutcliffe MC, Davidson JM: Effect of static stretching on elastin production by porcine aortic smooth muscle cells. *Matrix* 1990;10:148-153.
76. Hynes RO: Integrins: Versatility, modulation, and signaling in cell adhesion. *Cell* 1992;69:11-25.
77. Chan BMC, Kassner PD, Schiro JA, Byers HR, Kupper TS, Hemler ME: Distinct cellular functions mediated by different VLA integrin a subunit cytoplasmic domains. *Cell* 1992;68:1051-1060.
78. Delvoye P, Wiliquet P, Leveque JL, Nusgens BV, Lapiere CM: Measurement of mechanical forces generated by skin fibroblasts embedded in a three-dimensional collagen gel. *J Invest Dermatol* 1991;97:898-902.
79. L'Heureux N, Germain L, Labbe R, Auger FA: In vitro construction of a human blood vessel from cultured vascular cells: a morphologic study. *J Vasc Surg* 1993;17:499-509.
80. Clyman RI, McDonald KA, Kramer RH: Integrin receptors on aortic smooth muscle cells mediate adhesion to fibronectin, laminin, and collagen. *Circ Res* 1990;67:175-186.
81. Clyman RI, Mauray F, Kramer RH: b1 and b3 integrins have different roles in the adhesion and migration of vascular smooth muscle cells on extracellular matrix. *Exp Cell Res* 1992;200:272-284.
82. Wang N, Butler JP, Ingber DE: Mechanotransduction across the cell surface and through the cytoskeleton. *Science* 1993;260:1124-1127.
83. Sims JR, Karp S, Ingber DE: Altering the cellular mechanical force balance results in integrated changes in cell, cytoskeletal and nuclear shape. *J Cell Sci* 1992;103:1215-1222.
84. Elsdale T, Bard J: Collagen substrata for studies on cell behavior. *J Cell Biol* 1972;54:626-637.
85. Delvos U, Gajdusek C, Sage H, Harker LA, Schwartz SM: Interactions of vascular wall cells with collagen gels. *Lab Invest* 1982;46:61-72.

86. Madri JA, Pratt BM, Tucker AM: Phenotypic modulation of endothelial cells by transforming growth factor- β depends upon the composition and organization of the extracellular matrix. *J Cell Biol* 1988;106:1375-1384.
87. Tomasek JJ, Hay ED, Fujiwara K: Collagen modulates cell shape and cytoskeleton of embryonic corneal and fibroma fibroblasts: Distribution of actin, α -actinin, and myosin. *Dev Biol* 1982;92:107-122.
88. Nusgens B, Merrill C, Lapiere C, Bell E: Collagen biosynthesis by cells in a tissue equivalent matrix in vitro. *Collagen Rel Res* 1984;4:351-364.
89. Mauch C, Adelman-Grill B, Hatamochi A, Krieg T: Collagenase gene expression in fibroblasts is regulated by a three-dimensional contact with collagen. *FEBS Lett* 1989;250:301-305.
90. Quarnström EE, Kinsella MG, MacFarlane SA, Page RC, Wight TN: Modulation of proteoglycan metabolism by human fibroblasts maintained in an endogenous three-dimensional matrix. *Eur J Cell Biol* 1992;57:101-108.
91. Ehrmann RL, Gey GO: Growth of cells on a transparent gel of reconstituted rat-tail collagen. *J Nat Cancer Inst* 1956;16:1375-1403.
92. Yoshizato K, Taira T, Yamamoto N: Growth inhibition of human fibroblasts by reconstituted collagen fibrils. *Biomed Res* 1985;6:61-71.
93. Sarber R, Hull B, Merrill C, Soranno T, Bell E: Regulation of proliferation of fibroblasts of low and high population doubling levels grown in collagen lattices. *Mech Age Dev* 1981;17:107-117.
94. Thie M, Harrach B, Schönherr E, Kresse H, Robenek H, Rauterberg J: Responsiveness of aortic smooth muscle cells to soluble growth mediators is influenced by cell-matrix contact. *Arterioscler Thromb* 1993;13:994-1004.
95. Sumpio BE, Banes AJ, Link WG, Johnson GJ: Enhanced collagen production by smooth muscle cells during repetitive mechanical stretching. *Arch Surg* 1988;123:1233-1236.
96. Ip JH, Fuster V, Badimon L, Badimon J, Taubman MB, Chesebro JH: Syndromes of accelerated atherosclerosis: role of vascular injury and smooth muscle cell proliferation. *J Am Coll Cardiol* 1990;15:1667-1687.
97. Casscells W: Migration of smooth muscle and endothelial cells. Critical events in restenosis. *Circulation* 1992;86:723-729.
98. Davies MJ: A macro and micro view of coronary vascular insult in ischemic heart disease. *Circulation* 1990;82:II-38-II-46.

99. Klein CE, Dressel D, Steinmayer T, Mauch C, Eckes B, Krieg T, Bankert RB, Weber L: Integrin $\alpha 2\beta 1$ is upregulated in fibroblasts and highly aggressive melanoma cells in three-dimensional collagen lattices and mediates the reorganization of collagen I fibrils. *J Cell Biol* 1991;115:1427-1436.
100. Nakagawa S, Pawelek P, Grinnell F: Long-term culture of fibroblasts in contracted collagen gels: effects on cell growth and biosynthetic activity. *J Invest Dermatol* 1989;93:792-798.
101. Schiro JA, Chan BMC, Roswit WT, Kassner PD, Pentland AP, Hemler ME, Eisen AZ, Kupper TS: Integrin $\alpha 2\beta 1$ (VLA-2) mediates reorganization and contraction of collagen matrices by human cells. *Cell* 1991;67:403-410.
102. Hemler ME: VLA proteins in the integrin family: structures, functions, and their role on leukocytes. *Annu Rev Immunol* 1990;8:365-400.
103. Ingber DE: The riddle of morphogenesis: A question of solution chemistry or molecular cell engineering? *Cell* 1993;75:1249-1252.
104. Kirchofer D, Languino LR, Ruoslahti E, Pierschbacher MD: $\alpha 2\beta 1$ integrins from different cell types show different binding specificities. *J Biol Chem* 1990;265:615-618.
105. Elices MJ, Hemler ME: The human integrin VLA-2 is a collagen receptor on some cells and a collagen/laminin receptor on others. *Proc Natl Acad Sci USA* 1989;86:9906-9910.
106. Kupper TS, Ferguson TA: A potential pathophysiologic role for $\alpha 2\beta 1$ integrin in human eye diseases involving vitreoretinal traction. *FASEB J* 1993;7:1401-1406.
107. Hunt RC, Pakalanis VA, Choudhury P, Black EP: Cytokines and serum cause $\alpha 2\beta 1$ integrin-mediated contraction of collagen gels by cultures retinal pigment epithelial cells. *Invest Ophthalmol Vis Sci* 1994;35:955-963.
108. Clyman RI, Turner DC, Kramer RH: An $\alpha 1\beta 1$ -like integrin receptor on rat aortic smooth muscle cells mediates adhesion to laminin and collagen types I and IV. *Arteriosclerosis* 1990;10:402-409.
109. Akiyama SK, Yamada SS, Chen WT, Yamada KM: Analysis of fibronectin receptor function with monoclonal antibodies: roles in cell adhesion, migration, matrix assembly, and cytoskeletal organization. *J Cell Biol* 1989;109:863-875.
110. Bank I, Hemler ME, Brenner MB, Cohen D, Levy V, Belko J, Crouse C, Chess L: A novel monoclonal antibody, IB3.1, binds to a new epitope of the VLA-1 molecule. *Cellular Immunology* 1989;122:416-423.

111. Pischel KD, Hemler ME, Huang C, Bluestein HG, Woods VL: Use of the monoclonal antibody 12F1 to characterize the differentiation antigen VLA-2. *J Immunol* 1987;138:226-233.
112. Lemke H, Hammerling GJ, Hohmann C, Rajewsky K: Hybrid cell lines secreting monoclonal antibody specific for major histocompatibility antigens of the mouse. *Nature* 1978;271:249-251.
113. Hemler ME, Sanchez-Madrid F, Flotte TJ, Krensky AM, Burakoff SJ, Bhan AK, Springer TA, Strominger JL: Glycoproteins of 210,000 and 130,000 m.w. on activated T cells: cell distribution and antigenic relation to components on resting cells and T cell lines. *J Immunol* 1984;132:3011-3018.
114. Hemler ME, Huang C, Takada Y, Schwarz L, Strominger JL, Clabby ML: Characterization of the cell surface heterodimer VLA-4 and related peptides. *J Biol Chem* 1987;262:11478-11485.
115. Masumoto A, Hemler ME: Multiple activation states of VLA-4. *J Biol Chem* 1993;268:228-234.
116. Chan BMC, Hemler ME: Multiple functional forms of the integrin VLA-2 can be derived from a single $\alpha 2$ cDNA clone: interconversion of forms induced by an anti- $\beta 1$ antibody. *J Cell Biol* 1993;120:537-543.
117. Kawaguchi S, Hemler ME: Role of the α subunit cytoplasmic domain in regulation of adhesive activity mediated by the integrin VLA-2. *J Biol Chem* 1993;268:16279-16285.
118. Hemler ME, Huang C, Schwarz L: The VLA protein family. Characterization of five distinct cell surface heterodimers each with a common 130,000 molecular weight β subunit. *J Biol Chem* 1987;262:3300-3309.
119. Schmidt CE, Horwitz AF, Lauffenburger DA, Sheetz MP: Integrin-cytoskeletal interactions in migrating fibroblasts are dynamic, asymmetric, and regulated. *J Cell Biol* 1993;123:977-991.
120. Kuijpers TW, Mul EPJ, Blom M, Kovach NL, Gaeta FCA, Tollefson V, Elices MJ, Harlan JM: Freezing adhesion molecules in a state of high-avidity binding blocks eosinophil migration. *J Exp Med* 1993;178:279-284.
121. Loree HM, Grodzinsky AJ, Park SY, Gibson LJ, Lee RT: Static circumferential tangential modulus of human atherosclerotic tissue. *J Biomechanics* 1994;27:195-204.
122. Campbell JH, Campbell GR: Culture techniques and their applications to studies of vascular smooth muscle. *Clinical Science* 1993;85:501-513.

123. Dilley RJ, McGeachie JK, Prendergast FJ: A review of the proliferative behaviour, morphology and phenotypes of vascular smooth muscle. *Atherosclerosis* 1987;63:99-107.
124. Koteliansky VE, Belkin AM, Frid MG, Glukhova MA: Developmental changes in expression of adhesion-mediating proteins in human aortic smooth muscle. *Biochem Soc Trans* 1991;19:1072-1076.
125. Beklin VM, Belkin AM, Koteliansky VE: Human smooth muscle VLA-1 integrin: purification, substrate specificity, localization in aorta, and expression during development. *J Cell Biol* 1990;111:2159-2170.
126. Redecker-Beuke B, Thie M, Rautergerg J, Robenek H: Aortic smooth muscle cells in a three-dimensional collagen lattice culture. *Arterioscler Thromb* 1993;13:1572-1579.
127. Hajjar: Atherosclerosis. *Am Sci* 1995;83:460-467.
128. Falk E, Shah PK, Fuster V: Coronary plaque disruption. *Circulation* 1995;92:657-671.
129. Libby P: Molecular bases of the acute coronary syndromes. *Circulation* 1995;91:2844-2850.
130. Libby P, Schwartz D, Brogi E, Tanaka H, Clinton SK: A cascade model for restenosis: a special case of atherosclerosis progression. *Circulation* 1992;86 [suppl III]:III-47--III-52.
131. Stemme S, Hansson GK: Immune mechanisms in atherogenesis. *Ann Med* 1994;26:141-146.
132. Sudhir K, Wilson E, Chatterjee K, Ives HE: Mechanical strain and collagen potentiate mitogenic activity of angiotensin II in rat vascular smooth muscle cells. *J Clin Invest* 1993;92:3003-3007.
133. Indolfi C, Esposito G, Di Lorenzo E, Rapacciuolo A, Felicciello A, Porcellini A, Avvedimento VE, Condorelli M, Chiariello M: Smooth muscle cell proliferation is proportional to the degree of balloon injury in a rat model of angioplasty. *Circulation* 1995;92:1230-1235.
134. Guzman LA, Mick MJ, Arnold AM, Forudi F, Whitlow PL: Role of intimal hyperplasia and arterial remodeling after balloon angioplasty. *Arterioscler Thromb Vasc Biol* 1996;16:479-487.
135. Tan EML, Uitto J: Pathology of the extracellular matrix in atherosclerosis: in vivo and in vitro models, in White RA (ed): *Atherosclerosis and arteriosclerosis*. Boca Raton, FL, CRC Press, Inc., 1989, pp. 87-110.

136. Mayne R: Collagenous proteins of blood vessels. *Atherosclerosis* 1986;6:585-593.
137. Schönherr E, Järveläinen HT, Kinsella MG, Sandell LJ, Wight TN: Platelet-derived growth factor and transforming growth factor- β 1 differentially affect the synthesis of biglycan and decorin by monkey arterial smooth muscle cells. *Arterioscler Thromb* 1993;13:1026-1036.
138. Berrou E, Breton M, Deudon E, Picard J: Stimulation of large proteoglycan synthesis in cultured smooth muscle cells from pig aorta by endothelial cell-conditioned medium. *J Cell Physiol* 1991;149:436-443.
139. Mills I, Cohen CR, Sumpio BE: Cyclic strain and vascular biology, in Sumpio BE (ed): *Hemodynamic Forces and Vascular Cell Biology*. Austin, TX, RG Landes Company, 1993, pp. 66-89.
140. Thie M, Schlumberger W, Semich R, Rauterberg J, Robenek H: Aortic smooth muscle cells in collagen lattice culture: effects on ultrastructure, proliferation, and collagen synthesis. *Eur J Cell Biol* 1991;55:295-304.
141. Greve H, Blumberg P, Schmidt G, Schlumberger W, Rauterberg J, Kresse H: Influence of collagen lattice on the metabolism of small proteoglycan II by cultured fibroblasts. *Biochem J* 1990;269:149-155.
142. Ingber DE: Cellular tensegrity: defining new rules of biological design that govern the cytoskeleton. *J Cell Sci* 1993;104:613-627.
143. Gimbrone, Cotran: Human vascular smooth muscle in culture: growth and ultrastructure. *Lab Invest* 1975;33:16-27.
144. Libby P, Warner SK, Friedman GB: Interleukin-1: a mitogen for human vascular smooth muscle cells that induces the release of growth-inhibitory prostanoids. *J Clin Invest* 1988;81:487-498.
145. Karas RH, Patterson BL, Mendelsohn ME: Human vascular smooth muscle cells contain functional estrogen receptor. *Circulation* 1994;89:1943-1950.
146. Lee RT, Berdichevski F, Cheng GC, Hemler ME: Integrin-mediated collagen matrix reorganization by cultured human vascular smooth muscle cells. *Circ Res* 1995;76:209-214.
147. Kim Y-J, Sah RL-Y, Doong J-YH, Grodzinsky AJ: Fluorometric assay of DNA in cartilage explants using Hoechst 33258. *Ann Biochem* 1988;174:168-176.
148. Libby P, Schwartz D, Brogi E, Tanaka H, Clinton SK: A cascade model for restenosis: A special case of atherosclerosis progression. *Circulation* 1992;86:III-47-III-52.

149. Watson PA: Function follows form: generation of intracellular signals by cell deformation. *FASEB J* 1991;5:2013-2019.
150. Safar ME, Peronneau PA, Levenson JA, Toto-Moukouo JA, Simon AC: Pulsed doppler: diameter, blood flow velocity, and volumic flow of the brachial artery in sustained essential hypertension. *Circulation* 1981;63:393-400.
151. Lyall F, Deehan MR, Greer IA, Boswell F, Brown WC, McInnes GT: Mechanical stretch increases proto-oncogene expression and phosphoinositide turnover in vascular smooth muscle cells. *J Hypertension* 1994;12:1139-1145.
152. Rosenberg RD: Vascular smooth muscle cell proliferation: basic investigations and new therapeutic approaches. *Thromb Haemost* 1993;70:10-16.
153. Ross R, Raines EW, Bowen-Pope DF: The biology of platelet-derived growth factor. *Cell* 1986;46:155-169.
154. Majesky MW, Reidy MA, Bowen-Pope DF, Hart CE, Wilcox JN, Schwartz SM: PDGF ligand and receptor gene expression during repair of arterial injury. *J Cell Biol* 1990;111:2149-2158.
155. Miano JM, Vlastic N, Tota RR, Stemerman MB: Smooth muscle cell immediate-early gene and growth factor activation follows vascular injury: a putative in vivo mechanism for autocrine growth. *Arterioscler Thromb* 1993;13:211-219.
156. Ferns GAA, Raines EW, Sprugel KH, Motani AS, Reidy MA, Ross R: Inhibition of neointimal smooth muscle accumulation after angioplasty by an antibody to PDGF. *Science* 1991;253:1129-1132.
157. Vlodavsky I, Friedman R, Sullivan R, Sasse J, Klagsbrun M: Aortic endothelial cells synthesize basic fibroblast growth factor which remains cell-associated and platelet-derived growth factor-like protein which is secreted. *J Cell Physiol* 1987;131:402-428.
158. Gospodarowicz D, Ferrara N, Haaparanta T, Neufeld G: Basic fibroblast growth factor: expression in cultured bovine vascular smooth muscle cells. *Eur J Cell Biol* 1988;46:144-151.
159. Abraham JA, Whang JL, Tumolo A, Friedman J, Hjenild KA, Gospodarowicz D, Fiddes JC: Nucleotide sequence of a bovine clone encoding the angiogenic protein, basic fibroblast growth factor. *Science* 1986;233:545-548.
160. McNeil PL, Muthukrishnan L, Warder E, D'Amore PA: Growth factors are released by mechanically wounded endothelial cells. *J Cell Biol* 1989;109:811-822.

161. Muthukrishnan L, Warder E, McNeil PL: Basic fibroblast growth factor is efficiently released from a cytosolic storage site through plasma membrane disruptions of endothelial cells. *J Cell Physiol* 1991;148:1-16.
162. Clarke MSF, Khakee R, McNeil PL: Loss of cytoplasmic basic fibroblast growth factor from physiologically wounded myofibers of normal and dystrophic muscle. *J Cell Sci* 1993;106:121-133.
163. Fingerle J, Au YP, Clowes AW, Reidy MA: Intimal lesion formation in rat carotid arteries after endothelial denudation in absence of medial injury. *Arteriosclerosis* 1990;10:1082-1087.
164. Lindner V, Reidy MA: Proliferation of smooth muscle cells after vascular injury is inhibited by an antibody against basic fibroblast growth factor. *Proc Natl Acad Sci USA* 1991;88:3739-3743.
165. Fingerle J, Johnson R, Clowes AW, Majesky MW, Reidy MA: Role of platelets in smooth muscle cell proliferation and migration after vascular injury in rat carotid artery. *Proc Natl Acad Sci USA* 1989;86:8412-8416.
166. Lindner V, Reidy M: Expression of basic fibroblast growth factor and its receptor by smooth muscle cells and endothelium in injured rat arteries. *Circ Res* 1993;73:589-595.
167. Jackson CL, Reidy MA: Basic fibroblast growth factor: its role in the control of smooth muscle cell migration. *Am J Pathol* 1993;143:1024-1031.
168. Jawien AD, Bowen-Pope DF, Lindner V, Schwartz SM, Clowes AW: Platelet-derived growth factor promotes smooth muscle cell migration and intimal thickening in a rat model of balloon angioplasty. *J Clin Invest* 1992;89:507-511.
169. Lindner V, Lappi DA, Baird A, Majack RA, Reidy MA: Role of basic fibroblast growth factor in vascular lesion formation. *Circ Res* 1991;68:106-113.
170. Olson NE, Chao S, Lindner V, Reidy MA: Intimal smooth muscle cell proliferation after balloon injury: The role of basic fibroblast growth factor. *Am J Pathol* 1992;140:1017-1023.
171. Gajdusek CM, Carbon S: Injury-induced release of basic fibroblast growth factor from bovine aortic endothelium. *J Cell Physiol* 1989;139:570-579.
172. Mignatti P, Morimoto T, Rifkin DB: Basic fibroblast growth factor, a protein devoid of secretory signal sequence, is released by cells via a pathway independent of the endoplasmic reticulum-Golgi complex. *J Cell Physiol* 1992;151:81-93.

173. Bashkin P, Doctrow S, Klagsbrun M, Svahn CM, Folkman J, Vlodavsky I: Basic fibroblast growth factor binds to subendothelial extracellular matrix and is released by heparitinase and heparin-like molecules. *Biochem* 1989;28:1737-1743.
174. Majack RA, Majesky MW, Goodman LV: Role of PDGF-A expression in the control of vascular smooth muscle cell growth by transforming growth factor-beta. *J Cell Biol* 1990;111:239-247.
175. Fuster V, Badimon JJ, Badimon L: Clinical-pathological correlations of coronary disease progression and regression. *Circulation* 1992;86:1-11.
176. Hansson GK: Cytokines regulate proliferation and cytoskeletal organization of vascular smooth muscle cells. *Path Res Pract* 1994;190:891-894.
177. Dinarello CA: The interleukin-1 family: 10 years of discovery. *FASEB J* 1994;8:1314-1325.
178. Zhu X, Komiya H, Chirino A, Faham S, Fox GM, Arakawa T, Hsu BT, Rees DC: Three-dimensional structures of acidic and basic fibroblast growth factors. *Science* 1991;251:90-93.
179. Rubartelli A, Cozzolino F, Talio M, Sitia R: A novel secretory pathway for interleukin-1b, a protein lacking a signal sequence. *EMBO J* 1990;9:1503-1510.
180. Mizutani H, Black R, Kupper TS: Human keratinocytes produce but do not process pro-interleukin-1 (IL-1) beta: different strategies of IL-1 production and processing in monocytes and keratinocytes. *J Clin Invest* 1991;87:1066-1071.
181. Hung CT, Williams JL: A method for inducing equi-biaxial and uniform strains in elastomeric membranes used as cell substrates. *J Biomech* 1994;27:227-232.
182. D'Angelo G, Meininger GA: Transduction mechanisms involved in the regulation of myogenic activity. *Hypertension* 1994;23:1096-1105.
183. Zarins CK, Zatina MA, Giddens DP, Ku DN, Glagov S: Shear stress regulation of artery lumen diameter in experimental atherogenesis. *J Vasc Surg* 1987;5:413-420.
184. Dzau VJ, Gibbons GH, Morishita R, Pratt RE: New perspectives in hypertension research: potentials of vascular biology. *Hypertension* 1994;23:1132-1140.
185. Richardson PD, Davies MJ, Born GVR: Influence of plaque configuration and stress distribution on fissuring of coronary atherosclerotic plaques. *Lancet* 1989;941-944.
186. Ross R: The pathogenesis of atherosclerosis: a perspective for the 1990s. *Nature* 1992;362:801-809.

187. Mason IJ: The ins and outs of fibroblast growth factors. *Cell* 1994;78:547-552.
188. Powell PP, Klagsbrun M: Three forms of rat basic fibroblast growth factor are made from a single mRNA and localize to the nucleus. *J Cell Physiol* 1991;148:202-210.
189. Prats H, Kaghad M, Prats AC, Klagsbrun M, L  lias JM, Liauzun P, Chalon P, Tauber JP, Amalric F, Smith JA, Caput D: High molecular mass forms of basic fibroblast growth factor are initiated by alternative CUG codons. *Proc Natl Acad Sci USA* 1989;86:1836-1840.
190. Renko M, Quarto N, Morimoto T, Rifkin DB: Nuclear and cytoplasmic localization of different basic fibroblast growth factor species. *J Cell Physiol* 1990;144:108-114.
191. Biro S, Yu Zu-X, Fu Ya-M, Smale G, Sasse J, Sanchez J, Ferrans VJ, Casscells W: Expression and subcellular distribution of basic fibroblast growth factor are regulated during migration of endothelial cells. *Circ Res* 1994;74:485-494.
192. Anderson JE, Liu L, Kardami E: Distinctive patterns of basic fibroblast growth factor (bFGF) distribution in degenerating and regenerating areas of dystrophic (mdx) striated muscles. *Dev Biol* 1991;147:96-109.
193. Yu Zu-X, Biro S, Fu Ya-M, Sanchez J, Smale G, Sasse J, Ferrans VJ, Casscells W: Localization of basic fibroblast growth factor in bovine endothelial cells: immunohistochemical and biochemical studies. *Exp Cell Res* 1993;204:247-259.
194. Mignatti P, Rifkin DB: Release of basic fibroblast growth factor, an angiogenic factor devoid of secretory signal sequence: a trivial phenomenon or a novel secretion mechanism? *J Cell Biochem* 1991;47:201-207.
195. Ku PT, D'Amore PA: Regulation of basic fibroblast growth factor (bFGF) gene and protein expression following its release from sublethally injured endothelial cells. *J Cell Biochem* 1995;58:328-343.
196. Crowley ST, Ray CJ, Nawaz D, Majack RA, Horwitz LD: Multiple growth factors are released from mechanically injured vascular smooth muscle cells. *Am J Physiol* 1995;269:H1641-H1647.
197. Benzaquen LR, Nicholson-Weller A, Halperin JA: Terminal complement proteins C5b-9 release basic fibroblast growth factor and platelet-derived growth factor from endothelial cells. *J Exp Med* 1994;179:985-992.
198. Fukuo K, Inoue T, Morimoto S, Nakahashi T, Yasuda O, Kitano S, Sasada R, Ogihara T: Nitric oxide mediates cytotoxicity and basic fibroblast growth factor release in cultured vascular smooth muscle cells: a possible mechanism of neovascularization in atherosclerotic plaques. *J Clin Invest* 1995;95:669-676.

199. Calara F, Ameli S, Hultgardh-Nilsson A, Cercek B, Kupfer J, Hedin U, Forrester J, Shah PK, Nilsson J: Autocrine induction of DNA synthesis by mechanical injury of cultured smooth muscle cells: potential role of FGF and PDGF. *Arterioscler Thromb Vasc Biol* 1996;16:187-193.
200. Mignatti P, Morimoto T, Rifkin DB: Basic fibroblast growth factor released by single, isolated cells stimulates their migration in an autocrine manner. *Proc Natl Acad Sci USA* 1991;88:11007-11011.
201. Aviezer D, Hecht D, Safran M, Eisinger M, David G, Yayon A: Perlecan, basal lamina proteoglycan, promotes basic fibroblast growth factor-receptor binding, mitogenesis, and angiogenesis. *Cell* 1994;79:1005-1013.
202. Schlessinger J, Lax I, Lemmon M: Regulation of growth factor activation by proteoglycans: what is the role of the low affinity receptors. *Cell* 1995;83:357-360.
203. Roghani M, Mansukhani A, Dell'Era P, Bellosta P, Basilico C, Rifkin DB, Moscatelli D: Heparin increases the affinity of basic fibroblast growth factor for its receptor but is not required for binding. *J Biol Chem* 1994;269:3976-4984.
204. Moscatelli D: Basic fibroblast growth factor (bFGF) dissociates rapidly from heparan sulfates but slowly from receptors: implications for mechanisms of bFGF release from pericellular matrix. *J Biol Chem* 1992;267:25803-25809.
205. Presta M, Maier JAM, Rusnati M, Ragnotti G: Basic fibroblast growth factor is released from endothelial extracellular matrix in a biologically active form. *J Cell Physiol* 1989;140:68-74.
206. Saksela O, Rifkin DB: Release of basic fibroblast growth factor-heparan sulfate complexes from endothelial cells by plasminogen activator-mediated proteolytic activity. *J Cell Biol* 1990;110:767-775.
207. Flaumenhaft R, Moscatelli D, Saksela O, Rifkin DB: Role of extracellular matrix in the action of basic fibroblast growth factor: matrix as a source of growth factor for long-term stimulation of plasminogen activator production and DNA synthesis. *J Cell Physiol* 1989;140:75-81.
208. Cheng GC, Libby P, Grodzinsky AJ, Lee RT: Induction of DNA synthesis by a single transient mechanical stimulus of human vascular smooth muscle cells: role of fibroblast growth factor-2. *Circulation* 1996;93:99.
209. Moscatelli: High and low affinity binding sites for basic fibroblast growth factor on cultured cells: absence of a role for low affinity binding in the stimulation of

- plasminogen activator production by bovine capillary endothelial cells. *J Cell Physiol* 1987;131:123-130.
210. Moscatelli D: Metabolism of receptor-bound and matrix-bound basic fibroblast growth factor by bovine capillary endothelial cells. *J Cell Biol* 1988;107:753-759.
 211. Schweigerer L, Neufeld G, Friedman J, Abraham JA, Fiddes JC, Gospodarowicz D: Capillary endothelial cells express basic fibroblast growth factor, a mitogen that promotes their own growth. *Nature* 1987;325:257-259.
 212. Schmidt A, Skaletz-Rorowski, Breithardt G, Buddeck E: Growth status-dependent changes of bFGF compartmentalization and heparan sulfate structure in arterial smooth muscle cells. *Eur J Cell Biol* 1995;67:130-134.
 213. Ellis EF, McKinney JS, Willoughby KA, Liang S, Povlishock JT: A new model for rapid stretch-induced injury of cells in culture: characterization of the model using astrocytes. *J Neurotrauma* 1995;12:325-339.
 214. Jones KH, Senft JA: An improved method to determine cell viability by simultaneous staining with fluorescein diacetate-propidium iodide. *J Histochem Cytochem* 1985;33:77-79.
 215. Altman SA, Randers L, Rao G: Comparison of trypan blue exclusion and fluorometric assays for mammalian cell viability determinations. *Biotech Prog* 1993;9:671-674.
 216. McNeil PL, Ito S: Gastrointestinal cell plasma membrane wounding and resealing in vivo. *Gastroenterology* 1989;96:1238-1248.
 217. McNeil PL, Ito S: Molecular traffic through plasma membrane disruptions of cells in vivo. *J Cell Sci* 1990;96:549-556.
 218. Wilson E, Sudhir K, Ives HE: Mechanical strain of rat vascular smooth muscle cells is sensed by specific extracellular matrix/integrin interactions. *J Clin Invest* 1995;96:2364-2372.
 219. Nebe B, Rychly J, Knopp A, Bohn W: Mechanical induction of beta 1-integrin-mediated calcium signaling in a hepatocyte cell line. *Exp Cell Res* 1995;218:479-484.
 220. Lauffenburger DA, Horwitz AF: Cell migration: a physically integrated molecular process. *Cell* 1996;84:359-369.
 221. Saksela O, Moscatelli D, Sommer A, Rifkin DB: Endothelial cell-derived heparan sulfate binds basic fibroblast growth factor and protects it from proteolytic degradation. *J Cell Biol* 1988;107:743-751.

222. Spivak-Kroizman T, Lemmon MA, Dikic I, Ladbury JE, Pinchasi D, Huang J, Jaye M, Crumley G, Schlessinger J, Lax I: Heparin-induced oligomerization of FGF molecules is responsible for FGF receptor dimerization, activation, and cell proliferation. *Cell* 1994;79:1015-1024.
223. Vlodavsky I, Fuks Z, Ishai-Michaeli R, Bashkin P, Levi E, Korner G, Bar-Shavit R, Klagsbrun M: Extracellular matrix-resident basic fibroblast growth factor: implication for the control of angiogenesis. *J Cell Biochem* 1991;45:167-176.
224. Barbee KA, Macarak EJ, Thibault LE: Strain measurements in cultured vascular smooth muscle cells subjected to mechanical deformation. *Ann Biomed Eng* 1994;22:14-22.
225. Osol G: Mechanotransduction by vascular smooth muscle. *J Vasc Res* 1995;32:275-292.
226. Sadoshima J, Izumo S: Mechanical stretch rapidly activates multiple signal transduction pathways in cardiac myocytes: potential involvement of an autocrine/paracrine mechanism. *EMBO J* 1993;12:1681-1692.
227. Sumpio BE, Banes AJ, Levin LG, Johnson G: Mechanical stress stimulates aortic endothelial cells to proliferate. *J Vasc Surg* 1987;6:252-256.
228. Yang Z, Noll G, Lüscher T: Calcium antagonists differently inhibit proliferation of human coronary smooth muscle cells in response to pulsatile stretch and platelet-derived growth factor. *Circulation* 1993;88:832-836.
229. Sumpio BE, Banes AJ, Buckley M, Johnson GJ: Alterations in aortic endothelial cell morphology and cytoskeletal protein synthesis during cyclic tensional deformation. *J Vasc Surg* 1988;7:130-138.
230. Davies PF, Robotewskyi A, Griem ML: Quantitative studies of endothelial cell adhesion: directional remodeling of focal adhesion sites in response to flow forces. *J Clin Invest* 1994;93:2031-2038.
231. Carter AJ, Laird JR, Farb A, Kufs W, Wortham DC, Virmani R: Morphologic characteristics of lesion formation and time course of smooth muscle cell proliferation in a porcine proliferative restenosis model. *J Am Coll Cardiol* 1994;24:1398-1405.
232. Ruoslahti E: Control of cell motility and tumour invasion by extracellular matrix interactions. *Br J Cancer* 1992;66:239-242.
233. Lincoff AM, Topol EJ, Ellis SG: Local drug delivery for the prevention of restenosis. Fact, fancy, and future. *Circulation* 1994;90:2070-2084.

234. Cardarelli PM, Yamagata S, Taguchi I, Gorscan F, Chiang SL, Lobl T: The collagen receptor $\alpha_2\beta_1$, from MG-63 and HT 1080 cells, interacts with a cyclic RGD peptide. *J Biol Chem* 1992;267:23159-23164.
235. Thie M: Regulation of biosynthetic activity in aortic smooth muscle cells by extracellular matrix components, in Robenek H, Severs NJ (eds): *Cell interactions in atherosclerosis*. Boca Raton, FL, CRC Press, 1992, pp. 137-163.
236. Miano JM, Vlastic N, Tota RR, Stemerman MB: Localization of Fos and Jun proteins in rat aortic smooth muscle cells after vascular injury. *Am J Pathol* 1993;142:715-724.
237. Lee RT, Schoen FJ, Loree HM, Lark MW, Libby P: Circumferential stress and interstitial collagenase in human coronary atherosclerosis: implications for plaque rupture. 1996.